Electronic Theses and Dissertations

5-2018

# Exercise preconditioning and TFAM overexpression diminish skeletal muscle atrophy.

Nicholas Todd Theilen
*University of Louisville*

EXERCISE PRECONDITIONING AND TFAM OVEREXPRESSION DIMINISH
SKELETAL MUSCLE ATROPHY

By

Nicholas Todd Theilen
B.S., University of Louisville, 2009
M.S., University of South Florida, 2013
M.S., University of Louisville, 2017

A Dissertation
Submitted to the Faculty of the
School of Medicine of the University of Louisville
in Partial Fulfillment of the Requirements
for the Degree of

Doctor of Philosophy
in Physiology and Biophysics

Department of Physiology
University of Louisville
Louisville, Kentucky

May 2018

EXERCISE PRECONDITIONING AND TFAM OVEREXPRESSION DIMINISH
SKELETAL MUSCLE ATROPHY

By

Nicholas Todd Theilen
B.S., University of Louisville, 2009
M.S., University of South Florida, 2013
M.S., University of Louisville, 2017

A Dissertation Approved on

March 23, 2018

by the following Dissertation Committee:

_____
Dr. Suresh C. Tyagi

_____
Dr. Dale Schuschke

_____
Dr. Irving Joshua

_____
Dr. Sathnur Pushpakumar

_____
Dr. Adrienne Bratcher

## ACKNOWLEDGEMENTS

ABSTRACT

EXERCISE PRECONDITIONING AND TFAM OVEREXPRESSION DIMINISH
SKELETAL MUSCLE ATROPHY

Nicholas T. Theilen

March 23, 2018

This dissertation is an analysis of skeletal muscle atrophy and a molecular

assessment of potential preventative treatments. Chapter I begins with a background of

skeletal muscle atrophy along with an analysis of associated molecular pathways. Here,

we discuss how skeletal muscle atrophy is the consequence of protein degradation

exceeding protein synthesis and can occur when a muscle is abnormally disused. The

development of therapies prior to skeletal muscle atrophy settings to diminish protein

degradation is scarce and could be useful to prevent negative clinical outcomes of

patients who must unload and disuse musculature over extended periods. Mitochondrial

dysfunction is associated with skeletal muscle atrophy and contributes to the induction of

protein degradation and cell apoptosis through increased levels of ROS. This damages

mtDNA, leading to its degradation and mutation resulting in dysfunctional mitochondria.

Mitochondrial transcription factor A (TFAM) protects mtDNA from ROS and

degradation while increasing mitochondrial function and the transcription of

mitochondrial proteins. Exercise stimulates mitochondrial function by activating cell

signaling pathways that converge on and increase PGC-1α, a well-known activator of the

transcription of TFAM and mitochondrial biogenesis. Therefore, we first hypothesize

exercise training prior to muscle unloading and disuse will prevent skeletal muscle atrophy. Additionally, we hypothesize this protective effect of exercise in preventing skeletal muscle atrophy is associated with increased mitochondrial markers. In Chapter II, we test these hypotheses by first inducing skeletal muscle atrophy using hindlimb suspension (HLS) and exercising mice prior to this suspension. The results indicated exercising prior to HLS reduced many of the morphological and molecular changes within the muscle associated with atrophy. Also in Chapter II, we follow up these findings through mitochondrial molecular analyses with results showing exercise increasing mitochondrial-associated markers and redox balance. We also find decreases in TFAM after HLS, which led to further analyses through the use of a TFAM overexpression transgenic mouse model in HLS. We reason if HLS induces excessive ROS accumulation and decreases TFAM, overexpressing this gene may prevent mitochondrial dysfunction mechanisms associated with atrophy. Therefore, we hypothesize the overexpression of TFAM diminishes skeletal muscle atrophy and, secondarily, TFAM overexpression combined with exercise training will synergistically prevent atrophy caused by HLS. To assess these hypotheses, in Chapter III we subject TFAM mice to HLS as well as exercising TFAM mice prior to entering HLS. Results here reveal TFAM overexpression diminishes skeletal muscle atrophy caused by HLS and combining exercise and TFAM overexpression resulted in no significant difference compared to exercising prior to HLS in wild-type mice. Collectively, the data indicate an important role for exercise and TFAM in diminishing skeletal muscle atrophy.

TABLE OF CONTENTS

CHAPTER I

*TFAM OVEREXPRESSION DIMINISHES SKELETAL MUSCLE ATROPHY*

CHAPTER IV

*CONCLUDING DISCUSSION*………………………………………………...127

# LIST OF TABLES

LIST OF FIGURES

CHAPTER I

GENERAL INTRODUCTION


**<u>Skeletal Muscle Atrophy</u>**

Skeletal muscle serves many important functions affecting the human physiologic state. Standard perception of the function of skeletal muscle is generally in propulsion for locomotion and desired movement, such as the musculature of the upper legs contracting and relaxing to extend and retract the lower leg at the knee joint repetitiously as part of the coordination of walking. However, this tissue also serves as an important amino acid and glucose reservoir and is the largest metabolically active organ in the human body (117). Pathological loss of this tissue, known as skeletal muscle atrophy, is associated with numerous health abnormalities and can greatly affect quality of life.

Skeletal muscle atrophy is caused by a host of factors including disease, ageing, injury, nutritional decrements, and disuse. It is characterized by a decrease in the cross-sectional area of the muscle, a decline in force generative capabilities, decreases in functional proteins of the muscle mass, and a loss of oxidative ability making the tissue less resistant to fatigue (140). The scope of the present dissertation project will focus on the atrophic aspects of muscle disuse.

The abnormal disuse of muscle occurs for many reasons including bed rest from disease or injury, cast immobilization due to injury, spinal cord injury, weightlessness environments, and a sedentary lifestyle. Ultimately, reduced muscle contraction and mechanical stress from a lack of loading stimuli on the muscle encompasses disuse. When this happens, increased activation of protein signaling pathways leading to protein degradation and apoptosis arise with corresponding downregulation of protein synthesis pathways (140). This imbalance is depicted in *Figure 2*.

Skeletal muscle atrophy can be gravely debilitating and is associated with increased morbidity and mortality (113). One can imagine a scenario in which a patient is prescribed bedrest for an extended time, due to injury, and accumulates significant muscle atrophy which renders this person incapable of performing basic physical tasks, such as simply rising out of bed. Diminished force production from atrophic muscles is associated with the onset of fatigue and a potential, further reduction in physical ability. Not only is the patient's quality of life harshly diminished, healthcare costs in the form of medications and rehabilitation sharply increase to attempt to combat this condition. Therefore, it is important, both medically and fiscally, to study interventions that may potentially prevent atrophy.

There is a clear link in the literature with skeletal muscle atrophy to the dysfunction of the mitochondria (69, 96) and redox imbalance (114) to the induction of degradation and apoptotic pathways, which results in the physical reduction of the tissue. The study of these molecular mechanisms associated with atrophy is warranted to increase our understanding of this condition and potentially create molecularly directed

**Figure 1**. **Molecular scale of atrophy.** Scale representation of the molecular imbalance of skeletal muscle atrophy. Degradation and apoptosis exceeding protein synthesis results in atrophy over time.

FIGURE 1



Skeletal Muscle Atrophy

-Protein Synthesis

-Protein Degradation
-Apoptosis
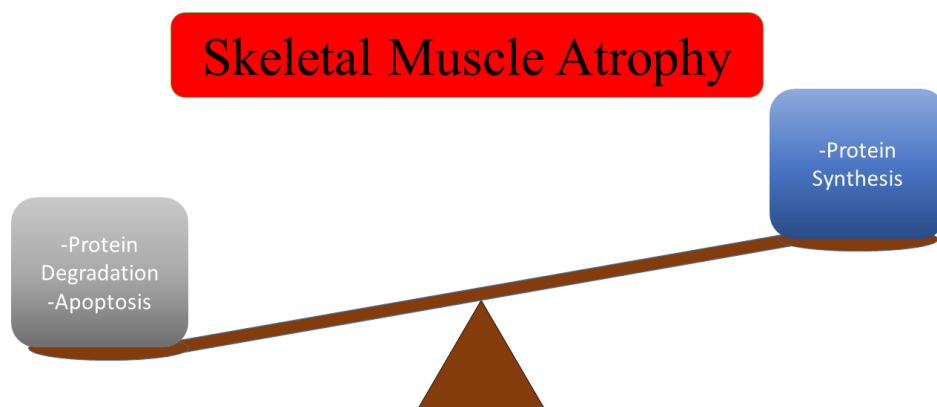
therapies of the future. To be able to do this, we must have a clear understanding of what causes atrophy to lead to how we can prevent the condition.

*Protein degradation.* Disuse-induced muscle atrophy has many causes, as previously stated. While the causes occur from different scenarios, they all similarly reduce mechanical stress and fiber contraction in the muscle. The mechanical stress of contracting skeletal muscle under a physical load in a healthy individual causes many changes throughout skeletal myocytes. Contraction induced by myosin and actin cross-bridging is sensed by the cell via proteins such as dystrophin and integrin complexes (5). Dystrophin is a cytoplasmic protein that interacts, on one end, with actin fibers under the cell surface and, on the opposite end, associates with membrane-bound proteins that form a dystrophin complex spanning the entire sarcolemmal membrane (40). During actin and myosin contraction, lateral force production is created in the myofilaments. Anchoring proteins, such as dystrophin and the associated complex, turn this lateral force into linear force to disperse across the sarcolemma. Through adhesion molecules, such as laminin, this linear force is converted back into lateral force as it transmits through the sarcolemma and into the extracellular matrix throughout the muscle. This acts as a "shock absorber" and provides stiffness to the contracting myocyte and prevents the initial lateral force of the myofilaments from being transferred into the sarcolemma inappropriately, causing deformation of the membrane.

Pasternak's group demonstrated this by using dystrophin knockout (mdx) mice lacking this protein (similar to humans with Duchenne muscular dystrophy). Mdx mice displayed fragile myotubes with roughly 4 times less stiffness than normal myotubes

(108). This important protein and its respective complex, along with other sensory

complexes (integrin), activates focal adhesion kinases (FAKs) and mediates the

prevention of apoptosis and activation of growth pathways (5). With unloading and

disuse, mechanical stress is greatly reduced and the corresponding growth signaling and

apoptosis prevention is prohibited. Further, lack of contraction leads to the activation of

catabolic pathways in skeletal muscle.

The ubiquitin-proteasome pathway is a main regulator of protein degradation.

Muscle ring finger-1 (Murf-1) and Atrogin-1/MAFbx are E3 ligases in skeletal muscle

that play a key role in ubiquitin marked degradation (45). These ligases are activated by

multiple stimuli, in particular ROS, inflammatory markers, and the unloading of muscle.

Activation of IκB kinase (IKK) occurs via these stimuli, which is associated with the

activation of nuclear factor kappa-light-chain-enhancer of activated B cells (NF-κB) (11).

NF-κB is a transcription factor responsible for transcription of many degradative genes.

In this case, NF-κB is able to translocate into the nucleus and play a role in the

transcription of Murf-1 and Atrogin-1/MAFbx. Mature Murf-1 and Atrogin-1/MAFbx

proteins polyubiquinate polypeptides in the muscle as a method of targeting the protein

for degradation. Skeletal muscles consist mostly of the myofibrillar proteins myosin and

actin involved in the functional aspect of the cells. Therefore, for significant atrophy to

occur, these proteins must be degraded.

Murf-1 is involved in targeting myosin light chains for degradation while atrogin-

1/MAFbx targets actin molecules (9). After these myofibrillar proteins are

polyubiquinated, proteasomes attach and degrade the protein resulting in atrophy. Tawa

et al. demonstrated the importance of the ubiquitin pathway by inhibiting proteasome

activity in the rat soleus muscle of three atrophy inducing pathological states (denervation, hyperthyroidism, sepsis). Without altering protein synthesis expression, protein balance increased with high percentages of reductions in proteolysis and an increase in ubiquinated proteins of the muscle was observed (139). This study, among others, delineated the ubiquitin-proteasome pathway as the key modulator of protein degradation and thus, should be considered when working with skeletal muscle atrophy models. It is possible that different pathways contribute to degradation in different settings based upon the conditions of the model and should also be considered when reviewing data.

Other protease contributors in skeletal muscle protein degradation include calpains and lysosomes (16). Calpains are intracellular proteases that are regulated by $Ca^{2+}$. In skeletal muscle, calpain-1, calpain-2, and calpain-3 are mainly expressed. Calpain-3 is downregulated during atrophy as well as in exercise suggesting that its absence is necessary for atrophy (4). Recently, Shenkman and colleagues used an inhibiting agent to diminish calpain-1 in a rat model while inducing skeletal muscle atrophy by hindlimb suspension for 3 days. The soleus muscle size was significantly reduced in rats that were only suspended while those suspended and treated with the calpain-1 inhibitor retained muscle size (126). Calpain-1 levels were increased in the suspension only model. Interestingly, levels of calpain-2 were not affected by hindlimb suspension induced atrophy, indicating a key role of calpain-1 in short-term (3 days) disuse. Inhibiting calpain-1 decreases MAFbx expression and inhibits protein ubiquitination. Studies increasing the atrophy duration should be done to further elucidate these changes in protein expression.

Lysosomal activity is also a contributing factor to protein degradation in muscle. Autophagy using lysosomal machinery (autophagy-lysosomal system) is upregulated during catabolic states of skeletal muscle (120). Normal contraction of muscle tissue over time causes damage to the contracting proteins as well as organelles of the cell. For these damaged proteins and organelles to be degraded and recycled to continue normal or enhanced function, the cells must have a self-selecting degradative system. This system is autophagy.

Again, NF-κB pathway is an important transcription factor inducing autophagy. Autophagosomes consume defective proteins of the cell and transport the defective material to lysosomes. Lysosomes are membrane-bound vesicles containing acid hydrolases that, when released, degrade the cellular components of the autophagosome (7). The process is also induced by multiple types of exercise (63, 124). This could be to enhance the removal of damaged proteins due to the stress of exercise contractions or may also be to provide energy for sustained contractions in the cell. While this process positively impacts the function of skeletal muscle tissue, excessive autophagy-lysosomal activity, as seen in many myopathies, leads to atrophy.

*Cell apoptosis.* Cells undergo a programmed cell death (apoptosis) due to specific biochemical interactions that cause blebbing of the cell membrane, condensation of chromatin, and cell fragment lysis resulting in the death of the cell. When skeletal muscle is not contracting over time, as occurs in disuse, an increase in cell apoptosis has been observed (130). As load and contractions of the muscle diminish, the removal of myonuclei occurs and is associated with apoptosis (5) along with the destruction of

cellular proteins. The myonuclear domain is reduced, resulting in diminished function in the myofiber.

Caspases are proteases within the cell that play a role in the disassembly of the nucleus and cytoskeleton while cleaving many other cellular proteins. Caspases are categorized as "initiators" and "executioners" with caspase-2, -6, -9, -10 being characterized as initiators while caspase-3, -7, and -8 are executioners (20). Specifically, caspase-3 is a major executioner involved in skeletal muscle atrophy. Signaling for caspase-3 includes both extrinsic and intrinsic factors. Extrinsic factors include binding of the tumor necrosis factor (TNF) ligand to TNF death receptors on transmembrane proteins. This TNF binding causes a signal cascade that results in procaspase-8 and the activation of the caspase-3 executioner. Capase-3 activates an endonuclease (CAD) that degrades DNA (32) and thus, the execution of apoptosis.

A major intrinsic pathway leading to caspase-3 activation includes the release of cytochrome c (Cyt c) from the mitochondria. Signals such as elevated levels of ROS and reactive-nitrogen species (RNS) increase mitochondrial membrane permeability that release Cyt c from the mitochondria (29). B-cell leukemia/lymphoma 2 (Bcl-2) and Bcl-XL block the release of Cyt c and serve an anti-apoptotic role. Members of the Bcl-2 associated death promoter (BAD) family, such as BAX and BAK, serve as pro-apoptotic factors and increase pore permeability of the mitochondria allowing the release of Cyt c (160). Cyt c is then involved in the activation of the initiator caspase-9, forming an apoptosome complex. This leads to the activation of the executioner caspase-3 and degradation of cellular components (152). Leeuwenburgh et al. performed hindlimb suspension on young and old rats over a 14-day period. Their results indicated an 84%

9

increase in caspase-3 activity in the soleus of young rats after inducing atrophy over 14 days (83). Furthermore, a study by Nagano and colleagues observed active caspase-3 activity in male Wistar rats after 3-weeks of hindlimb unloading (98). These studies indicate an apoptotic link between disuse-induced muscular atrophy and caspase-3.

There are caspase-dependent and caspase-independent pathways that induce apoptosis. Apoptosis-inducing factor (AIF) is released from the mitochondria upon stimulation from pro-apoptotic signals. This AIF activates apoptosis through chromosomal condensation and DNA fragmentation in a caspase-independent manner (62). EndonucleaseG (EndoG) is a protein released from the mitochondria after pro-apoptotic signaling. EndoG is caspase-independent and is associated with DNA fragmentation that coincides with apoptosis during muscle atrophy induced by hindlimb suspension in aged mice (29). With a multitude of cell signaling pathways involved in cell apoptosis, cross-talk is likely to occur between the various cascades.

*Protein synthesis.* The counterbalance to protein degradation in muscle cells is protein synthesis. As stated previously, when degradation exceeds synthesis over time, atrophy occurs. Signals for protein synthesis include many stimulatory factors such as mechanical loading of the muscle, hormone circulation, and nutrition. Conversely, protein synthesis signaling is inhibited by fasting, augmentation of growth factor release or binding, and muscular disuse. Many proteins play a role in the synthesis pathway but the previously mentioned mammalian target of rapamycin (mTOR) is consistently viewed as the major regulator of this process.

Two functional complexes are formed from mTOR termed mTOR complex-1 and mTOR complex-2 (mTORC1 and mTORC2). Although both mTORC1 and mTORC2 have a unique role, both complexes will be encompassed and referenced as 'mTOR' for the scope of the current review. Signaling from extracellular growth factors, such as IGF-1 and insulin, and amino acids (specifically branched-chain amino acids) lead to the activation of the PI3K/AKT pathway that is associated with the activation of mTOR (80). Mechanical loading via resistance exercise of the skeletal muscle also activates this pathway to activate mTOR (27, 103).

Activated mTOR interacts with many downstream effectors including two well-established proteins in particular, S6 kinase (S6K) ribosomal protein and eukaryotic translation initiation factor-4 (eIF-4E) binding protein (4E-BP) (94). The phosphorylation of 4E-BP by mTOR allows the unbinding and activation of eIF-4E. Similarly, other eIF-family proteins are activated with the phosphorylation and activation of S6K by mTOR. These signaling cascades increase translation initiation rates and thus, overall protein synthesis.

Speculatively, one could assume during skeletal muscle atrophy the rates of protein synthesis would decrease due to the lack of loading stimuli. In this case you could also assume you would observe diminished mTOR signaling. However, results from You et al. revealed an increase in mTOR activity after 7 days of hind limb immobilization in mice (161). Similarly, in a mouse hindlimb unloading model, Liu and colleagues observed increased 4E-BP binding and decreased eIF-4E activation (decreased protein synthesis) after 3 days and diminished binding and enhanced eIF-4E activation (increased protein synthesis) after 14 days. These results may be due to a compensatory or safety

mechanism in which protein synthesis signaling is induced to protect or save the muscle tissue from wasting after prolonged periods of disuse. Furthermore, as noted previously, during muscle atrophy we observe a decline in normal muscle tissue morphology and function. With variation in protein synthesis during atrophy, it appears the degradation process accompanying muscle disuse and the associated atrophy may outweigh any countering protein synthesis that is occurring.

However, the balance of synthesis and degradation lies at the foundation of the muscle cell net protein status. Therefore, the synthesis status of muscle is still a heavily weighted component when considering atrophy. For example, when we observe increases in AMPK, signaled by reduced cellular ATP levels, the result is an associated inactivation of mTOR (110). Speculatively, reduced mitochondrial function results in decreased cellular ATP and the activation of AMPK with the inactivation of mTOR. This inactivation may further shift the balance of the muscle tissue towards an atrophic state, with the mitochondria organelle playing a key role.

**Mitochondria and TFAM**

Mitochondria are cellular organelles responsible for the production of energy in the form of ATP and are also being analyzed for their role in skeletal muscle health. These organelles are believed to be directly descended from pro-bacteria forming an endosymbiotic relationship with an original eukaryotic host cell, leading to the self-replicating nature of mitochondria we observe today (60). As mentioned previously, the three major factors involved in the catabolic and anabolic status of skeletal muscle can be

greatly affected by ROS. These reactive molecules are specifically implicated in the

abnormal changes of the above pathways during disuse-induced atrophy (102). While

there are many sources of intracellular ROS, the mitochondria organelles appear to be a

major source of a specific ROS called superoxide anion. Certain centers in the electron

transport chain may leak electrons, which can reduce oxygen molecules to form

superoxide anion (144). The rate at which this leaking of electrons can occur varies

during acute events as well as a during chronic events. Many pathological states,

including disuse-atrophy, are correlated with disproportionate superoxide anion

accumulation leading to excessive oxidative stress (14).

Excessive ROS will activate degradation and apoptotic pathways and must be

neutralized by antioxidants to prevent abnormal cellular degradation. In the case of

superoxide anion, dismutation can occur in the presence of a family of particular

antioxidants called superoxide dismutases (SODs). SODs will catalyze the reaction of

superoxide anion to hydrogen peroxide, which can then be further reduced to water in the

presence of glutathione peroxidase (144). SOD-1 typically catalyzes this reaction in the

cell cytosol while SOD-2 (also called mtSOD) does this in the mitochondria. The

presence of increased superoxide anion without the appropriate increase in SOD-2 could

result in the deleterious effects of oxidative stress in the mitochondria, and may be

specifically linked to mtDNA.

*MtDNA.* The maternal genetics create the mitochondrial lineage of most animals (17).

Upon fertilization, paternal mitochondrial DNA (mtDNA) is selectively degraded by a

mitochondrial endonuclease. Along with protease and autophagy mechanisms, this

degradation leads to mitochondria from the paternal side being effectively abolished, allowing for maternal mtDNA to replicate and normal development of the organism (163).

MtDNA is a double-stranded, circular genome located in the inner mitochondrial matrix of the organelle, compartmentally separate from the nuclear DNA of the cell. MtDNA is approximately 16.5 kilobases coding for 37 genes. Thirteen of these genes encode functional subunits of the electron transport chain which are essential for oxidative phosphorylation (OXPHOS) (12, 60). Twenty-two genes encode transfer RNAs while 2 genes encode ribosomal RNAs, all of which are involved in the synthesis of mitochondrial proteins. The remaining protein of the mitochondria requires nuclear DNA, cytosolic translation, and effective import into the organelle.

MtDNA is essential to maintain energy homeostasis in the organism. Defects in mtDNA are associated with a multitude of mitochondrial related diseases and phenotypes such as diabetes, cancer, aging, and cardiovascular disease (13, 60, 149)  While many diseases may not originate in the mitochondria, there may still be an element of mitochondrial dysfunction involved in the disease genesis or progression. Alterations in the mitochondrial genome change the morphology and physiology of specific tissues. In skeletal muscle, Gehrig et al. observed a fiber-type switching from type I and more oxidative muscle fibers towards type II and more glycolytic muscle fibers in humans with mitochondrial myopathy (42). This type of mitochondrial defect changes the form and function of skeletal muscle leading to variations in the predominant energy sources used, increased muscle weakness, and decreased muscle health by a loss of oxidative capacity. These abnormalities of mtDNA occur in a variety of ways including DNA methylation,

DNA variants, reactive oxygen species (ROS) interactions, and transcriptional machinery defects. The consequence of these issues affects mtDNA copy number availability and interrupts typical synthesis of proteins in this organelle (132). In the skeletal muscle of aging humans, increases in mtDNA mutations and decreases in mtDNA copy numbers has been observed (127) and is typically associated with decreases in muscle mass (atrophy) and function. If the synthesis of mitochondrial and OXPHOS proteins is disrupted by an abnormality or a decrease in mtDNA copy number, a decrement in the efficient production of ATP (147) and the overproduction of ROS occurs. This increase in ROS further associates with mtDNA and leads to greater mutation and degradation creating a disturbance in energy homeostasis and an increased potential for association with disease. Excess ROS is also implicated in the activation of protein degradation and apoptosis pathways in muscle through ubiquitin-proteasome and caspase pathways, respectively (129, 141). An unbalanced increase in these pathways is highly correlated to skeletal muscle atrophy (16) and depicted in *Figure 3*. Therefore, we conclude maintaining the mtDNA structure and mtDNA copy number to transcribe mitochondrial proteins are vital components of proper health and function in skeletal muscle.

*TFAM.* As indicated in the literature, the protein responsible for maintaining properly functioning mtDNA is mitochondrial transcription factor A (TFAM) (79). TFAM is a diversely operating protein playing a role in mtDNA transcription, organization, and maintenance. Lack of this transcription factor in systemic TFAM knockout mice resulted in severe mtDNA depletion and embryonic lethality (134). A 2004 study using a combination of TFAM overexpression and knockout mice reveals mtDNA copy numbers

**Figure 2. Disuse leads to atrophy.** Flow chart of connecting muscle unloading and disuse to net protein loss and atrophy indicating mitochondrial dysfunction and redox imbalance being associated with this process.

**FIGURE 2**
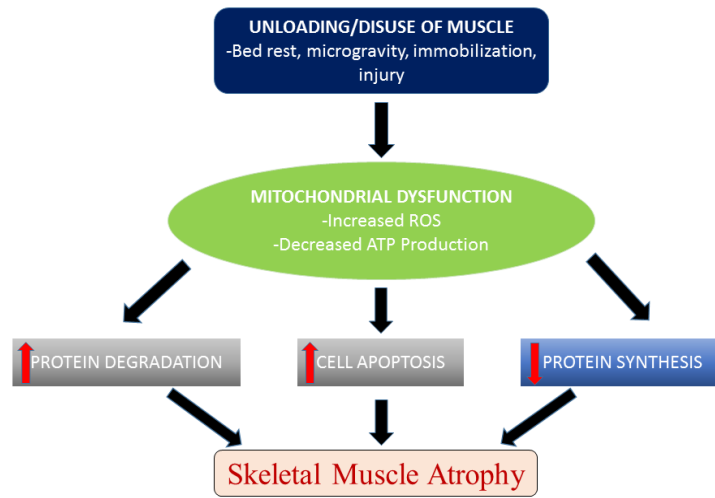
and embryonic lethality (134). A 2004 study using a combination of TFAM overexpression and knockout mice reveals mtDNA copy numbers are directly proportional to TFAM levels (31). Overexpression of TFAM in cardiac myocytes in a transgenic mouse model increased mtDNA copy number and diminished pathological hypertrophy after myocardial infarction. This subsequently led to an increase in survival rate (38). These studies provide evidence in an initial link between TFAM and mtDNA.

TFAM is a low molecular weight molecule (~25 kDa) with non-specific DNA binding properties encoded in the nucleus and transcribed in the cytosol as a pre-protein. From here, it is shuttled to the mitochondrion by a complex of cytosolic heat shock proteins (HSPs), HSP60 and HSP70, that act as protective chaperones and as a guide to locate the mitochondria. HSP protection prevents phosphorylation, promotes proper folding, and deters degradation during transport (79). The HSP60/HSP70 complex and attached pre-protein then bind to specific cytosolic receptors located on the translocase of the outer membrane complex (TOM) of the mitochondria, which serves as a main entry point for many mitochondrial proteins (107). The TFAM pre-protein will, next, pass from the TOM, through the intermembrane space, to a channel of the translocase of the inner membrane (TIM), specifically TIM23, using the selectivity of this complex for positively charged molecules (121). Entry into the matrix is achieved first by the binding of a mitochondrial heat shock-protein chaperone, mitochondrial HSP70, to TIM23 at a specific docking site (TIM44). TIM44-associated HSP70 causes conformational changes in HSP70 that either passively traps or actively pulls TFAM to the chaperone, as the precise mechanism is not completely understood (122). A mitochondrial processing peptidase (MPP) will cleave off the targeting sequence of the pre-protein on the matrix

side of TIM, while a chaperone, mtHSP60, along with mtHSP70, will re-fold the protein

into its mature form inside of the matrix (50). Again, in the inner mitochondrial matrix,

the mitochondrial heat shock protein complex mtHSP60/mtHSP70 serves as a protector

of TFAM from degradation. Specifically, the mitochondrial protease, LON, selectively

degrades oxidatively modified and improperly folded TFAM unbound to mtDNA (89).

After effective transport into the matrix, properly folded TFAM is able to come into close

proximity with mtDNA. The process of TFAM import is shown in *Figure 4.*

*TFAM binding: mtDNA transcription initiation and protection.* Free mtDNA and free

TFAM are both rapidly degraded in the matrix. As mentioned previously, mtDNA

interacting with ROS promotes a decrease in mtDNA copy number and unbound TFAM

is cleaved by Lon protease. TFAM interacting with mtDNA will form a protein-DNA

complex known as a mitochondrial nucleoid which prevents the degradation of each

component (70). This complex forms these nucleoid structures as TFAM binds and coats,

potentially, the entire mitochondrial genome. This provides the structural stability of the

mtDNA. Ekstrand et al. revealed that the levels of total TFAM were directly proportional

to the number of mtDNA copies in a mouse embryo model (31). Further, work done by

Larsson, et al., revealed that heterozygous TFAM depletion resulted in 35-40% decreases

in mtDNA copy numbers while homozygous TFAM depletion resulted in embryonic

lethality due to severe depletions of mtDNA copies and OXPHOS (82). These results

**Figure 3. TFAM import.** Process of mitochondrial import of TFAM. The process begins at number "1" in which TFAM mRNA is transcribed from nuclear DNA and ends at number "7" where TFAM binds mtDNA, protecting it from mutation.

FIGURE 3
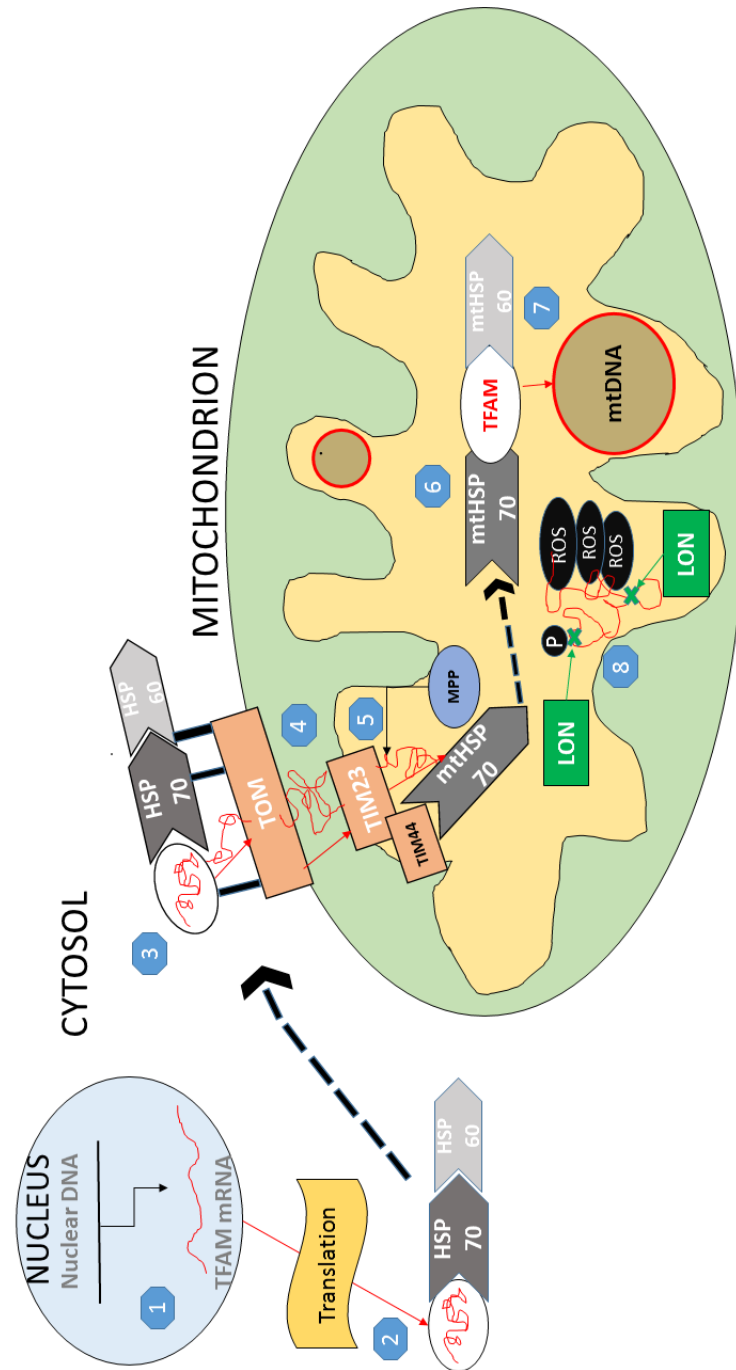
provide strong evidence of the correlation of TFAM and mtDNA and supports the role of TFAM preventing degradation of mtDNA.

TFAM will abundantly bind mtDNA both specifically and non-specifically. Two distinct promoter regions of mtDNA, light strand promoter (LSP) and heavy strand promoter 1 (HSP1), are bound by TFAM while other non-distinct regions of the mitochondrial genome are also able to bind. The specific binding of TFAM to these promoter regions activates transcription of the genome.

Specific binding of TFAM upstream of promoter sites induces bending of the genome and recruitment of transcriptional machinery. Two high mobility group-box domains (HMG-box A and HMG-box B) insert into grooves on the LSP, HSP1, or non-specific regions of mtDNA. These insertions cause distortion of the mtDNA and result in bending (100). Bending allows TFAM to interact with the transcriptional machinery, specifically mitochondrial RNA polymerase (POLRMT). POLRMT has sequence specific binding to TFAM and mtDNA promoter regions as well as upstream regions. This complex encourages binding of mitochondrial transcription factor B2 (TFB2M), resulting in a single RNA precursor in the mitochondrion and is the initiation of transcription (77). This process further advances to transcription elongation, transcription termination, initiation of translation, and translation elongation ultimately resulting in the synthesis of mature mitochondrial proteins (138). While the majority of mitochondrial proteins are nuclear encoded and require organelle import, intramitochondrial protein synthesis is still a highly necessary process to ensure proper function and maintenance of the mitochondrion and the OXPHOS system. TFAM is a key regulator of this process.

Interventions to improve mitochondrial dysfunction and promote normal function have been widely studied. Treatments include pharmacologic, nutritional supplementation, and exercise prescription. These treatments generally attempt to modulate one or more of the various signaling pathways involved in the creation of mitochondrial proteins, also termed mitochondrial biogenesis, to counteract dysfunctional effects (65, 84, 119). The effects of exercise specifically correlate with an increase in transcription factors of the mitochondria in skeletal muscle. A 90-minute bout of endurance exercise in mice increased nuclear encoded and mitochondrial encoded genes involved in mitochondrial biogenesis including key transcription factors and signaling proteins (119). Furthermore, a study inducing contractile activity of the rat tibialis anterior muscle by electrical stimulation revealed a significant increase in TFAM, a mtDNA regulatory protein. The stimulation increased TFAM mRNA levels after four days of stimulation while also increasing mitochondrial TFAM protein levels and mitochondrial specific enzymes after 5 days (44). This indicated TFAM expression is connected to the creation of new mitochondria with exercise. Thus, this project will emphasize the role of exercise in inducing mitochondrial biogenesis pathways associated with TFAM as a mechanism to preserve mtDNA and protect skeletal muscle tissue from atrophy.

## Exercise

Exercise enhances physical performance and is well known to be associated with many positive health benefits (155). A single bout of exercise causes a change in molecular expression in muscle that promotes specific adaptations. If the appropriate

duration, frequency, and intensity of contractile activity in muscle tissue occurs from physical exercise, specific signaling mechanisms will ensue, leading to the tissue adapting to the demand of the physical stress. Levels of circulating inflammatory markers, growth factors, and adrenergic compounds also increase during exercise. Exercise induces phenotypic changes of the muscle that include increased cross-sectional area, increased capillary density, fiber-type transitioning, and mitochondrial biogenesis resulting in increased mitochondrial density of the muscle cell (41, 159). This increased mitochondrial density is a part of an adaptive process allowing the organism experiencing the stress of exercise to increase functional proteins involved in the creation of energy (mitochondria and the OXPHOS system) to handle that specific stress in the future. A key component of exercise-induced mitochondrial biogenesis occurs via the effects of skeletal muscle contraction and the upregulation of TFAM (44).

For a skeletal muscle to contract, an action potential(s) must propagate from the motor cortex, through nerve fibers of the central nervous system, synapse at motor neurons located on the spinal cord down to the neuromuscular junction (NMJ). The signal must cross the NMJ and further propagate across the sarcolemma of the muscle and down into the t-tubules where voltage-gated dihydropyridine receptors (DHPRs) are able to interact with ryanodine receptors. Ryanodine receptor activation releases calcium from the sarcoplasmic reticulum (SR) into the cytoplasm of the muscle cell (115). From there, calcium can bind to troponin and remove tropomyosin from active binding sites of actin contractile proteins. Finally, in the presence of adequate ATP, muscle contractions can occur by the recycling of cross-bridging between myosin and actin proteins. During exercise, potentially high rates of this "excitation-contraction coupling" process occurs.

The release of calcium from the SR as well as the increased demand for ATP in this process leads to significant molecular changes within the cell.

The amount of cytosolic calcium released from the SR in skeletal myocytes during contraction not only depends on duration, frequency, and intensity of exercise of the muscle but also on the muscle fiber type. Isolated single muscle fiber calcium has been measured previously to be concentrated in the range of 30-50 nM. Upon stimulation, type I (slow-twitch) muscle fibers produced concentrations between 100-300 nM of calcium while type II fibers (fast-twitch) are capable of a drastically higher (~10x) 1-2 µM range (43). Baylor and colleagues report fast-twitch fibers capable of 3-4 times the amount of slow twitch (6). Nonetheless, cytoplasmic calcium concentrations in contracting fast-twitch muscle appear to be much greater than slow-twitch. This is important because specific types of exercise requiring higher relative intensities and perhaps longer relative durations recruit type II fibers at a greater rate than lower intensity exercise and disuse of the muscle (76). This leads to high levels of cytosolic calcium and increased intracellular signaling. Specifically, increased calcium activates calcium/calmodulin-dependent protein kinases (CAMKs) that are linked to increases in mitochondrial biogenesis (15, 19).

Increasing the intensity of physical activity also increases the AMP/ATP ratio in skeletal muscle (74, 153). As the previously described contraction process takes place and the cellular energy demand increases, the use of phosphate groups from ATP increases the amount of ADP and AMP, thus increasing the AMP/ATP ratio. AMP interacts with an AMP-activated protein kinase (AMPK) that is interrupted by high levels of ATP (48). The β-subunit of AMPK has a glycogen binding domain that, when bound,

inhibits the activation of AMPK (90). Exercise not only increases the AMP/ATP ratio but also depletes muscle glycogen, potentially releasing and activating AMPK. For these reasons AMPK is a cellular energy sensor and has been characterized as a "master switch" of metabolism (59). In response to exercise, activation of AMPK leads to downstream activators of mitochondrial biogenesis (8, 125).

Exercise will also acutely increase the levels of ROS in muscle (25). ROS has been implicated in many health disorders including muscle myopathies (95). The major contributors to ROS in skeletal muscle include xanthine oxidase (XO), NADPH-oxidases (NOXs), and mitochondria. In mitochondria, ROS production occurs due to electron leakage in the electron transport chain (ETC) (47). The ETC passes electrons through a series of protein complexes along the inner mitochondrial membrane with oxygen being the last acceptor of the electron. As oxygen accepts electrons in the ETC, it typically results in the formation of water. Oxygen that undergoes incomplete reductive processes results in radicals and the potential formation of ROS. Complex I and Complex III of the ETC appear to be the greatest contributors of ROS in the mitochondria. Although the precise contributions of each is poorly understood, these locations in muscle cells produce oxidants that are capable of negatively affecting cellular function while also activating potentially beneficial signaling pathways. An example of this was demonstrated in which male Wistar rat groups performed exercise and ate high antioxidant diets. The groups eating high antioxidant diets revealed decreased levels of mitochondrial biogenesis markers, regardless of exercise, indicating a potentially negative outcome of decreasing ROS signaling (135). The maintenance and balance of ROS through antioxidant defense systems and adaptations to the mitochondria are

important factors in skeletal muscle health and control potential mitochondrial biogenesis signaling.

Other major signaling mechanisms of exercise and mitochondrial biogenesis include the increased levels of inflammatory markers, epinephrine, and growth factors. Markers such as interleukins (IL-1,6) and tumor necrosis factor-alpha (TNF-α) bind cellular receptors and lead to increases in ROS production (73). Adrenal glands release epinephrine in response to exercise. Speculatively, this could be because of both the physical stress that is perceived as well as an emotional response that potentially occur during more intense forms of exercise, causing the release of epinephrine. Binding of epinephrine to β-adrenergic receptors of the cell lead to increases in cyclic AMP (cAMP), involved in biogenesis pathways. Growth factors such as insulin-like growth factor-1 (IGF-1) and insulin enter the cell and activate protein synthesis pathways, also implicated in the creation of mitochondrial proteins (93).

*Exercise and TFAM connection.* The various effects of skeletal muscle contraction and the stress of exercise connect to mitochondrial biogenesis in several ways. These upstream signals converge downstream to ultimately increase TFAM transcription. This convergence point is a major link of exercise to mitochondrial biogenesis and has received a great deal of attention in the literature and is known as the peroxisome proliferator-activated receptor-gamma coactivator 1-alpha (PGC-1α) and is activated in a multitude of ways (35, 105, 137).

PGC-1α is a transcriptional coactivator with formidable evidence of its correlation to exercise. Endurance exercise increases levels of PGC-1α in rat soleus muscle 18 hours post-exercise (137). Kang et al. subjected female Sprague-Dawley rats to anaerobic sprinting exercise and noticed a 5.6-fold increase in PGC-1α in the exercise group compared to the controls (68). Another group subjected rats to 20 minutes of aerobic treadmill running and increased PGC-1α mRNA levels 1.5-5 fold in soleus and gastrocnemius muscles while also noting 6 weeks of chronic exercise increased PGC-1α mRNA levels by ~25% in rat soleus muscle (10).

The aforementioned increase in cytosolic calcium with exercise activates CAMK which upregulates PGC-1α (15). CAMK is also a potent activator of myocyte-enhancer factor-2 (MEF2) (91). MEF2 is capable of binding to the nuclear promoter regions of the PGC-1α gene, enhancing its transcription (85). As AMP levels increase due to the demand of physical activity it interacts with AMPK, which also directly activates PGC-1α (125). ROS increases during exercise activate p38 mitogen-activated protein kinase (p38MAPK) that upregulates PGC-1α (3). ROS signaling also includes the activation of AMPK indirectly, although it is possible this is due to the decrease in ATP associated with stressful events (53). While ROS signaling leads to biogenesis of mitochondrial proteins, excessive ROS is detrimental to the cell. Furthermore, silent mating type information regulator 2 homolog (SIRT1) upregulation due to increased levels of nicotinamide adenine dinucleotide (NAD+) caused by exercise will deacetylate PGC-1α leading to its activation (131). Epinephrine released in response to exercise increases adenylyl cyclase leading to increased cAMP. A cAMP dependent protein kinase (PKA) activates with increased cAMP, and further interacts and upregulates cAMP response

element binding protein (CREB) that plays a role in PGC-1α upregulation. Growth factors (GFs) such as IGF-1 and insulin, as well as mechanical loading of muscle, activate mammalian target of rapamycin (mTOR), a major protein synthesis pathway that also promotes PGC-1α activation (21, 94).

PGC-1α is able to co-activate nuclear respiratory factors (NRFs), specifically NRF-1 and NRF-2, nuclear transcription factors responsible for activating many mitochondrial proteins (143). When this occurs, TFAM mRNA is transcribed from the nuclear genome by NRFs where it is able to be exported to the cytosol for translation, imported into the mitochondria, and maintain mtDNA and activate transcription of mitochondrial proteins (refer to *Figure 4*).

An exercise stimulus is a powerful metabolic signal, as shown above, that activates a multitude of signaling pathways in skeletal muscle leading to the transcription of TFAM, a key modulator of mitochondrial biogenesis. For these reasons, exercise and TFAM are attractive variables to study in skeletal muscle pathology. The above signaling pathways connecting these variables are summarized in *Figure 5*.

**Skeletal Muscle Protection**

Exercise induces a hormetic response in animals. That is, an appropriate dose of exercise over time leads to beneficial cellular adaptations to withstand the stress of exercise. This process of adaptation is at the essence of evolutionary biology. At extreme or high dosages, exercise can be toxic. When appropriate dosages of exercise are applied to an organism, the hormetic response plays a role in the prevention of pathological

**Figure 4. Exercise leading to TFAM.** Schematic representing multiple signaling pathways created by exercise converging on PGC-1α, which co-activates with NRF-1 and NRF-1. This coactivation results in the recruitment of transcriptional machinery to nuclear DNA, and ultimately transcribed TFAM mRNA. Through processes described above, translated TFAM is imported into the mitochondrion where it can interact with mtDNA.

FIGURE 4
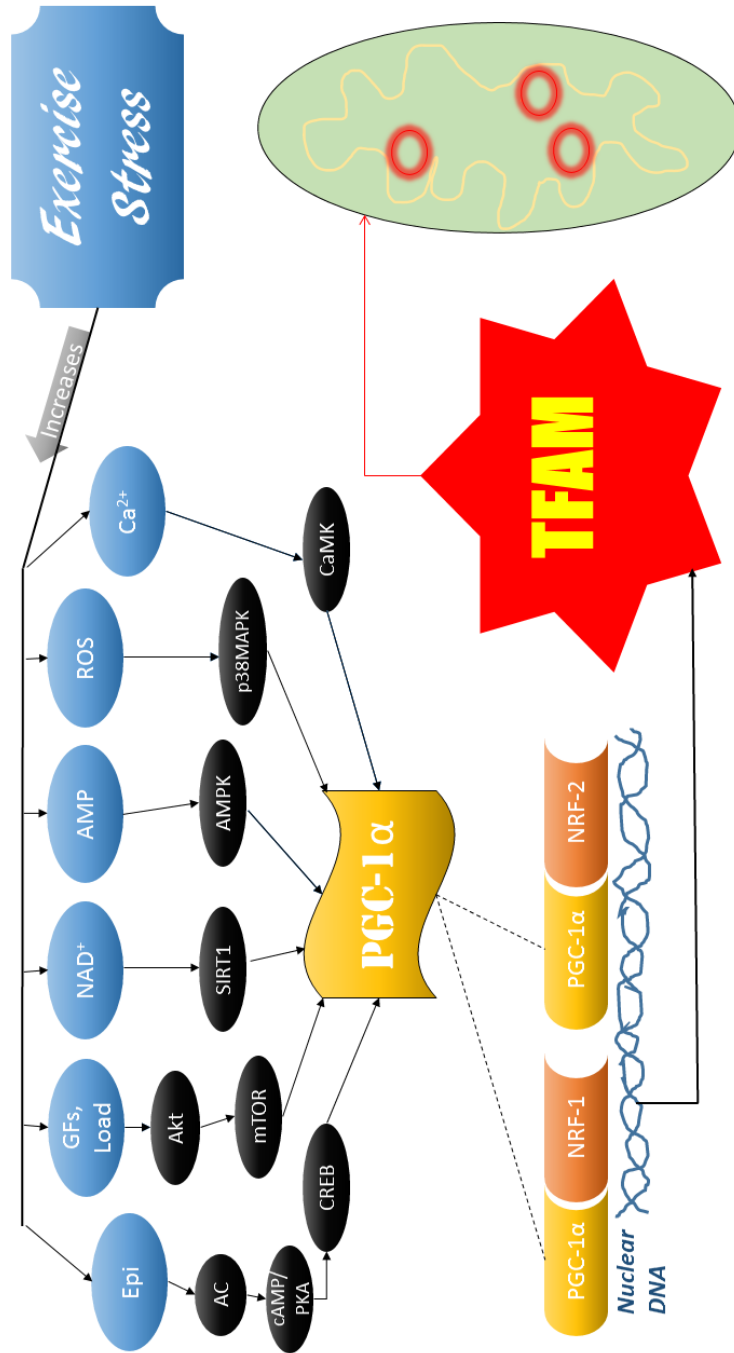
conditions. Exercise has been suggested to increase mitochondrial volume by up to 40% (87). This is due to factors of mitochondrial biogenesis being increased with exercise, signaling the increase in mitochondrial proteins to be synthesized (refer to *Figure 2*). In aging skeletal muscle, a rapid decline in muscle mass and muscle performance parameters are observed as are decreases in mitochondrial volume and biogenesis. Moderate exercise reverses or attenuates the decline in mitochondrial biogenesis markers and reduce the age-associated reduction in skeletal muscle mass (75). Although aging is its own respective form of skeletal muscle atrophy, this elucidates the idea that exercise is able to reverse the effects of atrophy through the induction of mitochondrial biogenesis.

The type of exercise, volume, intensity, and frequency as well as genetic capabilities of the organism will ultimately determine the extent to which muscle cells will adapt. Athletes that undergo intense physical exercise, especially endurance training, drastically increase the amount of mitochondrial proteins, antioxidant defense, and oxidative capabilities as an adaptation that more efficiently produces ATP to meet the demands of training. Those participating in lower levels of exercise and physical training will also increase mitochondrial proteins and efficiency (75), but generally to a lesser degree as stress is reduced and does not require higher levels of adaptation to meet the energy demand of the cell. With increased mitochondrial capabilities from exercise training, muscle cells will have a greater capacity to produce ATP and greater antioxidant scavenging enzymes (133). This adaptation allows the muscle cells to withstand larger levels of stress that would be incurred through physical training by a specific mechanism of reducing and neutralizing ROS. As stated previously, increased ROS activates many

pathways that cause skeletal muscle cellular proteins to be degraded, resulting in a net loss of protein over time and in the appearance of the negative effects of atrophy.

If the previously discussed processes that contribute to protein degradation, cell apoptosis, and variation in protein synthesis signaling in skeletal muscle atrophy are diminished during an atrophic setting, a reduction in atrophy is observed. Electronic stimulation of muscle tissue causing contraction throughout a 14 day hindlimb suspension protocol resulted in significant increases in soleus muscle mass compared to controls and to an increase in Bcl-2, preventing mitochondrial release of CytC and apoptosis (46). As we know, contractile activity, as occurs in exercise, also stimulates mitochondrial biogenesis and protein synthesis potentially leading to these results. The administration of branched chained amino acids (BCAAs) throughout a 14-day hindlimb suspension model of male Wistar rats diminished atrogin-1 and murf-1 protein expression and prevented a decrease in soleus mass (56). BCAAs are known to activate mTOR pathway signaling and protein synthesis while reducing degradation, resulting in the protection of muscle mass, while mTOR activation is implicated in mitochondrial biogenesis (*Figure 2*). In aging mice overexpressing catalase, a ROS reducing enzyme in the mitochondria, an improvement in muscle performance and lowered protein oxidation was observed compared to aged control mice indicating a crucial role for mitochondrial function protecting skeletal muscle (146).

The results above clearly indicate that different methods associated with improving mitochondrial function are capable of improving or preventing skeletal muscle loss during atrophy. A question that remains is whether or not the skeletal muscle can be protected from atrophy by interventions that occur prior to the atrophic setting?  The

abundance of evidence suggesting a correlation between mitochondrial dysfunction and atrophy indicate it may be beneficial to target mitochondrial biogenesis to mitigate excess ROS and alleviate the dysfunction of mitochondria and the efficiency of ATP production as a mechanism to diminish the processes of atrophy. If the muscle cells' adaptations can be sustained for any significant time during a period of unloading, atrophy may be at least diminished.

Fujino et al. analyzed soleus muscle mass in rats after 1 session of endurance exercise prior to HLS. This group exercising for one session prior to suspension trended higher than the suspension group without exercise in soleus muscle mass, although no significant differences were determined (37). These authors also noted a reduction in MHC I, a slow myosin heavy chain, protein expression after 14 days of HLS while the exercise prior to HLS group trended higher but not significantly. However, one exercise session may not be sufficient stress to induce adequate adaptive changes to provide significant protection of the muscle over an HLS protocol. A typical beginner exercising animal generally will not exercise completely during its first session, as it has not become familiarized to the procedure. Multiple training sessions over time allow the animal to understand the demands of the procedure while also allowing an exercise protocol to be applied that emphasizes a progression over time, leading to a compounding and an increased level of adaptation. These heightened adaptations could be key in protecting the muscle from atrophy during unloading and disuse.

Another group used swimming exercise, 3 sessions a week for 4 months, on female Wistar rats before immobilizing a hindlimb for 14 days to assess the effect of exercise on rehabilitation of atrophied skeletal muscle. The exercise prevented loss of

soleus muscle mass compared to rats that did not exercise. A feature of the present study was the use of swimming exercise, common in rehabilitation programs, as it does not load particular areas of the body that were injured previously while still allowing the muscle to contract. This also disallows increased mechanical loading that would be experienced in land based exercise, potentially providing different results. Furthermore, 4 months of exercise training may be difficult to retain adherence in humans. The question regarding shorter training protocols used to prevent muscle loss remains. Although this study used an immobilization protocol to induce atrophy, it does indicate a possible role of exercise in preventing atrophy during acute disuse.

*TFAM and skeletal muscle protection.* Mitochondrial biogenesis and function require TFAM to protect mtDNA from ROS and degradation while activating mtDNA transcription of specific proteins. TFAM proteins precede activity of mitochondrial biogenesis. Electrical stimulation of rat muscle at 10 Hz for 3 hours/day resulted in an initial 55% increase in TFAM by day 4 of stimulation. This was followed by a significant import of TFAM into intermyofibrillar mitochondria by day 5 and 7 and increased import protein machinery content. Further, by day 7 TFAM binding to the mitochondrial promoter increased 49%, the mitochondrial transcript cytochrome c oxidase (COX) III subunit protein content increased 65%, and COX enzyme activity increased by 72% (44). This study reveals a time schedule of TFAM preceding mitochondrial biogenesis processes and the intricate role TFAM plays in mitochondrial biogenesis that occurs during skeletal muscle contractile activity. Contractile activity occurs in exercise, and thus, the data of this study promotes further connection of TFAM and exercise.

Exercise creates an internal environment producing many signals inducing mitochondrial biogenesis. The activation of PGC-1α is of particular importance, as it is a convergence point of many of the signaling cascades activated by exercise. Kang et al. overexpressed PGC-1α in the tibialis anterior muscle of mice through in vivo transfection before immobilizing a randomly selected hindlimb for 14 days followed by 5 days of remobilization creating an acute period of unloading and disuse of the musculature. After 7 and 14 days of immobilization, control mice revealed a steady decline in PGC-1α and TFAM mRNA expression levels. PGC-1α overexpression resulted in a decrease in ROS, increase in mitochondrial functional markers, and reduction in inflammatory markers after immobilization and remobilization of the muscle. There was also an increase in mtDNA and mitochondrial density. This resulted in the preservation of soleus muscle mass after remobilizing previously immobilized muscle (69).

Cannavino et al. noted reductions in PGC-1α and mitochondrial complexes after 7 days of hindlimb unloading in mice. This reduction was associated with soleus skeletal muscle atrophy. The group further overexpressed PGC-1α in a transgenic mouse model and subjected these mice to a similar 7 days of hindlimb unloading. The overexpression of this gene prevented catabolic systems, reduced ROS, retained oxidative metabolism, and protected soleus muscle mass from atrophy caused by hindlimb unloading (14).

With the increase in TFAM being a downstream product of upregulating PGC-1α, the results of increased mtDNA copy number, mitochondrial density, and mitochondrial function are expected. Here we see creating a condition, i.e. overexpressing PGC-1α, correlating with TFAM and mitochondrial biogenesis prior to an atrophic protocol in skeletal muscle resulting in the protection of muscle. With TFAM being transcribed in

direct response to increased PGC-1α, the question of the importance of TFAM overexpression alone in skeletal muscle protection remains. The use of TFAM transgenic mouse models in the analysis of disuse-induced skeletal muscle atrophy has, to the best of our knowledge, not been previously shown. However, while the research using TFAM manipulations are scarce, there is data available to begin to analyze the effects of TFAM changes in different areas.

A germ line disruption of the mouse TFAM (TFAM $^{-/-}$) gene leads to extreme decreases in mtDNA and embryonic lethality (111). Nishiyama and colleagues mated transgenic mice overexpressing TFAM with mice of a mitochondrial disease model containing mutant mtDNA. This resulted in the amelioration of mitochondrial disease and prolonged lifespan by increasing mtDNA copy number due to the effects of overexpressing TFAM (101). A 2004 study using a combination of TFAM overexpression and knockout mice reveals mtDNA copy numbers are directly proportional to TFAM levels (31). These studies establish highly specific correlations between TFAM, mtDNA, and potential pathology.

A mouse model with skeletal-muscle specific disruption of TFAM leads to mitochondrial myopathy, ragged-red fibers, reduced muscle force, abnormal mitochondrial shape, and decreased respiratory chain activity (157). Iyer et al. report an *in vivo* treatment with recombinant TFAM results in increased motor endurance and complex-I respiration in mice (54), with both studies linking TFAM directly to skeletal muscle health decrements and reduced mitochondrial function. However, treating specific pathological conditions using TFAM overexpression are scarce.

Fujino et al. overexpressed a recombinant form of human TFAM (rhTFAM) in cultured cardiac myocytes. This rhTFAM rapidly entered the mitochondria and increased mtDNA copy number. Electron transport chain proteins (COX I and COX III) were elevated, as they are mtDNA encoded while nuclear DNA encoded proteins were not significantly elevated. Overexpression of rhTFAM also attenuated pathological hypertrophy by blocking the activation of nuclear factor of activated T-cells protein, known to induce pathological hypertrophy in cardiac myocytes (38). Again, the data shows a correlation between mtDNA copy number and attenuating pathology with this example being in cardiac muscle cells, implicating the possibility of TFAM overexpression in the treatment of mitochondrial related pathologies in skeletal muscle cells.

Similarly, Ikeda et al. used transgenic mice overexpressing TFAM in a volume-overload induced heart failure model to observe the effects of upregulated TFAM on cardiac muscle after myocardial infarction. TFAM mice exhibited improved cardiac function, diminished pathological hypertrophy, and a reduction in cardiac muscle ROS compared to control, heart failure mice. Mitochondrial enzymatic activity did not decline in the TFAM model, as is seen with the control heart failure mice. This group also used rat isolated cardiomyocytes to show an increase in mitochondrial ROS resulted in an increase in harmful, degrading proteinases (metallomatrix proteinases, specifically MMP-2 and MMP-9). Myocytes overexpressing human TFAM resulted in increased mtDNA copy number and a suppression of mitochondrial ROS and proteinase activity (51). The results of this study indicate TFAM increases mtDNA copy number in cardiac muscle

while also limiting oxidative stress. This also implicates a potential use in skeletal muscle to treat ROS-induced pathological conditions, such as atrophy.

Ikeuchi's group induced heart failure via myocardial infarction after ligation of the left coronary artery in wild-type and TFAM transgenic mice. TFAM mice had an attenuation of left-ventricular remodeling and failure as well as no reduction in mitochondrial complex activity compared to wild-type mice. Furthermore, TFAM mice had a higher survival rate compared to wild-type even with similar infarct sizes. Results here provide further evidence in the potential use of TFAM to treat pathological conditions in muscle tissue.

*Summary.* The literature discussed above shows that exercise induces mitochondrial biogenesis and function, efficient mitophagy, and increases the cell's ability to create ATP and neutralize ROS. These adaptations have been shown to reduce cell apoptosis, increase growth and protein synthesis signaling, and decrease protein degradation pathways. Beneficial changes such as these are all in opposition to the disuse-induced skeletal muscle atrophic state. Therefore, multiple questions are raised given these premises: Will exercise training as a treatment prior to a disuse-induced atrophic scenario provide a protective benefit to skeletal muscle?; and if so, is the protective mechanism associated with changes in markers of mitochondrial biogenesis and function? Furthermore, the above literature also reveals protective effects of PGC-1α during disuse-induced atrophy and shows beneficial effects of TFAM overexpression in cardiomyocytes during pathological scenarios that creates further research questions: If a major molecular signaling mechanism to transcribe TFAM is via PGC-1α, then will

overexpressing TFAM provide a similar protective benefit to skeletal muscle during an atrophic scenario?; If overexpressing TFAM is beneficial in cardiomyocytes, will the same benefit occur in skeletal muscle during disuse-atrophy? Finally, if both TFAM overexpression and exercise protect skeletal muscle, will combining both treatments have a synergistic effect? These research questions derived from evidence in the literature led to the development of multiple studies to attempt to address if exercise and TFAM prevent skeletal muscle atrophy. Refer to *Figure 5* for a summary schematic of the proposed research.

**FIGURE 5. Summary figure.** A graphical representation of what this project intends analyze: 1. This project intends to observe if exercise prior to a disuse-induce atrophic event will prevent atrophy.; 2. With exercise knowingly increasing PGC-1α and TFAM, will these mechanisms be associated with redox balance that, when imbalanced, has been previously shown to induce degradation and apoptosis as a mechanism of exercise-preconditioning preventing atrophy?; and 3. We intend to highlight the TFAM pathway through TFAM overexpression to see if this molecule is associated with redox balance and reduced atrophy.
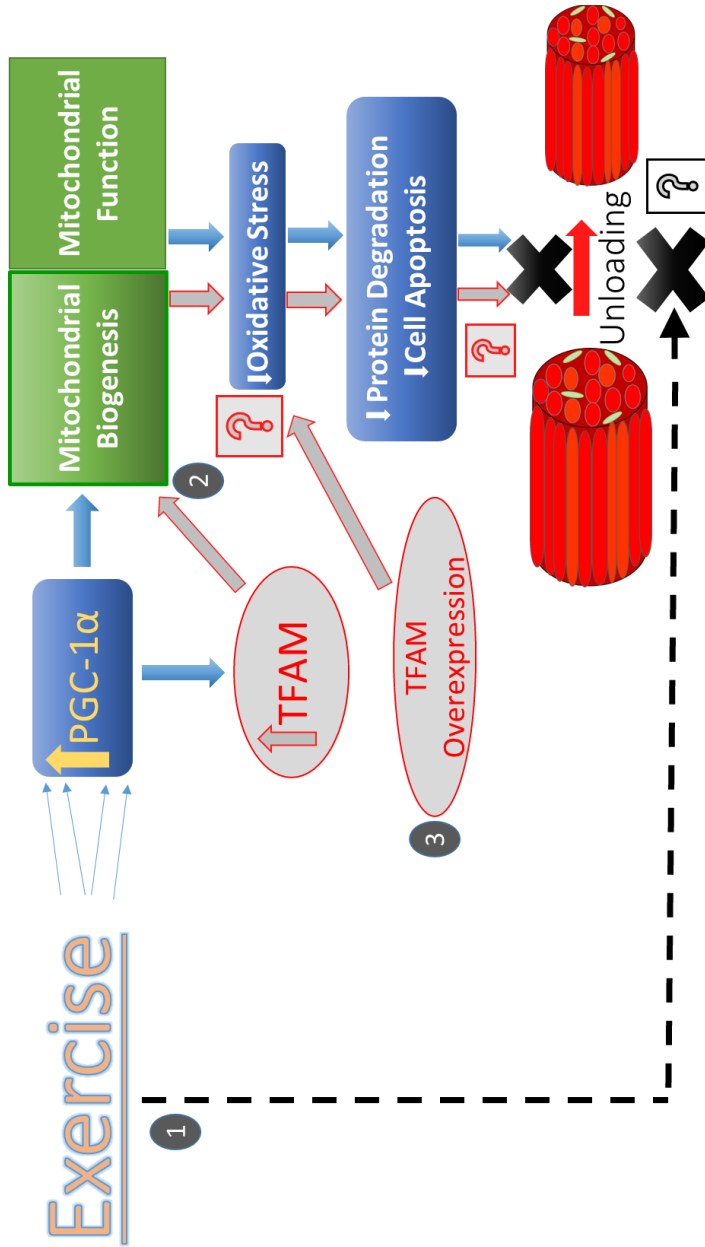
FIGURE 5

CHAPTER II

EXERCISE PRECONDITIONING DIMINISHES SKELETAL MUSCLE ATROPHY

## **Introduction**

Skeletal muscle atrophy results in the reduction of skeletal muscle mass and is associated with a decrease in health and quality of life. As muscle mass declines, the ability to perform physical tasks is greatly reduced leading to decreased independence and increased factors of morbidity and mortality (113). The study of associated molecular pathways is of great importance to understand this condition and guide research in the development of future therapies.

One cause of skeletal muscle atrophy occurs during prolonged mechanical unloading and disuse of muscle. This can be due to scenarios such as microgravity, sedentary lifestyle, bedrest, limb immobilization, and spinal cord injury. Ultimately, each of these scenarios encompass a lack of mechanical stress and muscle fiber contraction. Profound losses of skeletal muscle may occur under these conditions. As an example, many orthopedic injuries and non-orthopedic diseases require bedrest or body immobilization around the site of injury. An atrophy rate of approximately 0.5% of total muscle mass per day has been reported in the first 2-3 weeks under disuse atrophy

conditions (161). Therefore, the need to develop therapies to maintain skeletal muscle tissue when entering these settings is worth investigation.

Atrophy caused by unloading and disuse is characterized by reductions in size, weight, and function of the tissue (140). When this occurs, molecular changes leading to the net loss of functional protein in muscle tissue are observed. Moreover, previous data indicates correlations between muscle atrophy, mitochondrial dysfunction, and increased oxidative stress (102, 127). It is well established that excessive reactive oxygen species (ROS) observed during muscle atrophy activates protein degradation and cell apoptotic pathways while decreasing protein synthesis resulting in a net protein loss (22, 64, 97). Similarly, past research reveals ROS also damages functional components of the mitochondria leading to reductions in physiologic processes and mitochondrial dysfunction. More specifically, excessive ROS mutates unprotected mtDNA leading to the translation of defective mitochondrial proteins resulting in mitochondrial dysfunction (156).

Exercise is a powerful stimulator of mitochondrial function (128). On the molecular level, exercise activates the master regulator protein of mitochondrial biogenesis, peroxisome proliferator-activated receptor gamma coactivator 1-alpha (PGC-1α), via signaling cascades of acute and immediate changes in circulating and cellular molecules a part of the exercise response such as epinephrine, growth factors, AMP, and $Ca^{2+}$ (118). This master regulator co-activates with nuclear-respiratory factors 1 and 2, increasing the transcription of mitochondrial transcription factor A (TFAM), a well-known marker positively correlated with mtDNA copy number and mitochondrial function (148).

While many studies exist analyzing intra- and post-atrophic setting interventions to alleviate atrophy, the development of therapies to prevent these negative changes prior to a setting of unloading and disuse is scarce. When entering a known atrophy-causing scenario, such as prescribed bedrest or immobilization after elective surgery, being able to intervene physical or molecularly directed treatments to prevent muscular atrophy could be extremely beneficial for patient quality of life and in reducing financial burdens by mitigating medication and rehabilitation costs.

In a previous review of skeletal muscle atrophy, we proposed a protective effect of exercise prior to an atrophic setting and potential molecular mechanisms associated (140). Therefore, in the current study we hypothesize exercise training prior to skeletal muscle unloading and disuse will increase mitochondrial markers and protect skeletal muscle from atrophy. To test this, we use a 7-day hindlimb suspension (HLS) protocol to induce muscle atrophy in the hindlimbs of mice compared to mice performing an 18-day exercise protocol prior to 7 days of HLS. Results indicate exercise increases mitochondrial markers prior to entering HLS and this preconditioning is associated with the prevention of skeletal muscle atrophy post-HLS. Exercise is an attractive therapy to intervene prior to disuse settings.

**Methods**

*Animals and ethical approval.* The present study used male C57BL/6J mice (WT). Four groups of wild-type mice (WT) were used including a control, hindlimb suspension (HLS), exercise prior to hindlimb suspension (Ex+HLS), and exercise only (Ex). Mice were sacrificed immediately after HLS treatments and within 48 hours of exercise only treatments. The mice exercising before suspension were placed in HLS during the same

day of their last exercise session. All mice were 13±1 weeks of age at the time of

sacrifice. The mice were purchased from Jackson Laboratory (Bar Harbor, ME) and all

standard procedures and experiments involving animals conformed with the National

Institutes of Health guidelines and were approved by the Institutional Animal Care and

Use Committee of the University of Louisville.

*Hindlimb suspension.* Mice were suspended by the tail in custom built cages to unload

the hindlimb musculature and induce atrophy for a period of 7 continuous days. Cages

were constructed as previously shown (36). Briefly, mice were first placed under

continuous isoflurane anesthesia while a harness was fashioned to the tail. The tail was

cleaned and surrounded with tape cross-sectionally. A 27-gauge needle cap was cut

down, as to be open on each end, to ~2 centimeters in length. A small hole was drilled

into the sidewall of the needle cap and a piece of nylon string was tied into a loop through

this hole. This cap was then placed on the tail and taped into place roughly 1/3 of the tail

length from the base. The nylon loop could then be attached to the roof of the cage,

suspending the animal's hindlimbs while allowing the forelimbs to bear weight and the

animal to move around the cage. Mice could also access food and water *ad libitum* in this

manner. Bodyweights were recorded before and after suspension.

*Exercise protocol.* Exercise consisted of 14 training sessions over 18 days of treadmill

running in a concurrent style. Mice were acclimated to the treadmill during the first four

sessions. The subsequent 10 sessions consisted of 6 endurance training style exercise

sessions and 4 high-intensity interval style exercise sessions. All exercise program details (*Table 1*) were matched between exercising groups.

*Laser Doppler.* Gastrocnemius arterial blood flow imaging was done for each group using a laser Doppler imaging system (*Moor FLPI, Wilmington, DE*) to assess flux of the hindlimb after treatments. Mice were first administered tribromoethanol based on bodyweight. The musculature of the left, lower hindlimb was then exposed, revealing the musculature of the leg. Each mouse was placed in a prone position and the laser was positioned 15 cm from the area of interest. The laser was site directed to a prominent vessel on the posterior hindlimb, superficial to the gastrocnemius. Recordings of flux were measured for 2 minutes and quantified.

*Tissue extraction and weight.* Soleus and gastrocnemius tissues were excised and separated from each leg in all experimental groups, washed with 50 mmol/L phosphate buffer saline (PBS) pH of 7.4, weighed individually, snap frozen in liquid nitrogen, and stored at −80°C until use. All methods and timings of tissue extraction were equated across all groups.

**Table 1. Exercise protocol.** Mouse concurrent treadmill exercise protocol consisting of a "Week 1" acclimation, followed by progressive training "Week 2" and "Week 3". Three days per week (M,W,F) consisted of endurance-style exercise while two days per week (T,TH) consisted of higher-intensity interval sprint style of exercise.

**TABLE 1**

| WEEK 1 | Monday | Tuesday | Wednesday | Thursday | Friday |
|---|---|---|---|---|---|
| **Warmup** | | 7m/min. for 50m | 7m/min. for 50m | 7m/min. for 50m | 7m/min. for 50m |
| **Work Rate** | OFF | 7m/min. | 8m/min. | 9m/min | 10m/min. |
| **Rest** | | 3min. off/100m | 3min. off/100m | 3min. off/100m | 3min. off/100m |
| **Distance** | | 300m | 300m | 300m | 300m |

| WEEK 2 | Monday | Tuesday-Sprints | Wednesday | Thursday-Sprints | Friday |
|---|---|---|---|---|---|
| **Warmup** | 7m/min. for 50m | 7m/min. for 50m | 7m/min. for 50m | 7m/min. for 50m | 7m/min. for 50m |
| **Work Rate** | 11m/min. | 15m/min. for 10m | 12m/min. | 17m/min for 15m | 13m/min. |
| **Walk Rate** | - | 7m/min. for 10m | - | 7m/min. for 15m | - |
| **# of Sprints** | - | 8 | - | 10 | - |
| **Rest** | 3min. off/100m | 5mins after 5 sprints | 3min. off/100m | 5mins after 5 sprints | 3min. off/100m |
| **Distance** | 350m | 160m | 375m | 300m | 400m |

| WEEK 3 | Monday | Tuesday-Sprints | Wednesday | Thursday-Sprints | Friday |
|---|---|---|---|---|---|
| **Warmup** | 7m/min. for 50m | 7m/min. for 50m | 7m/min. for 50m | 7m/min. for 50m | 7m/min. for 50m |
| **Work Rate** | 13.5m/min. | 18m/min. for 15m | 14m/min. | 20m/min. for 20m | 14.5m/min. |
| **Walk Rate** | - | 7m/min. for 15m | - | 5x-7m/20m; 6x-7m/10m | - |
| **# of Sprints** | - | 11 | - | 11 | - |
| **Rest** | 3min. off/100m | 5mins after 5 sprints | 3min. off/100m | 5mins after 5 sprints | 3min. off/100m |
| **Distance** | 450m | 330m | 500m | 380m | 550m |

*Immunofluorescence.* A portion of each muscle was cut cross-sectionally at the midbelly and immersed in tissue-freezing medium (Triangle Biomedical Sciences, Durham, NC, USA) in disposable plastic tissue-embedding mold (Polysciences Inc., Warrington, PA, USA). The tissue blocks were immediately frozen and kept at -80°C until use. 7-10 µm thick sections were obtained from each muscle using a Cryocut System (CM 1850; Leica Microsystems, Buffalo Grove, IL, USA). Tissue sections were placed on Poly-L-Lysine coated microscope slides (Polysciences, Inc., Warrington, PA, USA). Tissue sections were fixated in acetone for 20 mins, washed in 1X PBS-T solution, and were incubated with permeabilization solution (0.2 g Bovine Serum Albumin, 3 ul Triton X-100 in 10ml 1X PBS) for 1 hour at RT followed by another washing step with 1X PBS-T. The sections were incubated with primary antibody (anti-Laminin; Abcam, Cambridge, MA, USA) dilution of 1:200 overnight at 4°C. After washing with 1X PBS-T the slides were incubated with a fluorescently labeled secondary antibody (goat anti-mouse Alexa flour 594; Invitrogen, Waltham, MA, USA) with a 1:300 dilution for 1 hour at RT. After another washing step, slides were mounted with mounting medium and glass cover slips, then visualized using a laser scanning confocal microscope (Olympus Fluo View 1000; Center Valley, PA, USA). Cross-sectional area measurements were acquired using laminin images by hand tracing single, stained muscle fibers in ImageJ software (123).

*DHE Staining.* After excision, each muscle was cross sectioned in half, immediately placed in tissue-freezing medium (Triangle Biomedical Sciences, Durham, NC, USA), snap frozen and stored at -80°C until use. Samples were then sectioned on a cryostat, placed on slides, and in situ superoxide generation was evaluated in each cryosection with the

oxidative fluorescent dye dihydroethidium (DHE). Cryosections (10 μm) were incubated with DHE (2 μmol/l) in PBS. After washing, slides were mounted with mounting medium and a cover slip, then visualized using a laser scanning confocal microscope (Olympus Fluo View 1000; Center Valley, PA, USA).

*Protein Estimation.* Muscle tissue samples were bead-homogenized in ice-cold RIPA (1 mmol/L) buffer with PMSF and protease inhibitor cocktails (1 $\mu$L/mL of lysis buffer, Sigma Aldrich, St. Louis, MO). The samples were then centrifuged at 12,000 g for 20 min at 4°C. The supernatant was extracted and stored at −80°C until use. Protein estimation was measured by the Bradford-dye (Bio-Rad, CA) method in a 96-well microliter plate against a Bovine Serum Albumin (BSA) standard. The plate was analyzed at 594 nm in a Spectra Max M2 plate reader (Molecular Devices Corporation, Sunnyvale, CA).

*Western Blot Analysis.* Protein lysates (40 μg) were prepared and heated at 95°C for 5 min and loaded in an SDS polyacrylamide gel in running buffer and run at a constant current (75 Volts). Proteins were then transferred to a PVDF membrane overnight at 120 mA at 4°. After transferring, the membranes were blocked in 5% nonfat milk for 1 hour at room temperature followed by overnight incubation with primary antibodies (Anti-PGC-1α, Anti-TFAM, Anti-SMHC, Anti-CS; Abcam, Cambridge, MA, USA.) at 4°C. After washing with TBS-T buffer, membranes were incubated with secondary antibodies (horse radish peroxidase- conjugated goat anti-mouse, goat anti- rabbit IgG; Santa Cruz Biotechnology, Dallas, TX, USA) for 1 hour at RT with 1:5000 dilution followed by washing. The membranes were developed with an ECL Western blotting detection system

(GE Healthcare, Piscataway, NJ, USA) and all images were recorded in the gel documentation system ChemiDoc XRS (Bio-Rad, Richmond, CA, USA). The membranes were stripped with stripping buffer (Boston BioProducts, Ashland, MA, USA) followed by a blocking step with 5% milk for 1 hour at RT. After washing, membranes were incubated with anti-Gapdh antibody (Millipore, Billerica, MA, USA) as a loading control protein. PGC-1α and SMHC were visualized on the same gel while TFAM and CS were visualized on the same gel, due to size similarities. The data were analyzed by Bio-Rad Image Lab densitometry software and normalized to anti-Gapdh bands.

*Quantitative PCR.* To assess mRNA expression of different genes in skeletal muscle, RNA was isolated with TRIzol® reagent (Life Technologies, Carlsbad, CA, USA) according to manufacturer's instructions. The RNA quantification and purity was assessed by nanodrop-1000 (Thermo Scientific, Walthan, MA, USA). Aliquots (2µg) of total RNA were reverse-transcribed into cDNA using a High Capacity cDNA Reverse Transcription Kit (Applied Biosystems, Foster City, CA) according to the manufacturer's protocol. q-PCR was performed for different genes (PGC-1α, TFAM, CS, Myh4, Myh7, SOD-1, SOD-2), in a final reaction volume of 20 µl containing 10 µl of PerfeCTa SYBR Green SuperMix, Low ROX (Quanta Biosciences, Gaithersburg, MD), 6 µl nuclease free water, 2µl cDNA, 40 picomoles of forward, and reverse primers. All sequence-specific oligonucleotide primers (Invitrogen, Carlsbad, CA, USA) are presented in (*Table 2*). The data reported from q-PCR is represented in fold expression, calculated as the cycle threshold difference between control and sample, normalized with the housekeeping genes *beta actin* and *18s*.

**Table 2. Nucleotide sequence.** All forward and reverse primers for each examined gene.

TABLE 2

| Gene | Forward Nucleotide Sequence | Reverse Nucleotide Sequence |
|------|------------------------------|------------------------------|
| Myh7 | 5'- ATCAAATCATCCAAGCCAACCC | 5'- GAGGAGTTGTCATTCCGAACTG |
| Myh4 | 5'- TTGTGGTGGATGCTAAGGAGTC | 5'- GTACTTGGGAGGGTTCATGGAG |
| CS | 5' - CACTGTTGAGATGGACACACTG | 5' – TCCTGAAGTCTGCATCATGACT |
| SOD-1 | 5'- GAACCAGTTGTGTTGTCAGGAC | 5'- GCCTTGTGTATTGTCCCCATAC |
| SOD-2 | 5'- GGTCACAGTTTCACAGTACACC | 5'- TCACAGCCTTGAGTTACAGAGT |
| TFAM | 5' - GAGAGCTACACTGGGAAACCACA | 5' – CATCAAGGACATCTGAGGAAAA |
| PGC-1a | 5'- CTTTCTGGGTGGATTGAAGTGG | 5'- CTCAAATATGTTCGCAGGCTCA |
| Rn18S | 5'- CACGGACAGGATTGACAGATTG | 5'- GACAAATCGCTCCACCAACTAA |
| ß-actin | 5'- CCCTGAAGTACCCCATTGAACA | 5'- CACACGCAGCTCATTGTAGAAG |

*Statistical Analysis.* All data were expressed as means ± SE. One-way ANOVA analyses were conducted on each data set with Tukey's post-hoc analysis used between groups after significance was obtained. Significance was determined as a p-value<.05.

## **Results**

*Exercise diminishes loss of CSA and weight.* Wet muscle weight was measured immediately after excision. Muscle weights were standardized to bodyweight (mg/g) to account for individual size variation (*Table 3*). HLS resulted in a significant decrease (p=.001) of 27.1% in soleus muscle and a significant decrease (p=.001) of 21.5% in gastrocnemius muscle weight to bodyweight ratio compared to Control. Exercising prior to HLS resulted in only a 5.6% non-significant decrease (p=.50) in soleus muscle and an 8.1% non-significant decrease (p=.16) in gastrocnemius weight to bodyweight ratio (*Table 3*). Both the soleus and gastrocnemius Ex+HLS group ratios were significantly greater than the HLS group (p=.001 and p=.007, respectively). Furthermore, cross-sectional area (µm$^2$) differences followed a similar trend with HLS resulting in a significant decrease compared to Control (p<.01), while Ex+HLS and Ex groups were both significantly greater than HLS (p<.01) (*Fig. 6 and 7*).

*Hindlimb blood flow is not a limiting factor.* Laser Doppler imaging of the left hindlimb assessed blood flow through a prominent posterior limb artery superior to the gastrocnemius (*Fig. 8*). This measurement is a function of red blood cell (RBC) content and the velocity of RBCs through the vessel of interest. Changes in RBC content and velocity to peripheral tissues could account for variations in the tissue if oxygen and

**Table 3**. **Bodyweight and muscle weights.** Bodyweight (BW) pre-HLS (g) and BW at time of sacrifice. Muscle weight of both the soleus and gastrocnemius. All data presented as means ± SE. Statistical significance (p<.05) between groups indicated by the superscript letter associated with each particular group (a: Control, b: HLS, c: Ex+HLS, d: Ex).

**TABLE 3**

| Group | Pre-HLS BW (g) | BW (g) | Sol MW (mg) | Gas MW (mg) | Sol MW/BW (mg/g) | Gas MW/BW (mg/g) |
|---|---|---|---|---|---|---|
| Control | - | $24.5 \pm .55$ | $7.8 \pm .17$ | $121.1 \pm 6.1$ | $.32 \pm .007$ | $4.9 \pm .164$ |
| HLS | $23.3 \pm .87$ | $22.0 \pm .79$ | **$5.1 \pm .15$[a,c,d]** | **$85.4 \pm 5.5$[a,c,d]** | **$.23 \pm .008$[a,c,d]** | **$3.9 \pm .236$[a,c,d]** |
| Ex+HLS | $24.3 \pm .78$ | $22.4 \pm .67$ | **$6.9 \pm .33$[a,b,d]** | **$103.8 \pm 4.3$[a,b]** | **$.30 \pm .012$[d]** | $4.5 \pm .065$ |
| Ex | - | $23.5 \pm .22$ | $7.9 \pm .12$ | $110.7 \pm 4.3$ | $.34 \pm .003$ | $4.7 \pm .151$ |

**Figure 6. Soleus CSA. A.** Immunofluorescence laminin staining of soleus muscle fibers. All pictures are 200 µm in width. **B.** Cross-sectional area ($\mu m^2$) measurement acquired using ImageJ software (n=6). Statistical significance (p<.05) indicated by the corresponding group letter (means ± SE).

**FIGURE 6**

**A.**



Ctrl          HLS          Ex+HLS          Ex

**B.**



Fiber Cross-Sectional Area

a: Control    b: HLS    c: Ex+HLS    d: Ex
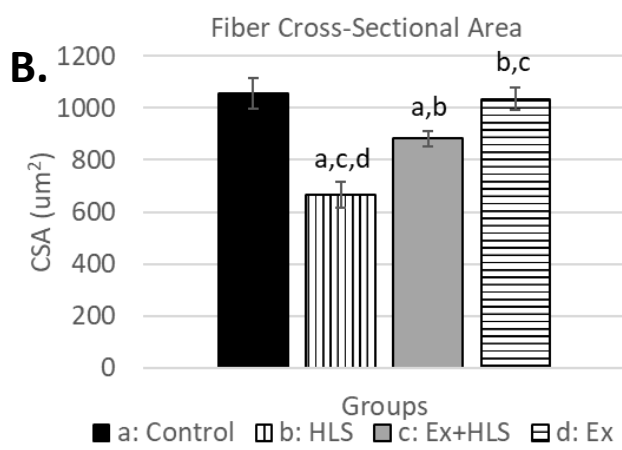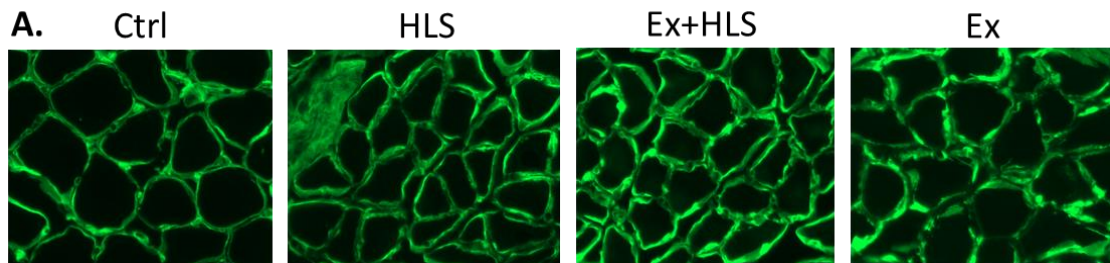
**Figure 7. Gastrocnemius CSA. A.** Immunofluorescence laminin staining of gastrocnemius muscle fibers. All pictures are 200 µm in width. **B.** Cross-sectional area (µm$^2$) measurement acquired using ImageJ software (n=6). Statistical significance (p<.05) indicated by the corresponding group letter (means ± SE).

**FIGURE 7**

**A.**



**B.**
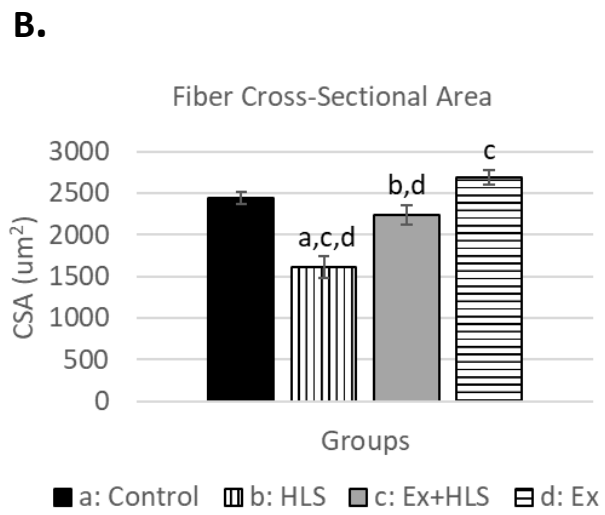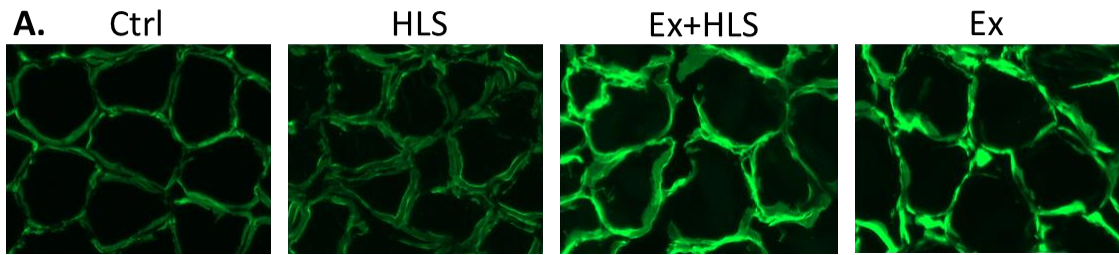
**Figure 8. Hindlimb blood flow. A.** Laser Doppler blood flow measurement of prominent vessel in the dorsal hindlimb. **B.** Blood flux measurement comparison between groups (n=6, p<.05). Statistical significance (p<.05) indicated by the corresponding group letter (means ± SE).

**FIGURE 8**
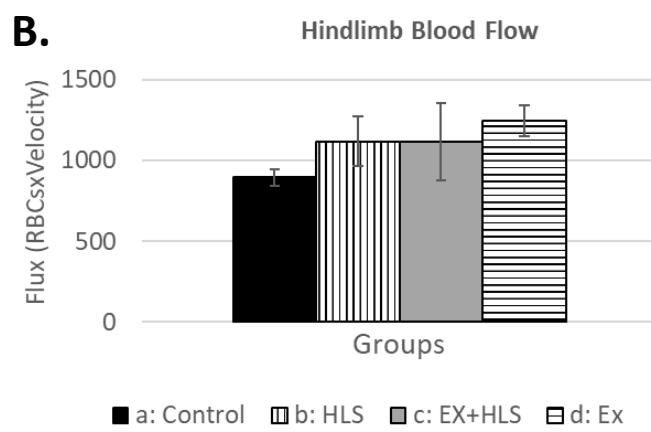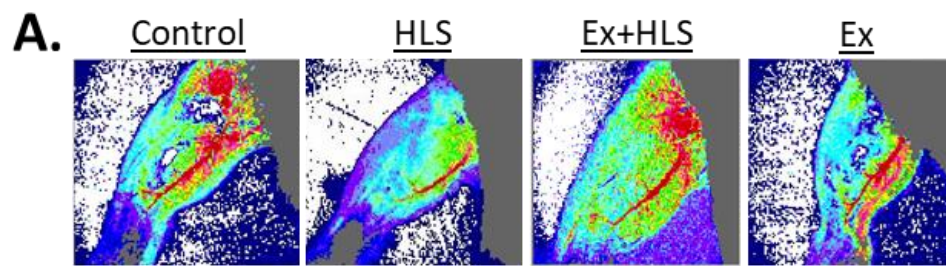
nutrient delivery along with waste removal are different between groups. Here we show while Ex tended to increase blood flow in this particular vessel, there were no significant differences between groups (p=.53).

*Exercise increases functional muscle protein.* According to Sliding Filament Theory, skeletal muscle contraction results from the cyclic interaction of actin and myosin molecules and the recycling of ATP (49). Loss of these protein molecules is an indicator of muscle atrophy and correlates with decreased fatigue resistance of the muscle (34, 57). HLS resulted in a no significant change in slow myosin heavy chain (SMHC) protein expression in the soleus muscle and a significant decrease in the gastrocnemius muscle (*Fig. 9 and 10*). However, exercise prior to HLS resulted in a significant increase in SMHC in the gastrocnemius compared to the HLS group (p<.05). Furthermore, exercise only significantly increased SMHC compared to controls in soleus (p=.014) and gastrocnemius (p<.01). Using qPCR, we followed up protein expression of SMHC with gene expression analysis of a slow myosin heavy chain gene, Myh7. In the soleus, Myh7 approached a significant decrease (p=.056) in HLS compared to Control (.94 vs. 1.1, respectively). In the gastrocnemius, Myh7 was significantly decreased in both HLS and Ex+HLS compared to Control and Ex with no difference being observed in the Ex group transcripts compared to control (*Fig. 10*).

Moreover, disuse of skeletal muscle and cessation of exercise training is associated with fiber-type transitioning from a slow, more oxidative muscle to a fast, more glycolytic muscle fiber-type composition (23). We therefore assessed the transcript levels of the faster, more glycolytic type IIb myosin heavy chain through qPCR analysis

**Figure 9. Soleus MHC analysis. A.** Soleus slow myosin heavy chain protein expression

(n=6). **B.** Western blot analysis of soleus SMHC. Statistical significance (p<.05) between

groups indicated by the corresponding group letter. **C.** Myosin heavy chain 7 (slow-

twitch muscle) gene expression analysis by qPCR. **D.** Myosin heavy chain 4 (fast-twitch

muscle) gene expression analysis by qPCR. (groups: n=6, p<.05, means ± SE)

**FIGURE 9**

**A.**



**B.**



SMHC Protein Expression

**C.**



Myh7 Gene Expression

**D.**



Soleus Myh4 Gene Expression
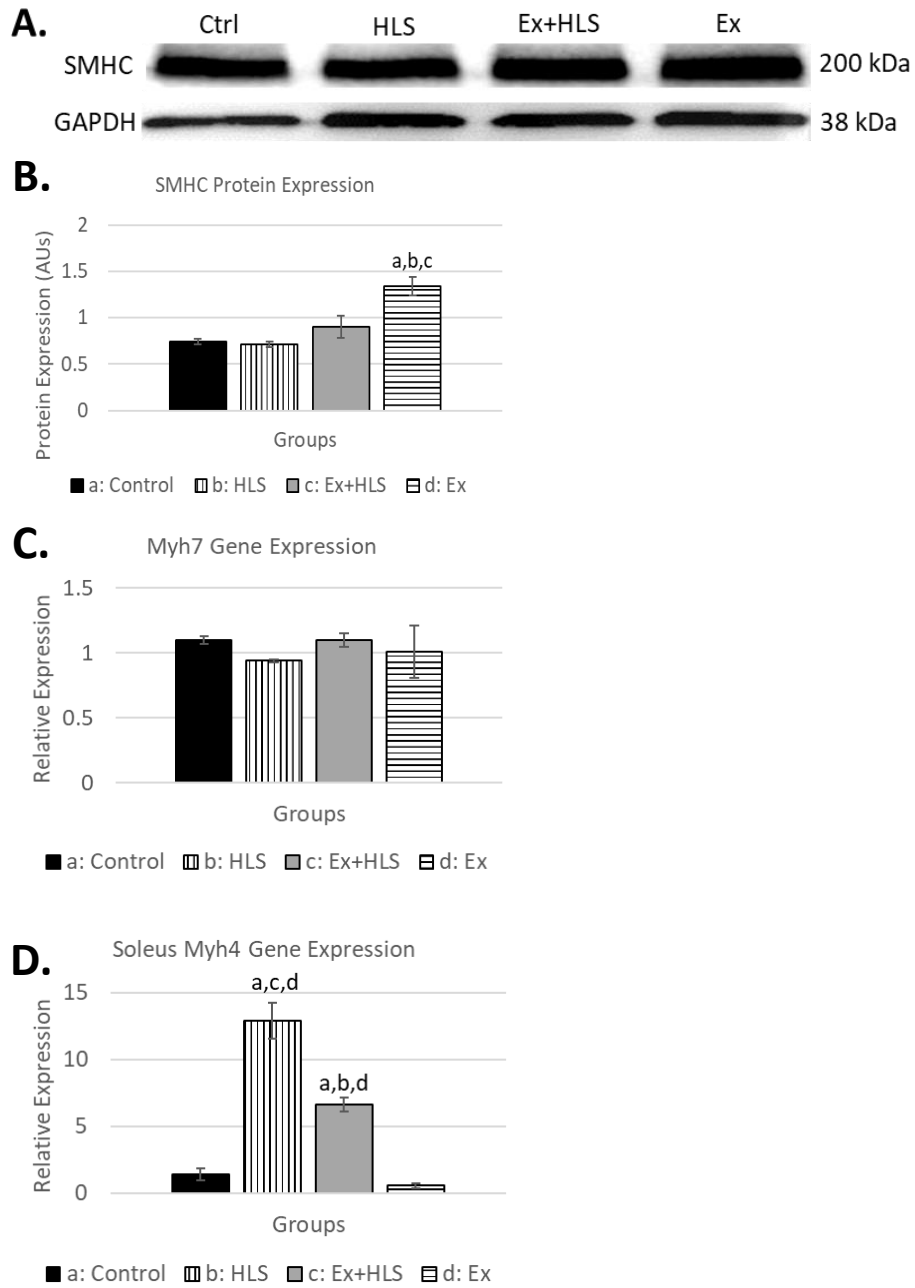
**Figure 10. Gastrocnemius MHC analysis. A.** Gastrocnemius slow myosin heavy chain

protein expression. **B.** Western blot analysis of gastrocnemius SMHC. Statistical

significance (p<.05) between groups indicated by the corresponding group letter. **C.**

Myosin heavy chain 7 (slow-twitch muscle) gene expression analysis by qPCR. (groups:

n=6, p<.05, means ± SE)

**FIGURE 10**

**A.**



**B.**



**C.**
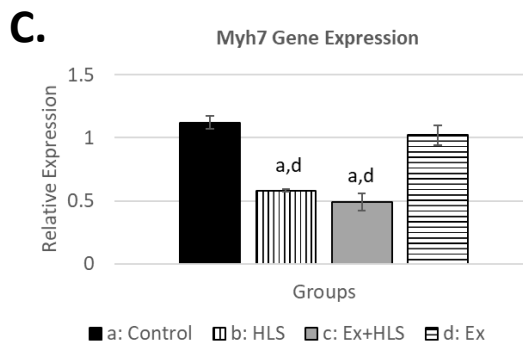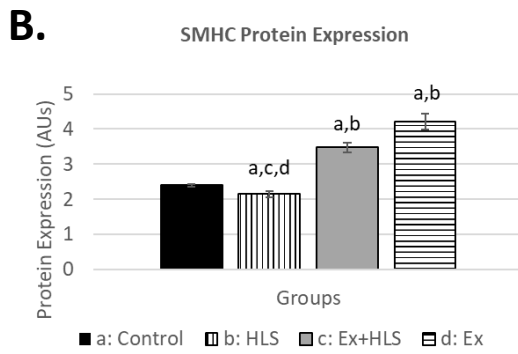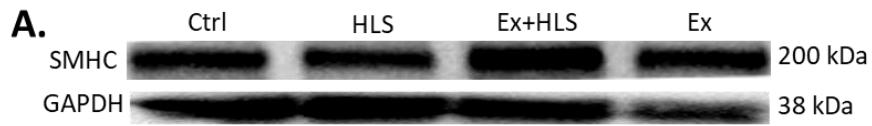
of the Myh4 gene. As expected, in soleus tissue HLS resulted in a significant increase in Myh4 mRNA compared to Control (21.34 vs 1.15, p<.01). Although Ex+HLS Myh4 transcript levels were significantly elevated from Control, results indicated less mRNA expression of Myh4 compared to HLS (p<.01) (*Fig. 9*).

*Mitochondrial markers increase with exercise.* Skeletal muscle atrophy is associated with mitochondrial dysfunction (86, 127). Markers of mitochondrial biogenesis and function were measured via qPCR and Western Blotting analyses to assess our hypothesis that exercise increases these markers which are correlated with the protection of muscle weight and size during HLS. To test this correlation, we assessed the transcript and protein expression of PGC-1α, TFAM, and CS.

In assessing mitochondrial biogenesis, we measured PGC-1α transcript expression to be significantly increased after the exercise protocol (Ex) in both soleus (*Fig. 11*) and gastrocnemius muscles (*Fig. 12*) compared to Control (2.3-fold and 1.6-fold, respectively). PGC-1α mRNA levels were significantly decreased in the gastrocnemius after HLS. The Ex+HLS group, while lower than Ex, was still significantly greater than HLS in the gastrocnemius (1.12 vs .87, p=.004). Transcript expression of PGC-1α between Control, HLS, and Ex+HLS in the soleus were not significantly different. Protein expression of PGC-1α in the soleus muscle (*Fig. 11*) was significantly greater in Ex compared to Control (p<.05) while HLS was significantly reduced (p<.05). Ex+HLS expression of PGC-1α was significantly greater than HLS alone (p<.05). In gastrocnemius muscle (*Fig. 12*), the Ex group revealed a nearly 2-fold increase in protein

**Figure 11. Soleus mitochondrial analysis. A.** Soleus protein expression via western blot of mitochondrial markers (SMHC/PGC-1α and TFAM/CS expression measured on same blots with same loading control, due to size similarities). **B.** Western blot analysis of soleus muscle mitochondrial markers. Statistical significance (p<.05) between groups indicated by the corresponding group letter. **C.** Gene expression analysis by qPCR of mitochondrial markers. (groups: n=6, p<.05, means ± SE)

**FIGURE 11**
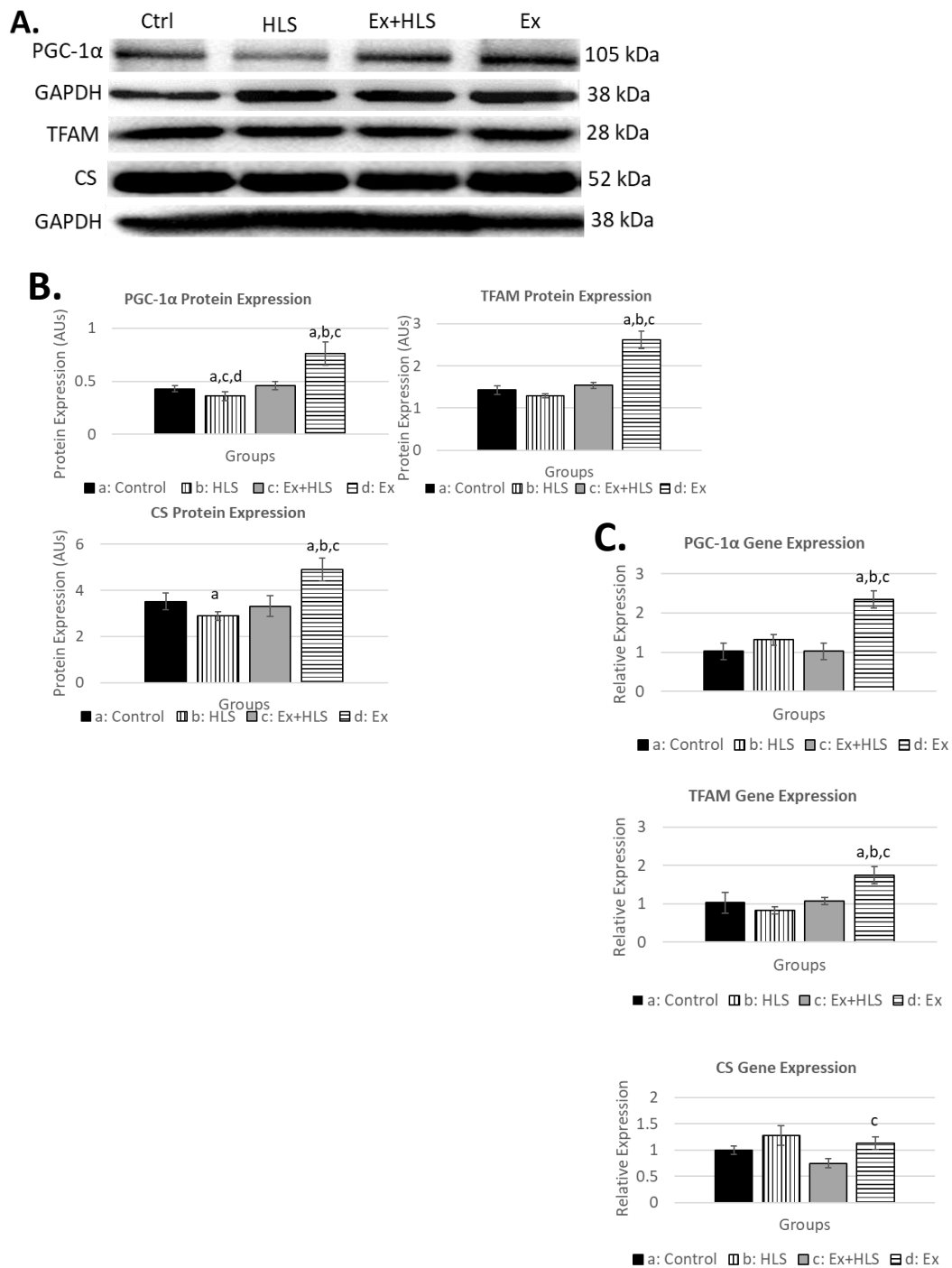
**Figure 12. Gastrocnemius mitochondrial analysis. A.** Gastrocnemius protein

expression via western blot of mitochondrial markers (SMHC/PGC-1α and TFAM/CS

expression measured on same blots with same loading control, due to size similarities). **B.**

Western blot analysis of soleus muscle mitochondrial markers. Statistical significance

($p<.05$) between groups indicated by the corresponding group letter. **C.** Gene expression

analysis by qPCR of mitochondrial markers. (groups: n=6, $p<.05$, means ± SE)

FIGURE 12
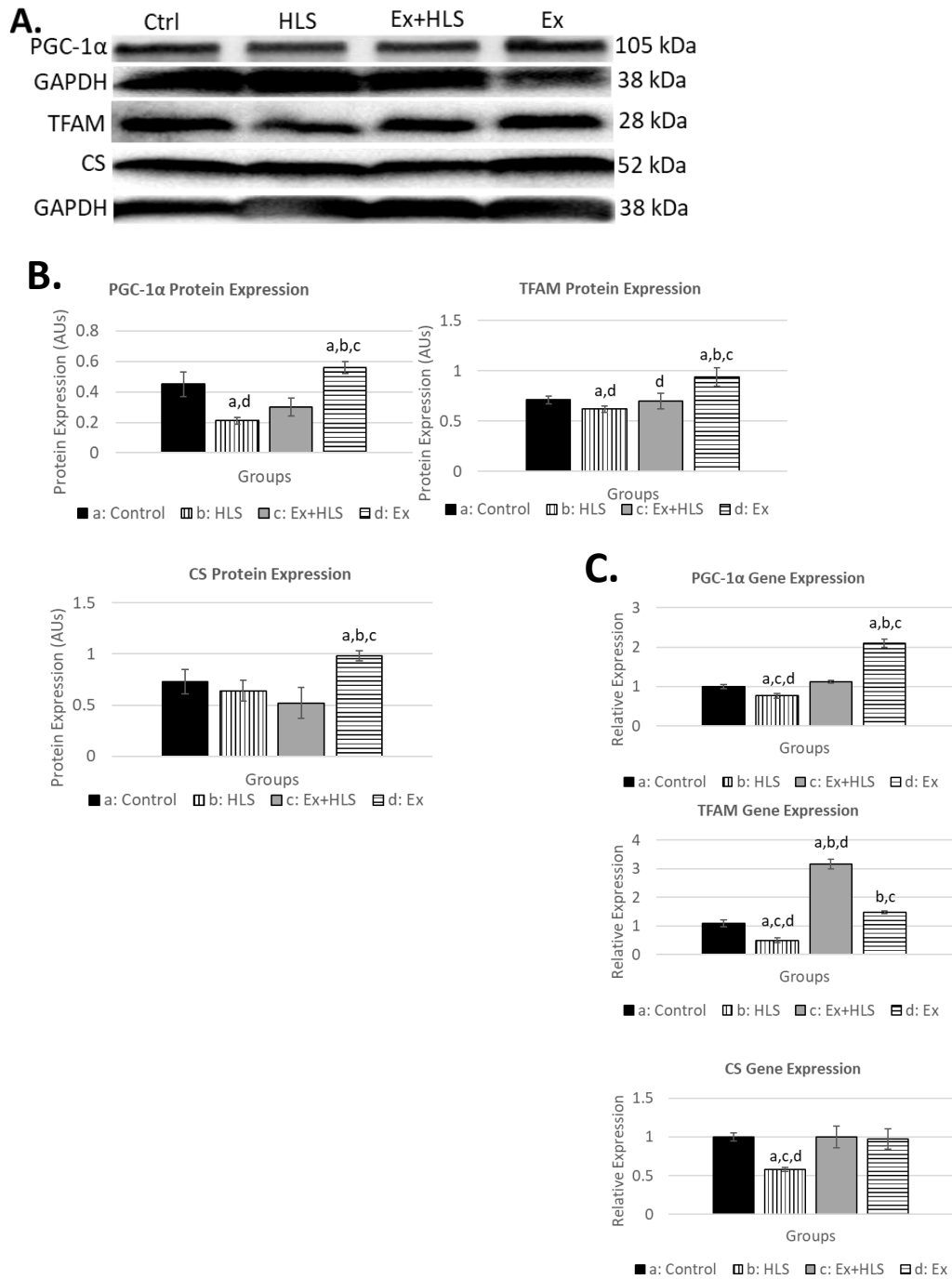
expression (p<.01). Furthermore, in gastrocnemius muscle HLS decreased PGC-1α compared to Control (p<.01). TFAM transcript expression significantly increased in the soleus (*Fig. 6*) and increased in trend in the gastrocnemius muscle (*Fig. 7*) after the exercise protocol (Ex) compared to Control (1.74 vs 1.03 [p<.05], 1.47 vs 1.09 [p=.30], respectively). Soleus muscle TFAM transcript levels were not significantly different between Control, HLS, and Ex+HLS (1.03 vs .83 vs 1.07, respectively) with Ex+HLS trending greater than HLS (p=.07). TFAM mRNA expression levels in the gastrocnemius significantly decreased after HLS (p=.016), with the Ex+HLS group being significantly greater than HLS (3.16 vs .49, p=.001). Protein expression of TFAM was found to be elevated in Ex compared to Control in both muscles (p<.05). HLS only resulted in no significant decrease in TFAM protein expression in the soleus and a significant decrease in the gastrocnemius (p<.05) (*Fig. 6 and 7*) compared to Control while TFAM of Ex+HLS was elevated significantly compared to HLS only in the gastrocnemius (p<.05).

Citrate synthetase is a tricarboxylic acid cycle enzyme catalyzing citrate from acetyl-CoA and oxaloacetate. It is a commonly used biomarker to assess mitochondrial function and density in skeletal muscle (151). Analysis of the mRNA expression in the soleus (*Fig. 6*) revealed greater CS expression in the HLS group compared to Ex+HLS (p<.05) with no differences between Control, HLS, and Ex groups. Soleus CS protein expression (*Fig. 7*) decreased in the HLS group compared to Controls (p<.05) while Ex+HLS trended greater than HLS but did not reach significance. Moreover, exercise increased CS protein in soleus muscle compared to all other groups (p<.05). In the gastrocnemius muscle (*Fig. 7*), CS mRNA transcripts were significantly reduced in HLS compared to control (.58 vs 1.01, p=.0001). Ex+HLS and Ex groups were not

significantly different compared to control but were both significantly greater than HLS (p<.05). Furthermore, Ex was significantly greater than HLS (p<.05). Protein expression of CS (*Fig. 7*) increased significantly in the Ex group compared to all other groups. However, there were no significant differences between Control, HLS, and Ex+HLS.

*Exercise prior to HLS may reduce ROS.* Reactive oxygen species are implicated in the induction of protein degradation and apoptotic pathways, potentially being an important contributor to the atrophic muscular condition (22). In order to visualize ROS accumulation, we used a dihydroethidium staining (DHE), solely as an observational assessment. DHE staining is commonly used to visualize ROS and in previous research is viewed as the least problematic and most specific ROS dye, due to its ability to easily permeate cell membranes and its specificity for superoxide anion (106). Observationally, there were clear differences between groups (*Fig. 13 and 14*). HLS, as expected, resulted in greater levels of ROS in both muscles. Ex+HLS appears to be reduced compared to the excessive positive staining for superoxide anion in the HLS group.

Superoxide dismutases are the main antioxidant defense system against superoxide anions (39). Therefore, we measured SOD-1 and SOD-2 (mitochondrial SOD) transcripts via qPCR and SOD-2 protein expression via Western blot to assess any differences between groups with these antioxidants. In the soleus we observed a

**Figure 13. Soleus ROS and antioxidants. A.** Observational soleus dihydroethidium staining for ROS. Bright spots are assumed to be positive staining for superoxide anion (n=6). **B.** Soleus protein expression via Western blot analysis for antioxidant enzyme SOD-2. Statistical significance (p<.05) between groups indicated by the corresponding group letter. **C.** Soleus SOD-1 and SOD-2 gene expression via qPCR. (groups: n=6, p<.05, means ± SE)

**FIGURE 13**



A. Control | HLS | Ex+HLS | Ex

B. SOD-2 / GAPDH western blot
Ctrl | HLS | Ex+HLS | Ex
SOD-2 — 26.6 kDa / 25 kDa
GAPDH — 38 kDa

SOD-2 Protein Expression

C. Soleus SOD-1 Gene Expression | SOD-2 Gene Expression
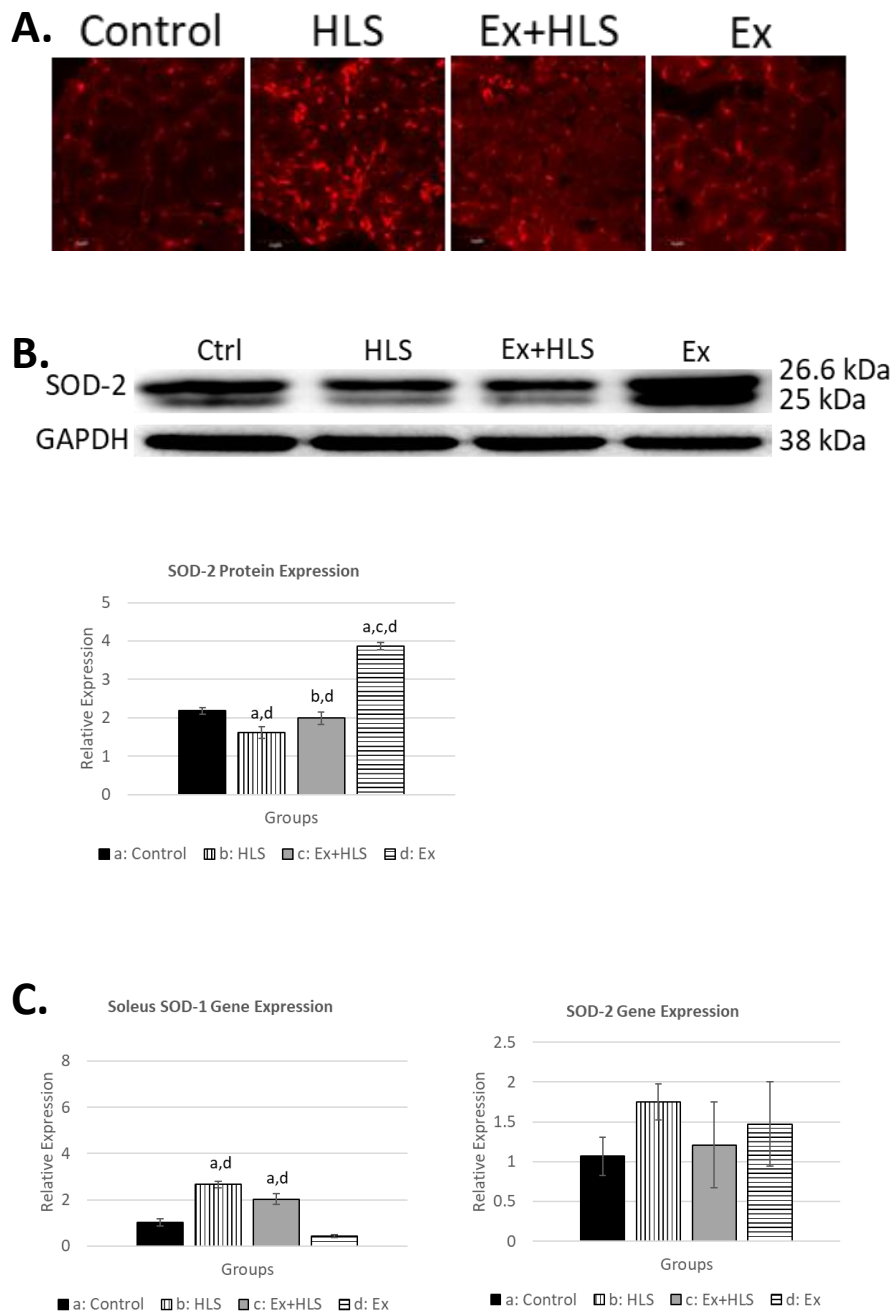
**Figure 14. Gastrocnemius ROS and antioxidants. A.** Observational gastrocnemius

dihydroethidium staining for ROS. Bright spots are assumed to be positive staining for

superoxide anion (n=6). **B.** Gastrocnemius protein expression via Western blot analysis

for antioxidant enzyme SOD-2. Statistical significance (p<.05) between groups indicated

by the corresponding group letter. **C.** SOD-1 and SOD-2 gene expression via qPCR.

(groups: n=6, p<.05, means ± SE)

**FIGURE 14**
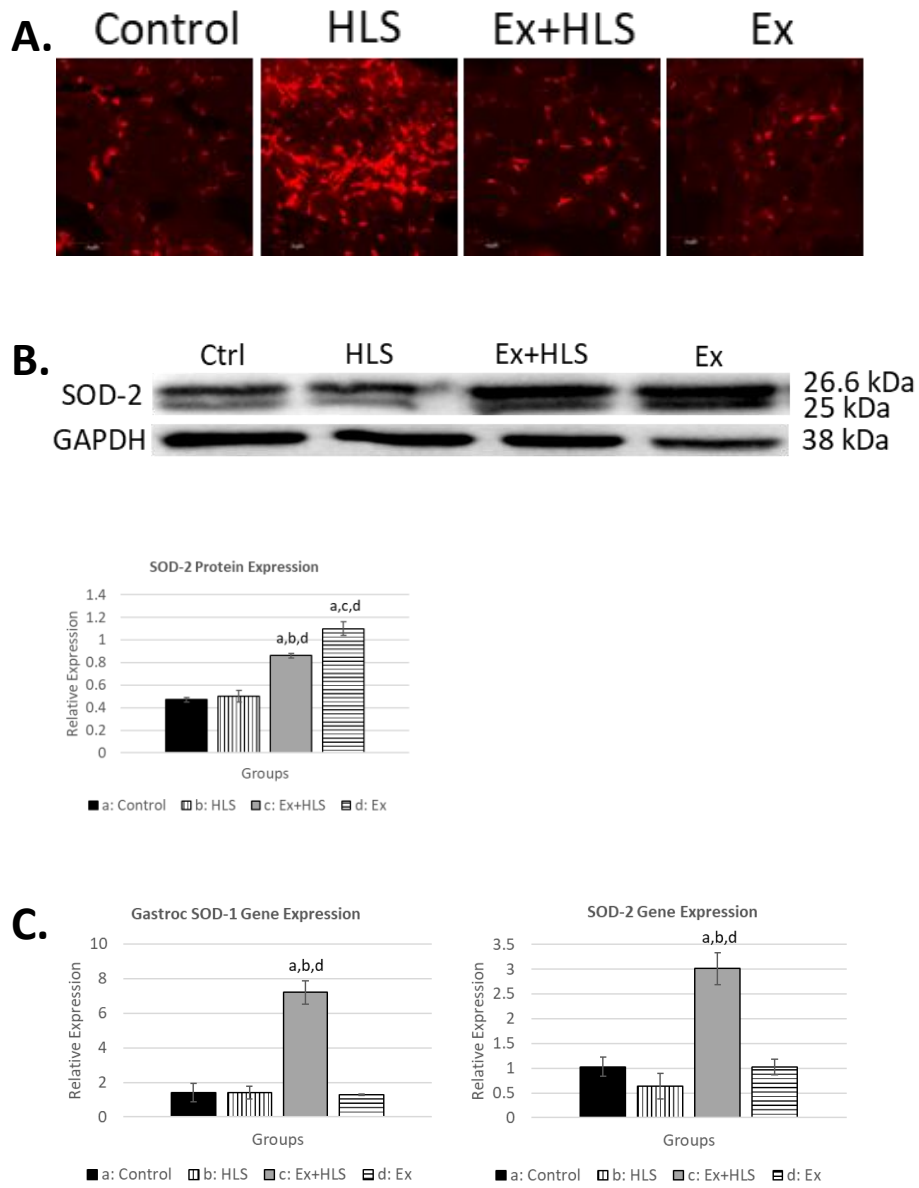
significant increase in SOD-2 protein expression after exercise (Ex) (P>.01) compared to all other groups with a trending decrease in SOD-2 expression in HLS. Gastrocnemius SOD-1 and SOD-2 mRNA expression of the Ex+HLS group was significantly greater than all other groups (p<.01). SOD-2 protein expression in this muscle was significantly greater in both Ex and Ex+HLS groups compared to both Control (p<.01) and HLS (p<.01), respectively.

## Discussion

Skeletal muscle atrophy is the result of an imbalance of protein degradation and protein synthesis. When degradation exceeds synthesis, the result is a loss of muscle mass. The correlation between skeletal muscle atrophy and reduced mitochondrial biogenesis and function (114, 116) as well as increased or unbalanced reactive oxygen species accumulation is well demonstrated in the literature (33, 102). Furthermore, a wealth of research reveals exercise training increases markers of mitochondrial function and biogenesis (44, 75, 87). Therefore, the aim of this study is to assess the effects of preconditioning the muscle tissue with a short-term exercise protocol prior to hindlimb unloading as a treatment to prevent atrophy. Secondarily, we aim to analyze mitochondrial molecular mechanisms associated with exercise preconditioning as a protective therapy.

Initially, Doppler laser technology used on the hindlimbs of all mice groups under anesthesia assessed blood flow. Differences in oxygen and nutrient delivery as well as waste removal in the muscle tissue via changes in blood flow could account for

differences in tissue health. Prior research in this area reveals a disconnect in blood flow assessment and atrophy. Nevertheless, according to a 2001 review of microvasculature changes with disuse atrophy by Tyml et al., multiple animal studies reveal no changes in blood flow in atrophied muscle as well as no differences in mean blood pressure and vascular resistance (145). Similarly, our measurements reveal no significant differences between all groups, indicating these tissues changes are not RBC and velocity related. Here, we did not account for capillarization and global microvasculature of each muscle, given our laser was solely directed at a more prominent vessel of the gastrocnemius due to the constraints of this particular technology. This assessment may account for group differences and is a limitation of the current study warranting future consideration.

In the disuse model of HLS in mice, previous research shows signs of muscle atrophy that include changes in muscle weight, CSA, and fiber-type transitioning. Atrophy may occur in as little as 3 days (14), while other studies reveal atrophy occurring after 7 or more days of disuse (56, 66, 116). In the present study, we similarly observe muscle atrophy occurring after 7 days of HLS in both the soleus and gastrocnemius muscles, indicated initially by reductions in the weight and size of the muscle.

Numerous studies have also intervened various treatments to reduce the effects of atrophy on skeletal muscles including electrical stimulation, nutrition, and exercise intra- or post-HLS (1, 46, 56, 104, 136). However, studies specifically measuring the effects of interventions, specifically exercise training, pre-HLS are scarce. Here we report greater muscle weight and cross-sectional area along with decreased slow-to-fast fiber-type transitioning in mice exercising prior to HLS compared to mice undergoing only HLS. Similar results of muscle weight and size were observed in a 2016 study in which rats

were treated with 4 months of swimming exercise before having their hindlimbs immobilized for 5 days in orthosis to induce atrophy (112). Although many differences exist between these studies, the researchers report exercise training prior to immobilization preserves soleus muscle mass compared to rats without exercise training.

Fujino et al. measured soleus muscle mass after treating rats with 1 session of endurance exercise prior to HLS and, while the exercise group trended higher than the suspension group, no significant differences were determined (37). This group also noted reductions in MHC I, a slow MHC, after 14 days of HLS while the group exercising before HLS trended higher but not significantly. However, a single exercise session may not be enough stress to induce adequate adaptive changes to provide significant protection of the muscle over an HLS protocol. Furthermore, adapting to exercise requires time and can be repetitiously surmounted to achieve, incrementally, greater adaptations. Such is the foundation of progressive exercise training (142). The use of a single session negates the factor of time to allow incremental increases in adaptation and potentially greater skeletal muscle protection. However, shorter-term exercise programs may be more translatable and useful in human adherence. Therefore, we used a concurrent protocol in this study that combines aerobic and anaerobic adaptive stressors over a shorter period (18 days) while still allowing enough time for adaptations to surmount. Our results indicate similar SMHC results as the Fujino et al. study in the soleus muscle between these groups and we also report a significant increase in gastrocnemius SMHC in the group exercising before HLS, potentially revealing muscle group differences in exercise adaptations and HLS effects.

It is well-established a reduction in markers of mitochondrial biogenesis and function are correlated with skeletal muscle atrophy (67, 99, 116). Liu et al. observed diminished mitochondrial respiration prior to activation of protein degradation pathways in a toxin-induced mouse atrophy model (86) while another group observed markers of mitochondrial biogenesis increasing prior to the regeneration of muscle after atrophy (28), indicating potential timelines of effect of mitochondrial function. The present research similarly revealed significant decreases in PGC-1α in both muscles while tending to decrease TFAM in the soleus and significantly decreasing TFAM in the gastrocnemius after HLS. We also observed decreases in trend and with significance of CS, a commonly used marker of mitochondrial function, across both muscles (81) establishing evidence for mitochondrial changes being correlated to the atrophy in the present study.

Based on this evidence, exercise was chosen as a preconditioning treatment to prevent disuse-associated atrophy because of the well-known inducing effect it has on mitochondrial biogenesis, particularly PGC-1 α and TFAM, and mitochondrial function (61, 87, 119). Indeed, our measurements of the Ex group mirrored this previous research, as we observed increases in gene expression and protein content across both muscles in many of these markers after the exercise protocol. It may be the increased molecular mitochondrial adaptations achieved by exercise provides enough lasting, anti-atrophic benefits over a 7-day HLS protocol to diminish the negative effects on skeletal muscle. Moreover, muscle protein synthesis is a high-ATP consuming process and studies suggest a mitochondrial dysfunction role being at the center of diminished muscle protein synthesis in atrophic conditions due to reduced ATP production (58). Exercise, by itself,

is also well known to activate protein synthesis pathways (Akt/mTOR) in skeletal muscle (24). Therefore, by concentrating on treating the mitochondria through exercise we attempt to shift the balance of degradation and synthesis towards saving muscle tissue.

We also find a wealth of evidence in prior research establishing protein degradation markers upregulated with muscle disuse (30, 56) and ROS as a prominent inducer of protein degradation pathways (ubiquitin-proteosome pathway, NF-κB, murf-1, atrogin-1/MAF-bx), apoptotic pathways, and mitochondrial dysfunction in skeletal muscle atrophy (22, 64, 97). Experiments quantifying ROS are generally variable, leading our account for ROS through DHE staining to be strictly observational in searching for particular trends between groups. Indeed, we observe high expression of ROS, specifically superoxide anion, in both muscles after HLS while exercising prior to HLS resulted in lower expression of ROS indicating a potential connection between ROS and muscle health in the present study. Cannavino et al. reported similar results through DHE staining, showing significant increases in superoxide anion after a 7-day hindlimb suspension in mice (14).

The mitochondrial respiratory chain is responsible for ATP production but also produces superoxide anion under normal physiologic circumstances, mainly from complex I and complex III (26). It is the excessive and unbalanced accumulation of ROS that leads to deleterious effects of mitochondrial and cellular proteins associated with atrophy. SOD-1 and SOD-2 (mtSOD) are antioxidants that neutralize ROS by accepting the unpaired electron of superoxide anion and converting to hydrogen peroxide, which is then further converted to water in the presence of glutathione peroxidase. Exercise acutely increases ROS leading to the transcription of antioxidants that neutralize

oxidative stress caused by increased respiration and results in an adaptation of increased levels of SOD over time to neutralize superoxide anions (133). Here, we also observe increased SOD-2 antioxidant expression in both muscles after the exercise protocol in the present study. The gastrocnemius revealed elevated levels of SOD-2 after Ex+HLS in both the mRNA and protein expression and not only after the exercise protocol (Ex) like that of the soleus. The gastrocnemius may be able to better withstand ROS accumulation during atrophic settings after exercise training due to a greater and more lengthy SOD-2 response. While the soleus muscle revealed increased SOD-2 after exercise, by the time the HLS protocol was over levels were not significantly different compared to HLS indicating potential differences among muscle fiber types. The change in antioxidants may potentially provide a protective effect against ROS that accumulates during disuse and further implicates exercise as an effective preconditioning treatment.

*Conclusions.* Skeletal muscle atrophy is correlated with reduced mitochondrial biogenesis and function along with excessive ROS leading to the activation of protein degradation and apoptotic pathways as well as reductions in protein synthesis. Here we show exercise training prior to an atrophic setting protects skeletal muscle from HLS-induced atrophy by inducing the potentially protective molecular effects of increased markers of mitochondrial biogenesis and function with increased antioxidant status. Exercise training prior to an atrophic setting may be a useful intervention to alleviate skeletal muscle atrophy caused by disuse and unloading. Furthermore, mitochondrial directed treatments could be a useful area of study in the prevention of muscle atrophy.

CHAPTER III


TFAM OVEREXPRESSION DIMINISHES SKELETAL MUSCLE ATROPHY



**<u>Introduction</u>**

Skeletal muscle functions not only in propulsion for locomotion but also as a glucose and amino acid reservoir (117). It is the largest organ in the body and functions as an endocrine secretory tissue (109). Notably, skeletal muscle strength is a key predictor of life span (92) and vitality. Being that this muscle functions in a variety of important processes, pathological losses can greatly affect health and quality of life.

Skeletal muscle atrophy is the loss of muscle tissue and is characterized by a decline in muscle mass leading to reductions in force production, decreased cross-sectional area of the muscle fibers, and diminished oxidative ability (140). As this tissue atrophies, the ability to perform physical tasks is greatly reduced and can significantly decrease the physical independence of the patient as well as increase factors of morbidity and mortality (113). Furthermore, when patients enter a scenario in which atrophy occurs, resources must be devoted to the mitigation and recovery process, such as pharmacological interventions or the use of rehab specialists. Therefore, preventing the condition of skeletal muscle atrophy is an important research endeavor to improve the patient condition, both physically and fiscally.

While many scenarios may cause skeletal muscle atrophy (disease, starvation, and aging), the mechanical unloading and disuse of muscle results in specific atrophic changes. Skeletal muscle is abnormally disused or unloaded during circumstances such as bedrest, limb immobilization, spinal cord injury, microgravity, and a sedentary lifestyle (162). During all of these scenarios, significant reductions in fiber contraction and mechanical stress on the muscle tissue occur, leading to potentially abrupt and reductive structural and molecular changes (55).

Disuse-induced atrophy results in the loss of muscle fiber size, weight, and function (16). When this occurs, decreases in molecular signaling pathways leading to protein synthesis and increases in molecular pathways leading to protein degradation and apoptosis are observed, resulting in a net loss of muscle protein (55, 141). These molecular mechanisms are also correlated with mitochondrial dysfunction and redox imbalance (102, 127). Dysfunctional mitochondria and excessive reactive oxygen species (ROS) accumulating during muscle atrophy reduces protein synthesis and activates protein catabolic mechanisms (22, 64, 97). ROS, in particular, can accumulate in the mitochondria and damage mtDNA, leading directly to dysfunction through the mutation of mtDNA and the transcription and translation of dysfunctional mitochondrial proteins (156).

Exercise powerfully stimulates mitochondrial function through small molecular changes that occur with physical activity and converge on the upregulation of the master-regulator protein, peroxisome proliferator-activated receptor gamma coactivator 1-alpha (PGC-1α) (118). This master regulator co-activates with nuclear-respiratory factors 1 and 2, increasing the transcription of mitochondrial transcription factor A (TFAM).

Translated TFAM is translocated into the inner-mitochondrial matrix and re-folded into its mature form where it can interact with mtDNA leading to increased mtDNA transcription. TFAM also abundantly binds mtDNA forming histone-like nucleoid structures to store, maintain, and protect mtDNA from binding and degradation via ROS (79).

Substantial evidence in prior research implicates the strong link of TFAM and mitochondrial health. Reviewing animal studies of TFAM, we see a germ line disruption of the mouse TFAM (TFAM $^{-/-}$) gene leading to extreme reductions in mtDNA and embryonic lethality (111). A 2004 study using a combination of TFAM overexpression and knockout mice reveals mtDNA copy numbers are directly proportional to TFAM levels (31). Balliet et al. showed a lack of TFAM resulted in mitochondrial dysfunction due to the loss of OXPHOS proteins (148). In contrast, an *in vivo* treatment with a recombinant form of TFAM resulted in increased motor endurance and complex-I respiration in mice (54).

There is evidence in a limited number of *in vivo* and *in vitro* TFAM overexpression studies that reveal decreased left-ventricular remodeling after myocardial infarction and an overall protective role of TFAM in cardiomyocytes (38, 52), establishing the important role of TFAM in a muscle tissue. In skeletal muscle, a mouse model with a skeletal-muscle specific disruption of TFAM led to mitochondrial myopathy, ragged-red fibers, reduced muscle force, abnormal mitochondrial shape, and decreased respiratory chain activity (157) specifically indicating its vital role in skeletal muscle. During skeletal muscle differentiation, increases in TFAM mRNA levels corresponded with increases in mitochondrial content and the authors concluded TFAM

protein levels are regulated by the availability of TFAM mRNA (18). Furthermore, we see overexpressing PGC-1α in a mouse model prevents disuse-induced skeletal muscle atrophy of the soleus (14). With TFAM being transcribed downstream of PGC-1α and tightly associated with mitochondrial function, a TFAM mechanism of skeletal muscle protection may exist. There are no known studies, to the best of our knowledge, analyzing TFAM overexpression in a mouse disuse-induced skeletal muscle atrophy model.

Therefore, we hypothesize overexpressing TFAM in mouse skeletal muscle will prevent or diminish unloading and disuse-induced atrophy. To test this, we use a 7-day hindlimb suspension (HLS) protocol to induce muscle atrophy in the hindlimbs of mice to be compared with wild-type mice entering the same HLS protocol. While we have separately shown exercise prior to HLS diminishes atrophy in wild-type mice (*article in submission*), here we further aim to observe if exercising TFAM overexpression transgenic mice prior to HLS results in a combination treatment effect to prevent muscle atrophy. Our results indicate overexpressing TFAM results in significantly diminished soleus and gastrocnemius atrophy prompting potential future research in genetic and molecularly directed therapies.

## Methods

*Animal and ethical approval.* Male C57BL/6J mice (WT) and male C57-based transgenic mice overexpressing the TFAM gene (*Cyagen Bioscience, Inc.*) were used for analysis. Genotyping confirmed the positive transgene in each mouse used in the present study.

The TFAM transgenic groups consisted of a control (T-Control), hindlimb suspension (T-HLS), and exercise prior to hindlimb suspension (T-Ex+HLS). Four groups of wild-type mice (WT) were used as comparison to transgenic groups including a Control, hindlimb suspension (HLS), exercise before hindlimb suspension (Ex+HLS), and exercise only (Ex) group. All data from WT mice are derived from our recent work and are being submitted in combination with the present study for publication. WT data will be used solely as comparative data for the objectives of this study. Mice that exercised prior to suspension were placed in HLS the same day after their last exercise session and all mice were sacrificed immediately after HLS. All mice were 13±1 weeks of age at the time of sacrifice. Wild-type mice were purchased from Jackson Laboratory (Bar Harbor, ME) and transgenic mice were purchased from *Cyagen Biosciences, Inc.* (Santa Clara, CA). All standard procedures and experiments involving animals were approved by the Institutional Animal Care and Use Committee of the University of Louisville and conformed with the National Institutes of Health guidelines.

*Hindlimb suspension.* Custom built cages were used to unload the hindlimb musculature and induce atrophy for 7 continuous days. Cage construction followed similar guidelines as previously shown (36).  Briefly, mice were first placed under continuous isoflurane anesthesia while a tail harness was attached. The tail was cleaned then taped cross-sectionally. A 27-gauge needle cap was cut down to ~2 centimeters in length with openings on each end. A small hole was created in the sidewall of the needle cap and a nylon string was used to tie a loop through this hole. This cap was placed over the tail and taped into place roughly 1/3 of the tail length from the base. The nylon loop and cap,

now taped to the tail, could then be attached to the roof of the cage, suspending the animal's hindlimbs. This also allowed the forelimbs to bear weight and the animal to move around the cage. Mice could also access food and water *ad libitum* in this manner. Bodyweights were recorded before and after suspension.

*Exercise Protocol.* Exercise consisted of 14 training sessions over 18 days of treadmill running in a concurrent style of exercise (combining more than one mode of exercise). An acclimation period to treadmill exercise occurred during the first four sessions. The following 10 sessions consisted of 6 endurance training style exercise sessions and 4 high-intensity interval style exercise sessions. All exercise program details (*Table 4*) were matched between exercising groups.

*Laser Doppler.* Laser Doppler imaging (*Moor FLPI, Wilmington, DE*) of lower, hindlimb blood flow was done for each group and used to assess flux of the hindlimb after treatments. Mice were first administered anesthesia (tribromoethanol) standardized to bodyweight. The musculature of the left, lower hindlimb was then exposed, revealing the musculature of the leg. Each mouse was placed in a prone position and the laser height was positioned roughly 15 cm from a prominent vessel superficial to the gastrocnemius. Flux measurements were recorded for 2 mins and quantified.

**Table 4. Exercise protocol.** Mouse concurrent treadmill exercise protocol consisting of a "Week 1" acclimation, followed by progressive training "Week 2" and "Week 3". Three days per week (M,W,F) consisted of endurance-style exercise while two days per week (T,TH) consisted of higher-intensity interval sprint style of exercise.

TABLE 4

| WEEK 1 | Monday | Tuesday | Wednesday | Thursday | Friday |
|---|---|---|---|---|---|
| Warmup | | 7m/min. for 50m | 7m/min. for 50m | 7m/min. for 50m | 7m/min. for 50m |
| Work Rate | OFF | 7m/min. | 8m/min. | 9m/min | 10m/min. |
| Rest | | 3min. off/100m | 3min. off/100m | 3min. off/100m | 3min. off/100m |
| Distance | | 300m | 300m | 300m | 300m |

| WEEK 2 | Monday | Tuesday-Sprints | Wednesday | Thursday-Sprints | Friday |
|---|---|---|---|---|---|
| Warmup | 7m/min. for 50m | 7m/min. for 50m | 7m/min. for 50m | 7m/min. for 50m | 7m/min. for 50m |
| Work Rate | 11m/min. | 15m/min. for 10m | 12m/min. | 17m/min for 15m | 13m/min. |
| Walk Rate | - | 7m/min. for 10m | - | 7m/min. for 15m | - |
| # of Sprints | - | 8 | - | 10 | - |
| Rest | 3min. off/100m | 5mins after 5 sprints | 3min. off/100m | 5mins after 5 sprints | 3min. off/100m |
| Distance | 350m | 160m | 375m | 300m | 400m |

| WEEK 3 | Monday | Tuesday-Sprints | Wednesday | Thursday-Sprints | Friday |
|---|---|---|---|---|---|
| Warmup | 7m/min. for 50m | 7m/min. for 50m | 7m/min. for 50m | 7m/min. for 50m | 7m/min. for 50m |
| Work Rate | 13.5m/min. | 18m/min. for 15m | 14m/min. | 20m/min. for 20m | 14.5m/min. |
| Walk Rate | - | 7m/min. for 15m | - | 5x-7m/20m; 6x-7m/10m | - |
| # of Sprints | - | 11 | - | 11 | - |
| Rest | 3min. off/100m | 5mins after 5 sprints | 3min. off/100m | 5mins after 5 sprints | 3min. off/100m |
| Distance | 450m | 330m | 500m | 380m | 550m |

*Tissue extraction and weight.* Both the soleus and gastrocnemius tissues were excised and separated from each leg for all experimental groups. Each muscle was washed with 50 mmol/L phosphate buffer saline (PBS) pH of 7.4, weighed individually, snap frozen in liquid nitrogen, and stored at −80°C until use. All tissue extraction methods and timings were equated across all groups.

*Immunofluorescence*. One of each muscle was cut cross-sectionally at the muscle midbelly and placed in tissue-freezing medium (Triangle Biomedical Sciences, Durham, NC, USA) in disposable plastic tissue-embedding molds (Polysciences Inc., Warrington, PA, USA). These tissue blocks were immediately frozen and stored at -80°C until use. Cryosections of each muscle, 7-10 µm thick, were obtained using a Cryocut System (CM 1850; Leica Microsystems, Buffalo Grove, IL, USA). These tissue sections were placed on Poly-L-Lysine coated microscope slides (Polysciences, Inc., Warrington, PA, USA) prior to use. Slides containing tissue sections were fixated in acetone for 20 mins, washed in 1X PBS-T solution, and incubated with a permeabilization solution (0.2 g Bovine Serum Albumin, 3 ul Triton X-100 in 10ml 1X PBS) for 1 hour at RT. This was followed by multiple washing steps with 1X PBS-T. The sections were incubated with a primary antibody (anti-Laminin; Abcam, Cambridge, MA, USA) solution with a dilution of 1:200 overnight at 4°C. After multiple washing steps with 1X PBS-T, the slides were incubated with a fluorescently labeled secondary antibody (goat anti-mouse Alexa flour 594; Invitrogen, Waltham, MA, USA) with a 1:300 dilution for 1 hour at RT. This was followed by another washing step, then slides were mounted with mounting medium and glass cover slips placed over the sections and air dried overnight in dark container. These samples could

then be visualized using a laser scanning confocal microscope (Olympus Fluo View 1000; Center Valley, PA, USA). Cross-sectional area (CSA) measurements were acquired using these laminin images by hand tracing single, stained muscle fibers in ImageJ software.

*DHE staining for ROS.* After tissue excision, each muscle was cross sectioned in half, immediately placed in tissue-freezing medium (Triangle Biomedical Sciences, Durham, NC, USA), snap frozen and stored at -80°C until use. Samples were sectioned on a cryostat, placed on slides, and in situ superoxide generation was evaluated in each cryosection with the oxidative fluorescent dye dihydroethidium (DHE). Cryosections (10 μm) were incubated with DHE (2 μmol/l) in a PBS solution. After multiple washing steps, slides were mounted with mounting medium and a cover slip and allowed to dry. These samples were then visualized using a laser scanning confocal microscope (Olympus Fluo View 1000; Center Valley, PA, USA).

*Protein Extraction and Protein Estimation.* Both muscle tissue samples from all groups were bead-homogenized in ice-cold RIPA (1 mmol/L) buffer with PMSF and protease inhibitor cocktails (1 $\mu$L/mL of lysis buffer, Sigma Aldrich, St. Louis, MO). Centrifugation followed with these samples at 12,000 g for 20 min at 4°C. All supernatant was extracted, placed in Eppendorf tubes, and immediately stored at −80°C until use. Protein estimation of each sample was measured by the Bradford-dye (Bio-Rad, CA) method in a 96-well microliter plate compared against a Bovine Serum Albumin (BSA) standards. This plate was analyzed at 594 nm in a Spectra Max M2 plate reader (Molecular Devices Corporation, Sunnyvale, CA).

*Western Blot Analysis.* Protein lysates (40 µg) were prepared and heated at 95°C for 5 min. These samples were then loaded into an SDS polyacrylamide gel submerged in running buffer and run at a constant current (75 Volts). Proteins were then transferred to a PVDF membrane overnight at 120 mA at 4°C. After the transfer, membranes were blocked in 5% nonfat milk for 1 hour at room temperature and then incubated overnight with the primary antibody (Anti-SOD2; GAPDH; Abcam, Cambridge, MA, USA.) at 4°C with slow agitation. Washing steps occurred the next day with a TBS-T buffer, then membranes were incubated with secondary antibody (horse radish peroxidase-conjugated goat anti-rabbit IgG, goat anti-mouse; Santa Cruz Biotechnology, Dallas, TX, USA) for 1 hour at RT with a 1:5000 dilution followed by another washing step. The membranes were developed using an ECL Western blotting detection system (GE Healthcare, Piscataway, NJ, USA) and all images were recorded in the gel documentation system ChemiDoc XRS (Bio-Rad, Richmond, CA, USA). Membranes, if being re-used, were stripped with stripping buffer (Boston BioProducts, Ashland, MA, USA) and blocked with 5% milk for 1 hour at RT under agitation. After washing, membranes were incubated with the anti-Gapdh antibody (Millipore, Billerica, MA, USA) as a loading control protein. The data were analyzed by Bio-Rad Image Lab densitometry software and normalized against anti-Gapdh bands.

*Quantitative PCR.* In the assessment of mRNA transcripts of specific genes in skeletal muscle, RNA was isolated with TRIzol® reagent (Life Technologies, Carlsbad, CA, USA) according to the instructions of the manufacturer. The RNA quantification and purity was assessed by nanodrop-1000 (Thermo Scientific, Walthan, MA, USA). Aliquots (2µg) of

total RNA were reverse-transcribed into cDNA using a High Capacity cDNA Reverse Transcription Kit (Applied Biosystems, Foster City, CA) according to the protocol of the manufacturer. Quantitative PCR (q-PCR) was performed for different genes (TFAM, Myh4, SOD-1, SOD-2), in a final reaction volume of 20 µl containing 10 µl PerfeCTa SYBR Green SuperMix, Low ROX (Quanta Biosciences, Gaithersburg, MD), 6 µl nuclease free water, 2µl cDNA, 40 picomoles of forward, and reverse primers. The information in *Table 5* presents all sequence-specific oligonucleotide primers (Invitrogen, Carlsbad, CA, USA). The data was represented in fold expression. This was calculated as the cycle threshold difference between control and sample normalized with the housekeeping genes *beta actin* and *18s*.

*Stastical Analysis*. All data were expressed as means ± SE. One-way ANOVA analyses were conducted on each data set with Tukey's post-hoc analysis used between groups within the same mouse line and the student t-test used between mouse line groups of relevance. Significance was determined as a p-value<.05.

## **Results**

*TFAM overexpression reduces atrophic changes.* Wet muscle weights were recorded immediately after tissue excision. A muscle weight to bodyweight (mg/g) standardization ratio was used to account for individual size variation. HLS resulted in non-significant decreases of 8.3% in soleus (*Fig. 15*) and 2.6% in gastrocnemius (*Fig. 16*) muscle weight to bodyweight ratio in mice overexpressing TFAM (T-HLS), compared to TFAM Control. Our conjoined work revealed a 27.1% decrease in wild-type soleus and a 21.5%

**Table 5. Nucleotide sequence - TFAM.** All forward and reverse primers for each

examined gene.

**TABLE 5**

| Gene | Forward Nucleotide Sequence | Reverse Nucleotide Sequence |
|---|---|---|
| Myh4 | 5'- TTGTGGTGGATGCTAAGGAGTC | 5'- GTACTTGGGAGGGTTCATGGAG |
| SOD-1 | 5'- GAACCAGTTGTGTTGTCAGGAC | 5'- GCCTTGTGTATTGTCCCCATAC |
| SOD-2 | 5'- GGTCACAGTTTCACAGTACACC | 5'- TCACAGCCTTGAGTTACAGAGT |
| TFAM | 5' - GAGAGCTACACTGGGAAACCACA | 5' – CATCAAGGACATCTGAGGAAAA |
| Rn18S | 5'- CACGGACAGGATTGACAGATTG | 5'- GACAAATCGCTCCACCAACTAA |
| ß-actin | 5'- CCCTGAAGTACCCCATTGAACA | 5'- CACACGCAGCTCATTGTAGAAG |

**Figure 15. Soleus weight and CSA. A.** Soleus muscle weight to bodyweight ratio (mg/g) of wild-type and TFAM transgenic groups (n=6). **B.** Immunofluorescence images of *anti-laminin* staining to visualize muscle fiber size and shape. All pictures are 200 µm in width. **C.** Mean cross-sectional area measurement comparison between groups of *anti-laminin* staining images calculated using *ImageJ* software (n=6). **D.** Myosin Heavy chain 4 (Myh4) gene expression analysis of the soleus muscle (n=6). Statistical significance (p<.05) indicated by the corresponding group letter (means ± SE).

**FIGURE 15**

**A.**
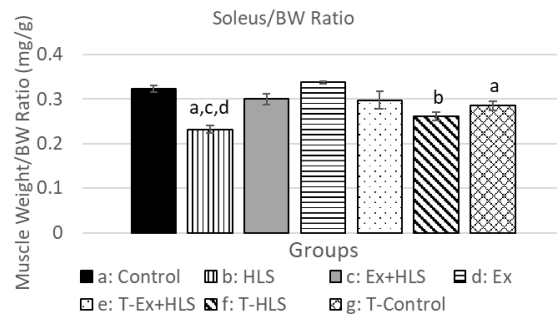


**B.**
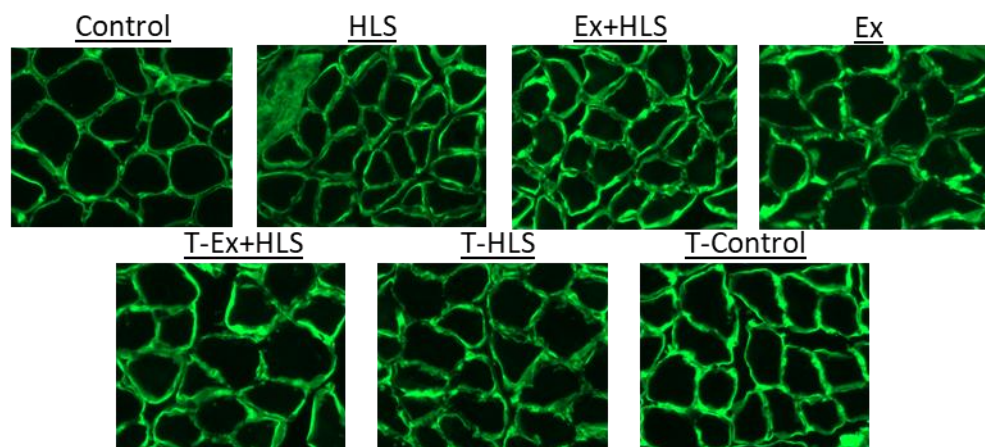


**C.**
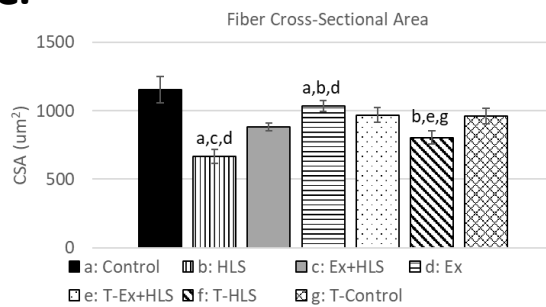


**D.**
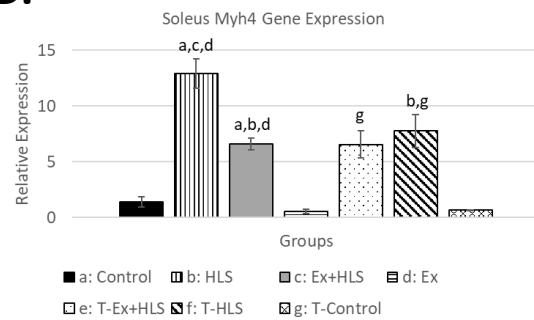
**Figure 16. Gastrocnemius weight and CSA. A.** Gastrocnemius muscle weight to bodyweight ratio (mg/g) of wild-type and TFAM transgenic groups (n=6). **B.** Immunofluorescence images of laminin staining to visualize muscle fiber size and shape. All pictures are 200 µm in width. **C.** Mean cross-sectional area measurement comparison between groups of *anti*-laminin staining images calculated using *ImageJ* software (n=6).

FIGURE 16

**A.**

Gastroc/BW Ratio



Muscle Weight/BW Ratio (mg/g)

a,c,d,f

b

Groups

■ a: Control    ▥ b: HLS    ▨ c: EX+HLS    ▤ d: Ex

▫ e: T-Ex+HLS    ◩ f: T-HLS    ⊠ g: T-Control

**B.**

| Control | HLS | Ex+HLS | Ex |

| T-Ex+HLS | T-HLS | T-Control |



**C.**

Fiber Cross-Sectional Area



CSA (um²)

b,c

a,c,d

b

■ a: Control    ▥ b: HLS    ▨ c: Ex+HLS    ▤ d: Ex

▫ e: T-Ex+HLS    ◩ f: T-HLS    ⊠ g: T-Control
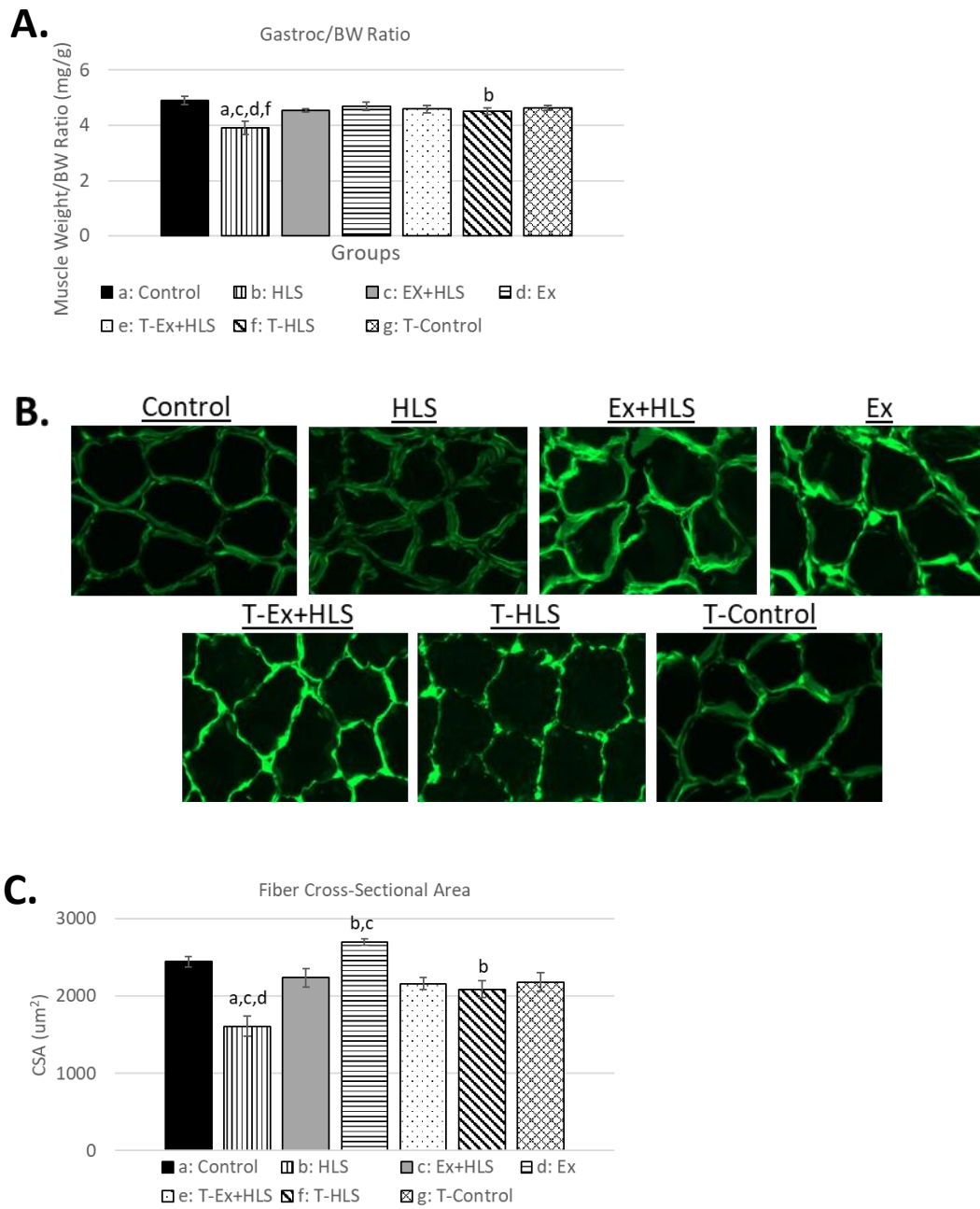
decrease in wild-type gastrocnemius in this ratio after HLS, compared to wild-type

Control TFAM Ex+HLS led to a non-significant increase of 4.5% in the soleus and

decrease of 0.7% in this ratio in T-HLS, compared to TFAM Control (*Fig. 15 and 16*).

Cross-sectional area measurements follow a similar, minor trend with T-HLS tending to

decrease in both muscles, although with no statistical significance between these groups,

with T-HLS being significantly greater (*Fig. 15 and 16*) than wild-type HLS in both

soleus [805um vs. 668um, p<.01] and gastrocnemius [2085um vs. 1605um, p<.01].

Moreover, fiber-type transitioning of the soleus muscle was measured through the qPCR

measurement of Myh4. Here, we see similar levels of Myh4 in both wild-type Ex+HLS

groups compared to T-Ex+HLS while T-HLS resulted in significantly lower levels of

Myh4 compared to wild-type HLS (12.89 vs. 7.75, p<.01).

*Greater TFAM expression in gastrocnemius.* To assess genetic expression of the TFAM

transgenic model, we completed qPCR analysis of the TFAM transcript across both

muscles (*Fig. 17*). Soleus TFAM expression in T-HLS mice was greater than wild-type

HLS (1.75 vs. .82, p<.01) while T-Control was greater than wild-type Control (2.35 vs.

1.02, p<.01). In the gastrocnemius, T-HLS was significantly greater than wild-type HLS

(4.23 vs. .49, p<.01) and T-Control was ~5-fold greater than wild-type Control (5.11 vs.

1.09, p<.01).

**Figure 17. TFAM gene expression. A.** Soleus TFAM gene expression (n=6). **B.**

Gastrocnemius TFAM gene expression. Statistical significance (p<.05) indicated by the

corresponding group letter (means ± SE).

FIGURE 17

**A.**

Soleus TFAM Gene Expression



**B.**

Gastroc TFAM Gene Expression
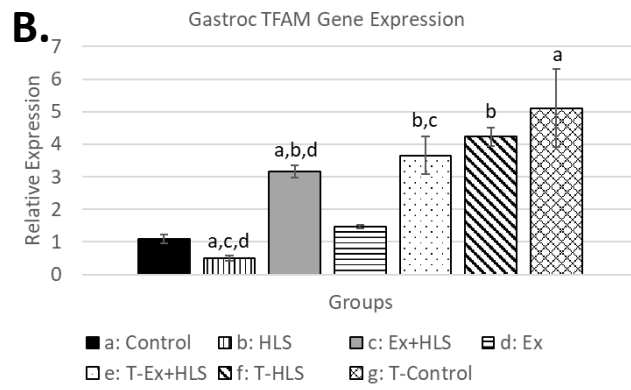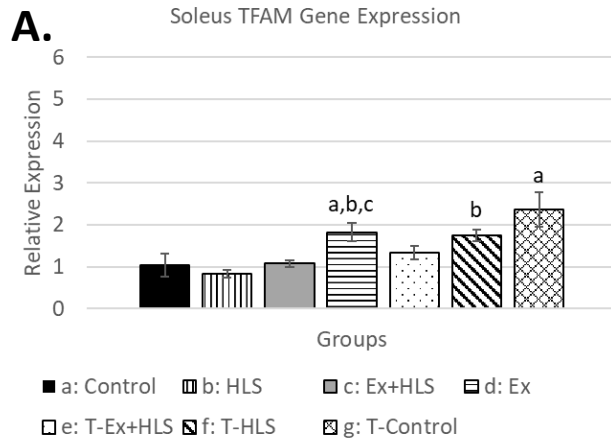
*Hindlimb bloodflow does not change.* Laser Doppler imaging of the left hindlimb assessed blood flow through a prominent posterior limb artery superior to the gastrocnemius (*Fig. 18*). Flux is a function of red blood cell (RBC) content and its velocity through the vessel of interest. Lack of RBC content to peripheral tissues may account for skeletal muscle changes if oxygen and nutrient delivery as well as waste removal are impaired. Here we show there were no significant differences in flux between all groups (p=.53).

*TFAM overexpression increases SOD-1 and SOD-2.* Skeletal muscle degradation and apoptotic pathways are induced by reactive oxygen species (22, 97). We assessed the accumulation of superoxide anion, observationally, through the use of DHE staining. In all TFAM transgenic groups, we consistently observed low positive staining markers after DHE staining across all groups (*Fig. 19*). In both soleus and gastrocnemius muscles, T-Ex+HLS resulted in minimal positive markers while, interestingly, T-Control and T-HLS appeared to have dull to low positive staining across multiple observations.

Superoxide dismutases (SODs) are antioxidant enzymes that catalyze the conversion of superoxide anions to hydrogen peroxide (39). Therefore, we measured SOD-1 (cytosolic) and SOD-2 (mitochondrial) transcripts via qPCR and SOD-2 protein expression via Western blot to assess inter-group antioxidant differences. SOD-1 mRNA analysis in the soleus (*Fig. 20*) revealed significantly greater expression of this gene in T-

**Figure 18. Hindlimb blood flow. A.** Laser Doppler blood flow measurement of a prominent vessel in the dorsal hindlimb. **B.** Blood flux measurement comparison between groups (n=6).

**FIGURE 18**
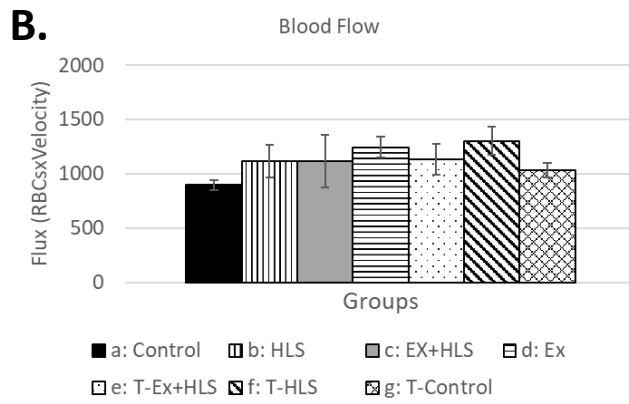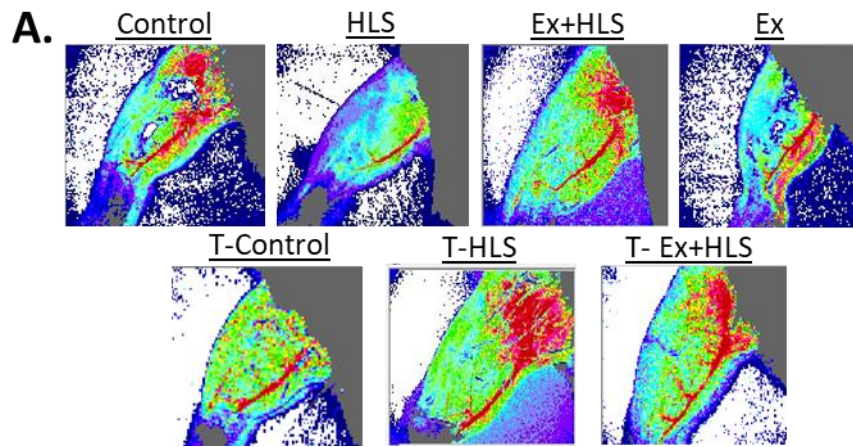
**Figure 19. Soleus and gastrocnemius ROS. A.** Observational soleus dihydroethidium staining for ROS. Bright spots are assumed to be positive staining for ROS (n=6). **B.** Observational gastrocnemius dihydroethidium staining for ROS. Bright spots are assumed to be positive staining for superoxide anion (n=6).

**FIGURE 19**

**A.**

Control      HLS      Ex+HLS      Ex

T-Ex+HLS      T-HLS      T-Control

**B.**

Control      HLS      Ex+HLS      Ex

T-Ex+HLS      T-HLS      T-Control
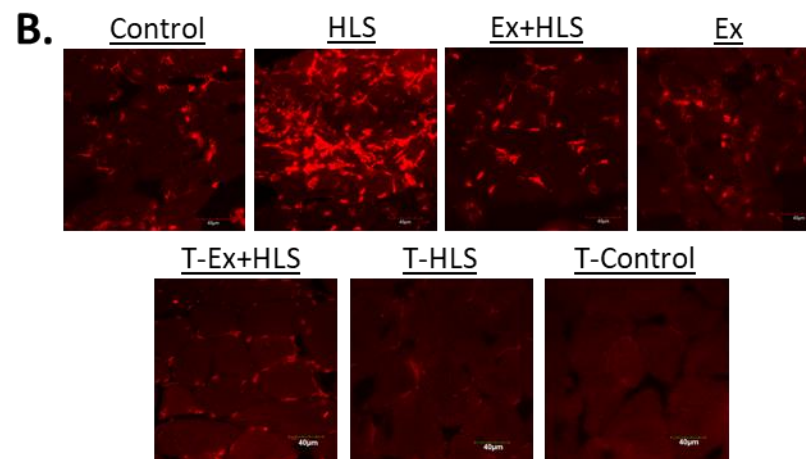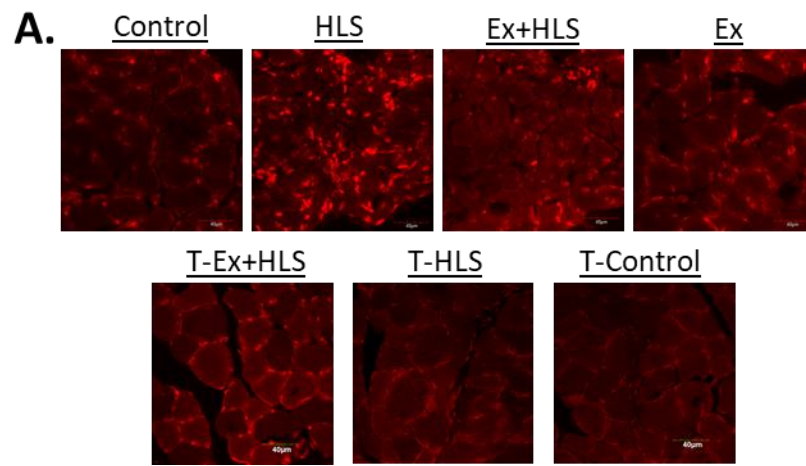
**Figure 20. Soleus antioxidants. A.** Soleus SOD-1 transcript expression (n=6). **B.** Soleus protein expression via Western blot analysis for antioxidant enzyme SOD-2 (n=6). **C.** Soleus SOD-2 gene transcript expression. Statistical significance (p<.05) indicated by the corresponding group letter (means ± SE).

**A.** Soleus SOD-1 Gene Expression

**FIGURE 20**

**B.**

| | Ctrl | HLS | Ex+HLS | Ex | T-Ex+HLS | T-HLS | T-Control | |
|---|---|---|---|---|---|---|---|---|
| SOD-2 | | | | | | | | 26.6 kDa / 25 kDa |
| GAPDH | | | | | | | | 42 kDa |

SOD-2 Protein Expression

**C.** SOD-2 Gene Expression
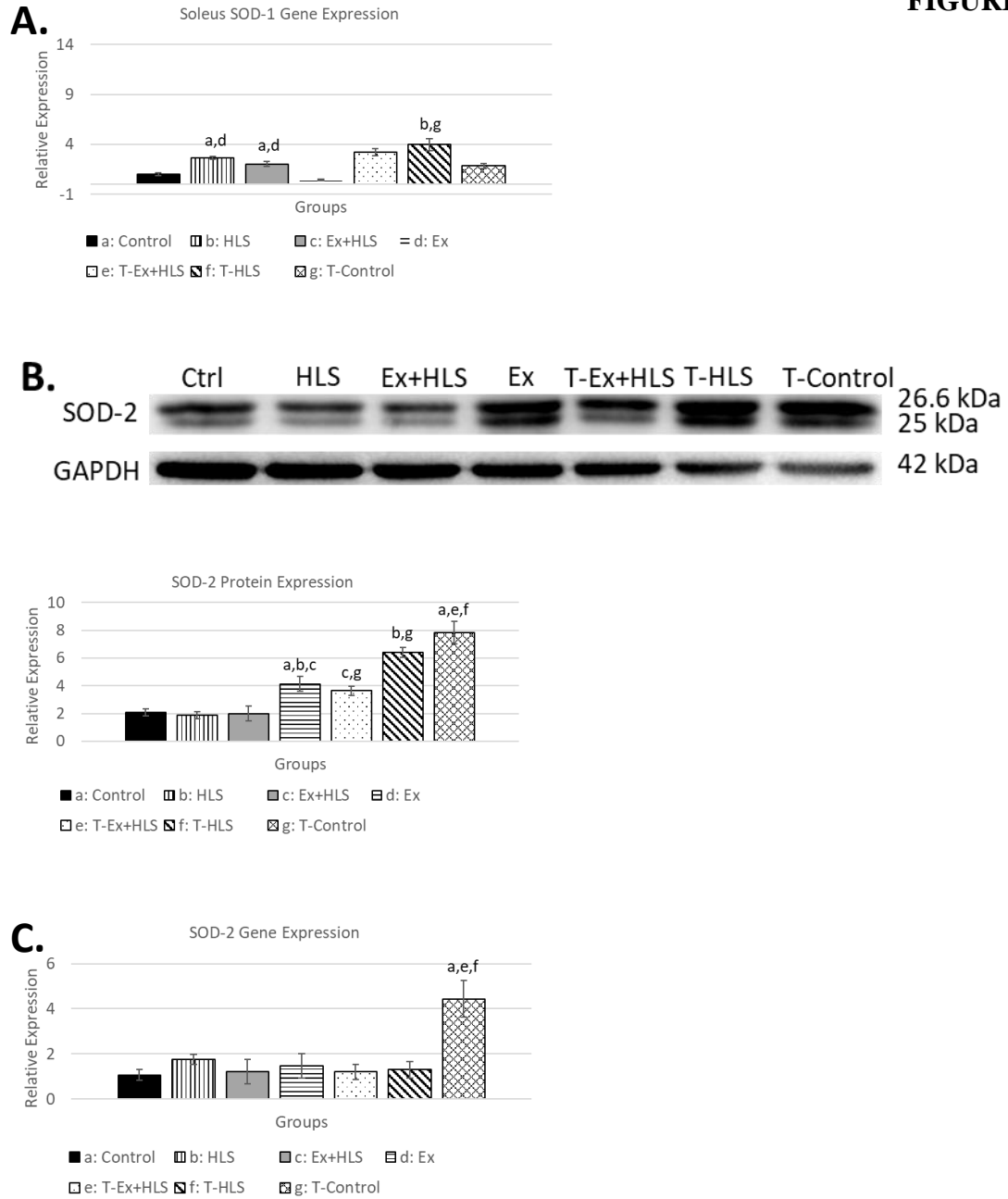
HLS mice compared to wild-type HLS (P<.05). In the gastrocnemius (*Fig. 21*), T-Control and T-HLS SOD-1 transcripts were both roughly 10-fold greater than wild-type Control and HLS (p<.01).

Transcript analysis of SOD-2 in the soleus (*Fig. 20*) reveals T-Control being ~4.5x greater than wild-type Control (p<.01). SOD-2 soleus protein expression was greater in T-HLS compared to wild-type HLS (p<.01) as well as T-Control compared to wild-type Control (p<.01). After observing gastrocnemius SOD-2 gene expression (Fig. 21), we see the T-Control group with a nearly 5.5-fold increase compared to Control (p<.01) and T-HLS nearly 6-fold greater than HLS (p<.01). Protein expression of this antioxidant in the gastrocnemius (*Fig. 21*) similarly shows increases in both T-HLS and T-Control compared to HLS and Control, respectively.

## Discussion

Atrophy of skeletal muscle arises when protein degradation and apoptosis exceeds protein synthesis and can occur when the musculature is unloaded or disused (140). Previously we have shown evidence of atrophy in both the soleus and gastrocnemius skeletal muscle of wild-type mice following a hindlimb-unloading protocol (*article in submission*). This skeletal muscle atrophy is associated with diminished markers of mitochondrial biogenesis and function, a reduced antioxidant state, as well as a potentially increased ROS status leading to redox imbalance.

**Figure 21. Gastrocnemius antioxidants. A.** Gastrocnemius SOD-1 transcript expression

(n=6). **B.** Gastrocnemius protein expression via Western blot analysis for antioxidant

enzyme SOD-2 (n=6). **C.** Gastrocnemius SOD-2 gene transcript expression (n=6).

Statistical significance (p<.05) indicated by the corresponding group letter (means ± SE).

**FIGURE 21**

**A.** Gastroc SOD-1 Gene Expression

**B.**

SOD-2 Protein Expression

**C.** SOD-2 Gene Expression

116
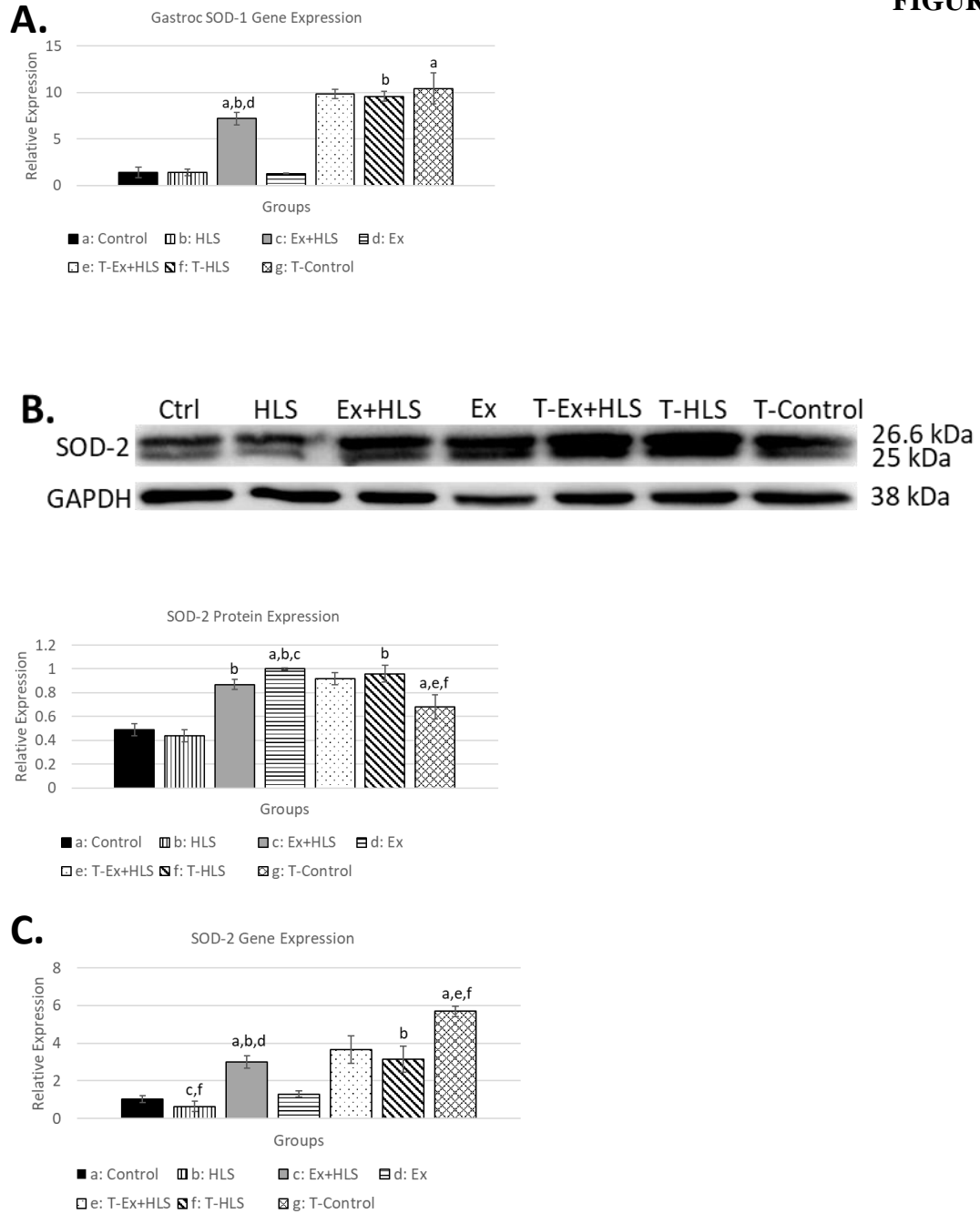
We successfully reduced atrophy by exercising the musculature prior to hindlimb suspension (*Table 6*), which was associated with improvements in many of these mitochondrial and redox markers. Specifically, we observed a trending decrease in TFAM gene and protein expression in the soleus and a greater, significant decrease in TFAM gene and protein expression in the gastrocnemius muscle after HLS. Therefore, in the present study we attempt to more specifically analyze the role of TFAM in muscle atrophy using a C57BL/6J-based TFAM overexpression transgenic mouse model in HLS, while also observing the effects of combining exercise with this transgenic model.

Previous research using TFAM transgenic animal models is scarce. A 2005 study reported the use of a TFAM transgenic mouse model in a myocardial infarction study and results indicate TFAM overexpression ameliorated left-ventricular remodeling, providing a cardiomyocyte protective effect (52). Other *in vitro* studies similarly reveal a cardiomyocyte protective role via TFAM overexpression (38, 51). Moreover, mitochondrial dysfunction in skeletal muscle atrophy is highly associated with excessive ROS. With TFAM protecting mtDNA from ROS as well as increasing mtDNA transcription, mtDNA copy number, and mitochondrial biogenesis, we chose to further investigate its role in skeletal muscle.

Initially, we assessed hindlimb blood flow via Doppler laser technology in a prominent vessel superior of the gastrocnemius. Blood flow could be a limiting factor in muscle atrophy due to decreases in the delivery of oxygen and nutrients and the ability to remove waste. There are discrepancies in the literature concerning muscle atrophy related blood flow changes. One would assume to see reductions in blood flow after HLS.

**Table 6. Bodyweight and muscle weights.** Bodyweight (BW) pre-HLS (g) and BW at time of sacrifice. Muscle weight of both the soleus and gastrocnemius. All data presented as means ± SE.  Statistical significance (p<.05) between groups indicated by the superscript letter associated with each particular group (a: Control, b: HLS, c: Ex+HLS, d: Ex).

TABLE 6

| Group | Pre-HLS BW (g) | BW (g) | Sol MW (mg) | Gas MW (mg) | Sol MW/BW (mg/g) | Gas MW/BW (mg/g) |
|---|---|---|---|---|---|---|
| Control | - | 24.5 ± .55 | 7.8 ± .17 | 121.1 ± 6.10 | .32 ± .01 | 4.9 ± .16 |
| HLS | 23.3 ± .87 | 22.0 ± .79 | **5.1 ± .15[a,c,d]** | **85.4 ± 5.5[a,d]** | **.23 ± .01[a,c,f]** | **3.9 ± .24[a,c,f]** |
| Ex+HLS | 24.3 ± .78 | 22.4 ± .67 | **6.9 ± .33[a,b,d]** | 103.8 ± 4.31 | **.30 ± .01[d]** | 4.5 ± .07 |
| Ex | | 23.5 ± .22 | 7.9 ± .12 | 110.7 ± 4.30 | .34 ± .003 | 4.7 ± .15 |
| T-Ex+HLS | 23.8 ± .47 | 22.9 ± .55 | 6.8 ± .44 | 105.2 ± 1.77 | .30 ± .03 | 4.59 ± .14 |
| T-HLS | 26.1 ± .63 | 23.8 ± .59 | **6.3 ± .27[b,g]** | **105.9 ± 2.60[b]** | **.261 ± .01[b]** | **4.5 ± .12 [b]** |
| T-Control | - | 26.9 ± .27 | **7.7 ± .32[f]** | 124.5 ± 3.42 | **.29 ± .01[a]** | 4.63 ± .09 |

However, according to Tyml et al. in a 2001 review of the microvasculature changes in disused muscle, this assumption may be incorrect. Multiple animal studies reported here on muscle disuse reveal no changes in blood flow in atrophied muscles, indicating no changes in mean blood pressure and vascular resistance (145). We similarly observe these effects in blood flow with no differences between groups. However, this assessment does not specifically analyze capillarization or microvasculature of each muscle, which may reveal differences. This limitation in conjunction with the current findings warrants future investigation.

After HLS in transgenic mice we observe muscle wet weight, muscle weight/bodyweight ratio, and cross-sectional area are all significantly greater in both the soleus and gastrocnemius of the T-HLS group compared to the wild-type HLS group, indicating an initial, potential protective role of TFAM overexpression (*Fig. 22, Table 6*). TFAM abundantly binds and protects mtDNA from mitochondrial ROS. As greater TFAM comes in contact with mtDNA, greater protection is expected (78). TFAM expression is also positively correlated with mtDNA copy number (31). Therefore, results from the current study suggest supra-physiologic gene expression of TFAM may lead to, speculatively, increased mtDNA protection during an atrophic setting with increased ROS, preserving muscle tissue from atrophy via mitochondrial protection.

**Figure 22. Exposed lower hindlimb.** Dorsal view of the exposed lower left hindlimb with mice, under anesthesia, placed in a prone position. Observational differences between groups.

**FIGURE 22**



Control    HLS    Ex+HLS    Ex

T-Ex+HLS    T-HLS    T-Control
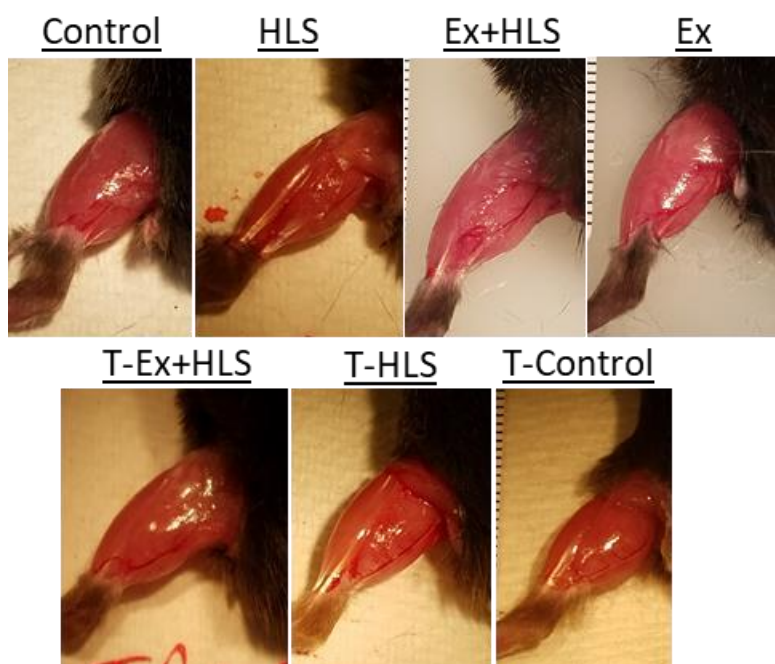
In the present study, the transgenic gastrocnemius muscle appears to have a more pronounced protective effect from atrophy with minimal reductions in muscle weight, size, and shape compared to the greater changes observed in the transgenic soleus. Our recent research indicates mitochondrial biogenesis markers, particularly TFAM gene and protein expression, in the wild-type gastrocnemius is more affected by 7 days of HLS (*article in submission*). Yajid et al. also report muscle group mitochondrial differences where they conclude mitochondrial respiration is most affected in the gastrocnemius after HLS in rats. Here the researchers analyzed mitochondrial respiration in 4 separate muscles, including the soleus, and noted a 59% decrease in gastrocnemius state 3 respiration with disuse atrophy (158). The implication is muscle groups with very different fiber-type makeups may respond to atrophy differently, and thus should be analyzed separately when creating therapeutics.

Nonetheless, while it appears the gastrocnemius may be more susceptible to mitochondrial changes during disuse and potentially able to respond better to mitochondrial treatment via the overexpression of the TFAM gene, we must also emphasize muscle fiber-type differences between muscle groups. In the analysis of C57BL/6J mouse muscle fiber-type composition, the soleus muscle reportedly consists of much higher oxidative fibers with 37% type-I fibers and 38% type-IIA fibers while the gastrocnemius consisted of much lower oxidative fibers with only ~6% type-I and ~6% type-IIA but over 54% type-IIB fibers (2). Oxidative fibers tend to have greater mitochondrial content and density while fast-glycolytic fibers tend to have less mitochondrial content (88). In speculation, due to the lower volume of mitochondria in the gastrocnemius, there may be a greater sensitivity to even minor mitochondrial

changes, such as the decreases in TFAM we observe in HLS. By overexpressing this highly important gene in mitochondrial health and function that directly protects mtDNA copy number and activates mtDNA transcription, it may blunt the gastrocnemius sensitivity to mitochondrial fluctuations. While the gastrocnemius in wild-type mice revealed a significant decline in TFAM gene and protein expression after HLS, there was no significant difference in soleus TFAM gene and protein expression in wild-type mice after HLS. The soleus, with greater mitochondrial densities and no significant decreases in TFAM, did not benefit from increased TFAM transcript expression to the same extent while the gastrocnemius, with significant declines in TFAM after HLS, had the physiologic capacity to benefit from overexpression.

We also observed differences in expression levels between muscles in the transgenic mice. To investigate this further, measurements of TFAM mRNA expression in transgenic mice against wild-type mice revealed a nearly 2.5-fold increase in transgenic soleus TFAM mRNA compared to ~5-fold increase in transgenic gastrocnemius TFAM mRNA (*Fig. 17*). This difference was similar across all transgenic treatment groups indicating a potential difference in fiber-type response to the random integration of the TFAM transgenic construct. Interestingly, in a study using a PGC-1α overexpression mouse model, the authors note the potential for certain promoters to be more highly expressed in fast-fibers compared to slow-fibers (14). Although purely speculation, this may play a role in the current study to account for expression differences between muscle types.

We previously observed increased superoxide anion after HLS in wild-type mice, which was similar to DHE staining results in skeletal muscle after 7-day HLS by

124

Cannavino et al. (14). In the present study, we observe much lower expression of ROS across both muscles of all transgenic groups compared to wild-type. Also, we see increases in SOD-1 gene expression and SOD-2 protein expression of both muscles, with the transgenic gastrocnemius revealing more pronounced levels of gene expression of both antioxidants compared to the transgenic soleus. These findings are unexpected and links TFAM gene overexpression with increased antioxidant status. Interestingly, a 2009 study isolating mtDNA nucleoids revealed the presence of SOD-2 within each nucleoid, potentially acting as a front-line antioxidant defense barrier for mtDNA (72). Speculatively, it is possible overexpressing TFAM results in increased mtDNA binding and greater nucleoid formation, leading to a higher presence of SOD-2 expression antioxidant defense overall. The exact mechanism between these two molecules appears to be unknown, to our knowledge, and worthy of future investigation.


*Conclusion.* Skeletal muscle atrophy is highly correlated with reduced mitochondrial biogenesis and function along with excessive ROS leading to the activation of protein degradation and apoptotic pathways and the reduction in protein synthesis. Here we follow up on our recent research that correlated diminished mitochondrial markers with skeletal muscle atrophy and attempt to display a protective role of TFAM in disuse-induced skeletal muscle atrophy. Moreover, there may be a more pronounced effect in the gastrocnemius muscle to TFAM overexpression, which should be considered in future research. Our results indicate the overexpression of the TFAM gene is associated with increased antioxidant expression as a possible mechanism to prevent catabolic pathway induction in skeletal muscle disuse. TFAM directed pharmaceuticals or therapies to

manipulate this molecule is an attractive area of research in preventing skeletal muscle

atrophy. Future research into this molecule could also focus on other tissues and

pathologic areas in which mitochondrial biogenesis and dysfunction plays a major role.

CHAPTER IV

CONCLUDING DISCUSSION

The studies presented in this project were meant to further our knowledge of the effect of exercise on skeletal muscle and to attempt to prevent the unwanted effects of atrophy during disuse. We reasoned since reductions in markers of mitochondrial biogenesis and function as well as redox imbalances were highly correlated with skeletal muscle atrophy in numerous research studies, observing and treating this mechanism to prevent atrophy may be a useful research endeavor. First, we hypothesized that exercise training prior to a disuse-induced atrophic setting would prevent skeletal muscle atrophy. Second, we hypothesized that this prevention of atrophy would be associated with changes in mitochondrial markers.

To test our initial hypothesis, we first needed to determine if a 7-day hindlimb suspension protocol would induce atrophy and if exercise training prior to this atrophic event was linked to atrophy prevention. To test our secondary hypothesis, we had to assess the molecular changes associated with this treatment. As discussed in Chapter II, HLS results in a 27.1% and 21.5% decrease in soleus and gastrocnemius muscle weight to bodyweight ratio in WT mice, respectively, indicating the HLS protocol induced atrophy. Exercising prior to HLS resulted in a 5.6% and 8.1% decrease in soleus and gastrocnemius weight to bodyweight ratio, respectively.

Exercise increased mitochondrial associated markers (PGC-1α, TFAM, CS, SOD-2), Slow myosin heavy chain (SMHC) expression, and reduced fiber-type transitioning (Myh4). Observationally, Ex+HLS reveals decreased ROS expression compared to HLS. Our data indicates the time prior to an atrophic setting, particularly caused by muscle unloading, may be a useful period to intervene progressive exercise training to prevent skeletal muscle atrophy and is associated with mitochondrial function and redox balance.

Based on the results of Chapter II, we created a third hypothesis that was two-fold in which we state TFAM overexpression will prevent skeletal muscle atrophy and combining TFAM overexpression with exercise will act synergistically to prevent atrophy during HLS. To test this, we had to first obtain a viable C57Bl/6J-based transgenic mouse model that positively overexpressed the TFAM gene and subject these mice with the same HLS and exercise protocols as the wild-type mice in Chapter II. As we see in Chapter III, all transgenic mice were first genotyped to confirm a positive overexpression. Overexpressing TFAM results in a decrease of 8.3% in soleus and 2.6% in gastrocnemius muscle weight to bodyweight ratio after only HLS compared to wild-type mice incurring a loss of 27.1% in soleus and 21.5% in gastrocnemius muscle after HLS. Our data indicates TFAM may play a critical role in protecting skeletal muscle from disuse atrophy and is correlated with increased expression of antioxidants (SOD-2) and potential redox balance. Moreover, combining exercise with TFAM overexpression had no synergistic effect compared to wild-type Ex+HLS. TFAM may be an attractive molecule of interest for potential, future therapeutic development.

Combining the results from these studies, the data supports the hypotheses that exercise training prior to a disuse-induced atrophy scenario prevents skeletal muscle atrophy and this is associated with reductions in markers of mitochondrial biogenesis and function. Additionally, TFAM overexpression further results in the prevention of disuse-induced atrophy while combining exercise with TFAM overexpression appeared to have no additional benefit. A mitochondrial mechanism increased by exercise that includes the TFAM molecule appears to be an important factor in the prevention of skeletal muscle atrophy and in the soleus and gastrocnemius. Refer to *Figure 1* for a summary outline.

## **Exercise and TFAM Protect Skeletal Muscle**

The goal of skeletal muscle atrophy research is ultimately prevention. Preventing pathological tissue loss may sustain functional and metabolic activity of the muscle. The patient prescribed bedrest after an orthopedic surgery, or any other atrophy scenario, has not only a quality of life interest to preserve muscle, but also a financial interest to reduce pharmaceutical and rehabilitation costs. The need to study interventions to prevent disuse-induced muscle atrophy and the molecular mechanisms associated is warranted to create treatments that improve the human condition.

The molecular processes resulting in atrophy can be viewed more simply as the balance of protein degradation and cell apoptosis with protein synthesis. When degradation and apoptosis exceed synthesis, a net protein loss occurs and the muscle atrophies over time. Any treatment developed to prevent this condition must, in some combination, reduce excessive degradation and apoptosis while increasing or maintaining

levels of protein synthesis. The main goal of the project was to prevent this imbalance with exercise and observe mitochondria variables associated with this prevention as a possible mechanism.

The most prominent findings of this project are: (1) a short-term, concurrent exercise training protocol prior to skeletal muscle unloading and disuse diminishes skeletal muscle atrophy, (2) atrophy is associated with diminished mitochondrial markers of biogenesis and function while exercising prior to disuse is associated with an increase in these markers, and (3) the overexpression of the TFAM mitochondrial marker diminishes atrophy associated with disuse. Our finding that exercise preconditioning diminishes disuse atrophy could lead to changes in instructions to patients prior to atrophy-inducing scenarios. In the case of the patient prescribed bedrest post-surgery, the overseeing physician may consider prescribing an exercise protocol pre-surgery, if the patient status allows, to attempt to prevent the negative consequences of bedrest on skeletal muscle. Similarly, an astronaut going into a microgravity environment for a shorter period of time could be prescribed exercise training pre-space travel to prevent the unloading-induced atrophy typically observed in space flight (150). The findings that this prevention is associated with increased mitochondrial markers, and particularly the TFAM molecule, is a new area of introspection in skeletal muscle atrophy research. This evidence could lead to molecularly directed pharmaceuticals in the future that attempt to manipulate the mitochondria and TFAM to sustain mitochondrial biogenesis and function pathways and protect mtDNA during muscle disuse and unloading. Further, the finding that TFAM overexpression is also potentially linked to increased antioxidant expression has not been fully elucidated in the literature and presents new opportunities of research.

A more detailed explanation of these findings with the associated results from Chapter II and Chapter III is discussed in the following sections.

*Exercise preconditioning diminishes skeletal muscle atrophy.* A principle finding of this project was the reduction of disuse-induce atrophy using an exercise training treatment prior to HLS. Our initial physiologic measurement of each group used Doppler laser technology to assess blood flow of the lower hindlimb. Changes in blood flow to any tissue may influence tissue health due to potential decrements in oxygen and nutrient delivery as well as in waste removal. The research in this area is mixed. However, in a more specific review of the microvasculature of disuse-induced skeletal muscle atrophy, the authors note multiple animal studies reveal no differences in blood flow, mean blood pressure, or vascular resistance in atrophied muscle (145). Similarly, we observed no significant differences across all groups in blood flow, indicating initially that atrophy was not flow-limited. This measurement is a function of RBCs and velocity and was observed in a prominent vessel superior to the gastrocnemius in the hindlimb. While there were no measurable differences in this vessel, microvasculature measurements may have provided useful data in assessing the present results, as we did not account for capillarization.

Prior research using HLS in mice reveal changes in muscle weight, CSA, and fiber-type transitioning. Atrophy has been shown to occur in as little as 3 days (14), or after 7 or more days of unloading and disuse (56, 66, 116). Here, we similarly observe signs of atrophy occurring after 7 days of hindlimb suspension in both the soleus and gastrocnemius of wild-type mice. These results indicated our atrophy protocol was viable

and could be a target for treatment. Furthermore, while changes in nutrition status could create variation between groups, bodyweights were recorded prior to and after HLS to ensure no drastic reductions occurred while in HLS and food and water consumption was monitored daily. In the current project, there were no significant differences in bodyweight measurements in this regard. This finding was similar to Ferreira et al. in which food intake and bodyweight were both recorded with no significant difference after 14 days of HLS (36).

Interventions in the literature to prevent atrophy include electrical stimulation, nutrition, and exercise intra- or post-HLS (1, 46, 56, 104, 136). Interventions prior to the atrophic setting to improve the atrophic condition are scarce. In Chapter II, we show exercise training intervened prior to HLS prevented the loss of muscle weight and size. Similarly, a 2016 study using a 4-month swimming protocol prior to immobilizing the hindlimb of rats for 5 days in orthosis, which induces atrophy, revealed greater soleus muscle weight and size compared to the non-exercise group. Although these treatments constructs are very different, the theme of exercise preconditioning prior to disuse was similar.

Fujino et al. measured soleus muscle mass after rats completed 1 session of endurance exercise prior to HLS. While the exercise group trended greater in these parameters, no significant differences were determined (37). This group also noted reductions in MHC I after HLS with the exercise group trending higher but not significantly. However, many of these results may be due to the use of a single exercise session. A single session may not stress the musculature adequately to induce the adaptive changes that provide significant protection of muscle in an HLS protocol.

Furthermore, a single session removes the factor of progressive exercise training. Adapting to exercise requires time and can be repetitiously surmounted to achieve, incrementally, even greater adaptations. This method is the foundation of progressive exercise training (142). Progressive training over time results in these incremental increases and greater adaptations and possibly lead to greater skeletal muscle protection. However, the translatable nature of a single session may be more useful for human adherence. Therefore, we used a concurrent protocol in this study combining moderate and more intense exercise over a shorter period (18 days) while still allowing enough time for adaptations to surmount. We similarly observed nonsignificant soleus decreases after HLS but also report significant decreases of SMHC in the gastrocnemius, revealing potential muscle group differences in atrophy susceptibility. This could be due to the differences in fiber-type makeup of each muscle and the associated characteristics of each fiber type that may make some muscle fibers more prone to atrophy.

When a muscle is disused, it not only atrophies but the fiber-type makeup will also remodel and transition from a slow fiber-type to a fast fiber-type (154). Through the measurement of a fast-twitch fiber transitioning marker (Myh4) in the soleus, we found when the hindlimbs were exposed to suspension, drastic increases in Myh4 were observed indicating a decline in muscle quality occurred. When an exercise treatment was intervened prior to suspension, this decline in quality was comparatively reduced, indicating improved muscle quality. This is an important measurement to assess muscle quality as a function of oxidative ability and resistance to fatigue. The same muscle group with increased levels of fast-twitch fiber mRNA tend to be less resistant to fatigue to those with lower levels of this transitioning marker, and vice versa. Part of the decline in

muscle function observed in patients with significant atrophy may be due to this decreased resistance to fatigue caused by a remodeled muscle.

*Mitochondrial markers are associated with exercise protection.* After establishing the HLS protocol induces atrophy and an exercise intervention prior to HLS prevented atrophy, a molecular analysis of mitochondrial markers was completed. Exercise was chosen as a preconditioning treatment to prevent disuse-associated atrophy because of the well-known inducing effect it has on mitochondrial biogenesis, particularly PGC-1 α and TFAM, and mitochondrial function (61, 87, 119). Our analysis similarly led to the important establishment that exercise increased markers of mitochondrial biogenesis and function as well as antioxidant expression variably across both muscles.

In prior research, Liu et al. observed decreased mitochondrial respiration prior to the activation of protein degradation pathways in a toxin-induced mouse atrophy model (86). Another study observed markers of mitochondrial biogenesis increasing prior to the regeneration of muscle after an initial atrophying scenario (28). Therefore, atrophy and regeneration seemed to be preceded by changes in mitochondrial function and thus, establishing mitochondrial importance with this tissue. In Chapter II, we show decreases in markers of the mitochondria after HLS. Decreased mitochondrial biogenesis and function markers suggests reductions in overall mitochondrial health. More specifically, a reduction in TFAM is highly correlated with reduced mtDNA copy number and decreased mitochondrial function (31). Our analysis reveal significant reductions of TFAM in the gastrocnemius and trending decrease in the soleus. Based on this evidence

and the literature data, the assumption made in this project is mtDNA copy number and function are also diminished by the HLS protocol. This could be associated with the reduction of ATP synthesis leading to reduced protein synthesis pathways, and redox imbalance leading to the accumulation of ROS and the induction of apoptotic and degradation pathways causing an imbalance in the skeletal muscle and a net protein loss over the HLS protocol. Notably, most of these markers increased after exercise training potentially providing an increased mitochondrial adaptation prior to entering HLS that could sustain muscle health over the 7-day atrophying period according to the above mechanisms.

When we examined redox imbalance, we observed increased superoxide anion after HLS in both muscles and found SOD-2 expression generally decreased after HLS. Similar superoxide anion results were observed by Cannavino et al. after a 7-day HLS protocol in mice (14). Here, exercise training increased SOD-2 and links exercise leading to greater redox balance. This balance could reduce excessive ROS accumulation that is implicated in degradation aspects of skeletal muscle atrophy and may be due to the combined factors of increased antioxidant expression and overall greater mitochondrial health with exercise training. The combination of increased mitochondrial markers and greater redox balance provides the framework for the associated molecular mechanisms of exercise protecting skeletal muscle from atrophying during disuse.

*TFAM overexpression diminishes skeletal muscle atrophy.* Another major finding of this project is the prevention of skeletal muscle atrophy via TFAM overexpression in a

transgenic mouse model. This finding is particularly important, as it is the first time, to our knowledge, a TFAM overexpression model has been used in the analysis of disuse-induce skeletal muscle atrophy. We hypothesized this finding based on the evidence in the literature that indicated a possible role for TFAM in atrophy.

Initially, we see results from Kang et al. displaying the idea of a protective effect of PGC-1α overexpression on mice skeletal muscle during limb immobilization (66). Cannavino et al. similarly show overexpressing PGC-1α in transgenic mice diminished skeletal muscle atrophy during hindlimb unloading (14). PGC-1α coactivating with NRF-1 and NRF-2 initiates the transcription of TFAM from nuclear DNA. Although PGC-1α is a diverse protein with many powerful interactions, its role in mitochondrial health includes the transcription of the TFAM molecule and is worth isolating in research for further study.

TFAM overexpression research is scarce in pathological scenarios. A 2005 study reported the use of a TFAM transgenic mouse model in a myocardial infarction study and results indicate TFAM overexpression ameliorated left ventricular remodeling, providing a cardiomyocyte protective effect (52). Other *in vitro* studies similarly reveal a cardiomyocyte protective role via TFAM overexpression (38, 51). Reviewing the protective effects in cardiac muscle also provides evidence for a potential use in skeletal muscle, even though there are differences between the tissues. From a redox balance standpoint, mitochondrial dysfunction is highly correlated with excessive ROS and is a variable that should be considered when attempting to improve muscle health. As previous research has already shown, TFAM protects mtDNA from degradation via ROS binding while also increasing mtDNA transcription, mtDNA copy number, and

mitochondrial biogenesis. This data provides evidence that the overexpression of this molecule can prevent atrophy, as atrophy is correlated to diminished mitochondrial factors. In Chapter II we found decreases in TFAM after the HLS protocol. Based on this finding, in Chapter III we tested TFAM overexpression in HLS which led to greater skeletal muscle weight to bodyweight ratios and CSA of muscle fibers and echoed our hypothesis that TFAM would improve this condition. Increased TFAM transcripts may have led to increased TFAM protein translation and import into the mitochondria. Assumingly, this protein could interact with mtDNA and protect it from the excessive ROS that accrues during HLS and increase or sustain mitochondrial biogenesis and function by activating transcription of mtDNA and retaining mitochondrial function with subsequent ATP synthesis and redox balance. As discussed previously, these aspects of are of key importance in protein degradation, apoptosis, and protein synthesis in skeletal muscle.

Kang's group, in the analysis of skeletal muscle using a PGC-1α overexpression mouse transgenic model after limb immobilization-remobilization, note decreased superoxide and increased SOD-2 expression in the transgenic mouse model (66). This positive correlation between PGC-1α and antioxidants has also been shown previously in skeletal muscle (67). In Chapter II, we observe increased antioxidant status across both muscles in all TFAM transgenic groups, including controls. This observation is important because the above research on PGC-1α link the increase in antioxidants to mechanisms preceding or outside of TFAM. Here we are linking increased antioxidants specifically to TFAM overexpression while data in the literature on this connection is scarce. However, a 2009 study isolating mtDNA nucleoids revealed the presence of SOD-2 within each

nucleoid, potentially acting as a front-line antioxidant defense barrier for mtDNA (72). Speculatively, it could be overexpressing TFAM results in increased mtDNA-TFAM protein interaction and greater nucleoid formation, leading to greater SOD-2 expression within these nucleoids. A specific mechanism here, however, appears to be unknown and worth investigation. Through increased TFAM overexpression and increased antioxidant expression, the typical inducer of protein degradation and mitochondrial based apoptotic pathways (i.e. ROS) could be neutralized during muscle disuse. Many of the major molecular degradation factors leading to muscle atrophy are therefore prevented or diminished and could account for the positive effects of TFAM overexpression preventing skeletal muscle atrophy. Indeed, here we observed diminished ROS accumulation in the form of superoxide anion across all TFAM groups as observational evidence of this potential mechanism.

Another point of emphasis in this project was to compare the results of two separate muscles with very different fiber-type makeups in the soleus and gastrocnemius. While both muscles appeared to atrophy in wild-type mice after HLS, TFAM overexpression mice were both significantly greater than wild-type HLS. The gastrocnemius responded, potentially, to a greater extent to TFAM overexpression compared to the soleus. TFAM HLS gastrocnemius muscle weight to body weight ratio was nearly identical to TFAM Control, with CSA and immunofluorescence imaging of the muscle fibers revealing similar results. In Chapter II, we show a significant decrease in TFAM in the gastrocnemius and not in the soleus after HLS. These results combined with the more robust response of the gastrocnemius to TFAM overexpression may indicate the gastrocnemius is more susceptible to mitochondrial changes and thus, a

better responder to TFAM overexpression. We also observed greater TFAM mRNA levels in the gastrocnemius compared to the soleus in transgenic groups. The gastrocnemius, with a greater fast-twitch fiber makeup, may also be more receptive to the random integration of the TFAM transgenic construct. In the Cannavino et al. study, the authors note the potential for certain promoters to be more highly expressed in fast-fibers compared to slow-fibers (14). Speculatively, this may account for expression differences between muscle types.

A final finding of this project is that combining exercise training with TFAM overexpression resulted in no synergistic effects in diminishing skeletal muscle atrophy. One could assume, due to the diverse signaling response to exercise, adding an exercise treatment to TFAM overexpression would further prevent muscle atrophy. Here, in most measures, TFAM Ex+HLS was not significantly different when compared to wild-type Ex+HLS, which countered our proposed hypothesis. This could be due to possible physiological limitations in available mRNA and messaging pathways leading to mitochondrial protection. With the TFAM gene already being overexpressed in transgenic mice, adding in mitochondrial biogenesis signals in the form of exercise may not have been able to further affect this process. Due to these observations we conclude this combination of treatments was not superior to either treatment alone.

## Future Directions

We have demonstrated through the results of this project that exercise training prior to muscle unloading clearly attenuates disuse-induced skeletal muscle atrophy and

is associated with changes in particular mitochondrial markers, most notably TFAM, which can be manipulated to also play a protective role. However, the acquisition of new knowledge brings forth the attainment of new questions, which we find to be the same here. For example, what changes occur to the markers of degradation and synthesis during HLS? Two prominent degradation molecules and E3 ubiquitin ligases, muscle RING finger-1 (Murf-1) and muscle atrophy F-Box (MAFbx)/Atrogin-1, have been shown to be transcriptionally increased during skeletal muscle atrophy in over 10 years of research (11). While multiple studies mentioned previously have linked mitochondrial dysfunction and ROS to these degradation markers, future research into a comprehensive connection of degradation and apoptotic markers to the treatments in this project and atrophy prevention is warranted. Did exercise prior to HLS reduce degradation molecules? Did TFAM overexpression reduce pathways to cell apoptosis? These questions could build upon our molecular understanding of the current research.

While previously mentioned research linked decreases in protein synthesis pathways to mitochondrial dysfunction and ROS, direct measurement of these pathways was not conducted in the present study. A useful study design could be the analysis of the Akt/mTOR pathway in conjunction with TFAM overexpression and exercise treatments. Particularly in exercise, a known inducer of mTOR (71), a protein synthesis analysis study could provide useful data. Furthermore, different types of exercise could be studied to observe any superiority in training styles. For example, while resistance training appears to activate protein synthesis greater than other forms of exercise, will this type of exercise alone or in conjunction with other forms or exercise provide superior results due to increased synthesis levels going in to HLS?

Another potential area to explore based off the current data derived from this project is a deeper mitochondrial analysis. While many of the markers measured here have been thoroughly linked to mitochondrial dysfunction, a specific functional study analyzing mtDNA, respiration markers, O2 consumption and ATP synthesis rates, and possibly transmission electron microscopy to visualize mitochondrial size and number would be useful to explore. Similarly, while our ROS measurements matched previous research in HLS, an in-depth analysis of ROS using multiple measurement techniques during skeletal muscle atrophy and the associated mitochondrial effects could also be another useful endeavor to elucidate ROS in atrophy.

Due to the results of TFAM overexpression, pharmaceutical and therapeutic options that are TFAM-directed may be useful to study. If TFAM transcription can be pharmacologically stimulated or if the role of TFAM can be pharmacologically replicated, a medicinal intervention could be synthesized. Provided greater basic research is needed, the use of a medicinal intervention to protect mtDNA and potentially mitochondrial function during scenarios of skeletal muscle disuse could reduce healthcare costs and improve the quality of lives of numerous patients every year. Translationally, a project using human subjects choosing elective surgery that will be prescribed bedrest post-surgery could be directed into an exercise protocol prior to going into surgery. This could translate the results of our basic research and is an obvious next step that we believe should be undertaken.

Collectively, the results of this project provide useful data into the prevention of disuse-induced skeletal muscle atrophy. Through the highlighting of exercise and TFAM,

it is my sincerest hope this information will be used to build upon viable treatment

options of the future.

REFERENCES

1.      **Alway SE, Pereira SL, Edens NK, Hao Y, and Bennett BT**. beta-Hydroxy-beta-

methylbutyrate (HMB) enhances the proliferation of satellite cells in fast muscles of aged rats

during recovery from disuse atrophy. *Experimental gerontology* 48: 973-984, 2013.

2.      **Augusto VP, Carlos Roberto ; Campos, Gerson Eduardo Rocha**. Skeletal muscle types in

C57BL6J mice. *Braz j morphol sci* 21: 89-94, 2004.

3.      **Bartlett JD, Close GL, Drust B, and Morton JP**. The emerging role of p53 in exercise

metabolism. *Sports medicine (Auckland, NZ)* 44: 303-309, 2014.

4.      **Bartoli M, and Richard I**. Calpains in muscle wasting. *The international journal of

biochemistry & cell biology* 37: 2115-2133, 2005.

5.      **Barton E, and Morris C**. Mechanisms and strategies to counter muscle atrophy. *The

journals of gerontology Series A, Biological sciences and medical sciences* 58: M923-926, 2003.

6.      **Baylor SM, and Hollingworth S**. Intracellular calcium movements during excitation-

contraction coupling in mammalian slow-twitch and fast-twitch muscle fibers. *J Gen Physiol* 139:

261-272, 2012.

7.      **Bechet D, Tassa A, Taillandier D, Combaret L, and Attaix D**. Lysosomal proteolysis in

skeletal muscle. *The international journal of biochemistry & cell biology* 37: 2098-2114, 2005.

8.      **Bergeron R, Ren JM, Cadman KS, Moore IK, Perret P, Pypaert M, Young LH,

Semenkovich CF, and Shulman GI**. Chronic activation of AMP kinase results in NRF-1 activation

and mitochondrial biogenesis. *American journal of physiology Endocrinology and metabolism* 281: E1340-1346, 2001.

9.      **Bilodeau PA, Coyne ES, and Wing SS**. The Ubiquitin Proteasome System in Atrophying Skeletal Muscle - Roles & Regulation. *American journal of physiology Cell physiology* ajpcell.00125.02016, 2016.

10.     **Bocco BM, Louzada RA, Silvestre DH, Santos MC, Anne-Palmer E, Rangel IF, Abdalla S, Ferreira AC, Ribeiro MO, Gereben B, Carvalho DP, Bianco AC, and Werneck-de-Castro JP**. Thyroid hormone activation by type 2 deiodinase mediates exercise-induced peroxisome proliferator-activated receptor-gamma coactivator-1alpha expression in skeletal muscle. *The Journal of physiology* 594: 5255-5269, 2016.

11.     **Bodine SC, and Baehr LM**. Skeletal muscle atrophy and the E3 ubiquitin ligases MuRF1 and MAFbx/atrogin-1. *American Journal of Physiology - Endocrinology and Metabolism* 307: E469-E484, 2014.

12.     **Bolisetty S, and Jaimes EA**. Mitochondria and reactive oxygen species: physiology and pathophysiology. *International journal of molecular sciences* 14: 6306-6344, 2013.

13.     **Campbell CT, Kolesar JE, and Kaufman BA**. Mitochondrial transcription factor A regulates mitochondrial transcription initiation, DNA packaging, and genome copy number. *Biochimica et biophysica acta* 1819: 921-929, 2012.

14.     **Cannavino J, Brocca L, Sandri M, Bottinelli R, and Pellegrino MA**. PGC1-alpha over-expression prevents metabolic alterations and soleus muscle atrophy in hindlimb unloaded mice. *The Journal of physiology* 592: 4575-4589, 2014.

15.      **Chin ER**. Role of Ca2+/calmodulin-dependent kinases in skeletal muscle plasticity. *Journal of applied physiology (Bethesda, Md : 1985)* 99: 414-423, 2005.

16.      **Chopard A, Hillock S, and Jasmin BJ**. Molecular events and signalling pathways involved in skeletal muscle disuse-induced atrophy and the impact of countermeasures. *Journal of cellular and molecular medicine* 13: 3032-3050, 2009.

17.      **Cloonan SM, and Choi AM**. Mitochondria in lung disease. *The Journal of clinical investigation* 126: 809-820, 2016.

18.      **Collu-Marchese M, Shuen M, Pauly M, Saleem A, and Hood DA**. The regulation of mitochondrial transcription factor A (Tfam) expression during skeletal muscle cell differentiation. *Bioscience reports* 35: 2015.

19.      **Combes A, Dekerle J, Webborn N, Watt P, Bougault V, and Daussin FN**. Exercise-induced metabolic fluctuations influence AMPK, p38-MAPK and CaMKII phosphorylation in human skeletal muscle. *Physiological reports* 3: 2015.

20.      **Connolly PF, Jager R, and Fearnhead HO**. New roles for old enzymes: killer caspases as the engine of cell behavior changes. *Frontiers in physiology* 5: 149, 2014.

21.      **Cunningham JT, Rodgers JT, Arlow DH, Vazquez F, Mootha VK, and Puigserver P**. mTOR controls mitochondrial oxidative function through a YY1-PGC-1alpha transcriptional complex. *Nature* 450: 736-740, 2007.

22.      **Dam AD, Mitchell AS, Rush JW, and Quadrilatero J**. Elevated skeletal muscle apoptotic signaling following glutathione depletion. *Apoptosis : an international journal on programmed cell death* 17: 48-60, 2012.

23.     **Desaphy JF, Pierno S, Liantonio A, Giannuzzi V, Digennaro C, Dinardo MM, Camerino GM, Ricciuti P, Brocca L, Pellegrino MA, Bottinelli R, and Camerino DC**. Antioxidant treatment of hindlimb-unloaded mouse counteracts fiber type transition but not atrophy of disused muscles. *Pharmacological research* 61: 553-563, 2010.

24.     **Dickinson JM, Volpi E, and Rasmussen BB**. Exercise and nutrition to target protein synthesis impairments in aging skeletal muscle. *Exerc Sport Sci Rev* 41: 216-223, 2013.

25.     **Dimauro I, Mercatelli N, and Caporossi D**. Exercise-induced ROS in heat shock proteins response. *Free radical biology & medicine* 98: 46-55, 2016.

26.     **Drose S, and Brandt U**. The mechanism of mitochondrial superoxide production by the cytochrome bc1 complex. *J Biol Chem* 283: 21649-21654, 2008.

27.     **Drummond MJ, Fry CS, Glynn EL, Dreyer HC, Dhanani S, Timmerman KL, Volpi E, and Rasmussen BB**. Rapamycin administration in humans blocks the contraction-induced increase in skeletal muscle protein synthesis. *The Journal of physiology* 587: 1535-1546, 2009.

28.     **Duguez S, Feasson L, Denis C, and Freyssenet D**. Mitochondrial biogenesis during skeletal muscle regeneration. *American journal of physiology Endocrinology and metabolism* 282: E802-809, 2002.

29.     **Dupont-Versteegden EE**. Apoptosis in skeletal muscle and its relevance to atrophy. *World Journal of Gastroenterology : WJG* 12: 7463-7466, 2006.

30.     **Egawa T, Goto A, Ohno Y, Yokoyama S, Ikuta A, Suzuki M, Sugiura T, Ohira Y, Yoshioka T, Hayashi T, and Goto K**. Involvement of AMPK in regulating slow-twitch muscle atrophy during hindlimb unloading in mice. *American journal of physiology Endocrinology and metabolism* 309: E651-662, 2015.

31.     **Ekstrand MI, Falkenberg M, Rantanen A, Park CB, Gaspari M, Hultenby K, Rustin P, Gustafsson CM, and Larsson NG**. Mitochondrial transcription factor A regulates mtDNA copy number in mammals. *Human molecular genetics* 13: 935-944, 2004.

32.     **Elmore S**. Apoptosis: A Review of Programmed Cell Death. *Toxicologic pathology* 35: 495-516, 2007.

33.     **Espinosa A, Henriquez-Olguin C, and Jaimovich E**. Reactive oxygen species and calcium signals in skeletal muscle: A crosstalk involved in both normal signaling and disease. *Cell calcium* 60: 172-179, 2016.

34.     **Feng HZ, Chen X, Malek MH, and Jin JP**. Slow recovery of the impaired fatigue resistance in postunloading mouse soleus muscle corresponding to decreased mitochondrial function and a compensatory increase in type I slow fibers. *American journal of physiology Cell physiology* 310: C27-40, 2016.

35.     **Fernandez-Marcos PJ, and Auwerx J**. Regulation of PGC-1α, a nodal regulator of mitochondrial biogenesis. *The American Journal of Clinical Nutrition* 93: 884S-890S, 2011.

36.     **Ferreira JA, Crissey JM, and Brown M**. An Alternant Method to the Traditional NASA Hindlimb Unloading Model in Mice. e2467, 2011.

37.     **Fujino H, Ishihara A, Murakami S, Yasuhara T, Kondo H, Mohri S, Takeda I, and Roy RR**. Protective effects of exercise preconditioning on hindlimb unloading-induced atrophy of rat soleus muscle. *Acta physiologica (Oxford, England)* 197: 65-74, 2009.

38.     **Fujino T, Ide T, Yoshida M, Onitsuka K, Tanaka A, Hata Y, Nishida M, Takehara T, Kanemaru T, Kitajima N, Takazaki S, Kurose H, Kang D, and Sunagawa K**. Recombinant

mitochondrial transcription factor A protein inhibits nuclear factor of activated T cells signaling and attenuates pathological hypertrophy of cardiac myocytes. *Mitochondrion* 12: 449-458, 2012.

39. **Fukai T, and Ushio-Fukai M**. Superoxide dismutases: role in redox signaling, vascular function, and diseases. *Antioxidants & redox signaling* 15: 1583-1606, 2011.

40. **Gao QQ, and McNally EM**. The Dystrophin Complex: Structure, Function, and Implications for Therapy. *Comprehensive Physiology* 5: 1223-1239, 2015.

41. **Garatachea N, Pareja-Galeano H, Sanchis-Gomar F, Santos-Lozano A, Fiuza-Luces C, Morán M, Emanuele E, Joyner MJ, and Lucia A**. Exercise Attenuates the Major Hallmarks of Aging. *Rejuvenation Research* 18: 57-89, 2015.

42. **Gehrig SM, Mihaylova V, Frese S, Mueller SM, Ligon-Auer M, Spengler CM, Petersen JA, Lundby C, and Jung HH**. Altered skeletal muscle (mitochondrial) properties in patients with mitochondrial DNA single deletion myopathy. *Orphanet journal of rare diseases* 11: 105, 2016.

43. **Godin R, Ascah A, and Daussin FN**. Intensity-dependent activation of intracellular signalling pathways in skeletal muscle: role of fibre type recruitment during exercise. *The Journal of physiology* 588: 4073-4074, 2010.

44. **Gordon JW, Rungi AA, Inagaki H, and Hood DA**. Effects of contractile activity on mitochondrial transcription factor A expression in skeletal muscle. *Journal of applied physiology (Bethesda, Md : 1985)* 90: 389-396, 2001.

45. **Gumucio JP, and Mendias CL**. Atrogin-1, MuRF-1, and sarcopenia. *Endocrine* 43: 12-21, 2013.

46.     **Guo B-S, Cheung K-K, Yeung SS, Zhang B-T, and Yeung EW**. Electrical Stimulation Influences Satellite Cell Proliferation and Apoptosis in Unloading-Induced Muscle Atrophy in Mice. *PLoS ONE* 7: e30348, 2012.

47.     **Gutterman DD**. Mitochondria and Reactive Oxygen Species: An Evolution in Function. *Circulation Research* 97: 302-304, 2005.

48.     **Hardie DG**. The AMP-activated protein kinase pathway – new players upstream and downstream. *Journal of Cell Science* 117: 5479-5487, 2004.

49.     **Herzog W**. The role of titin in eccentric muscle contraction. *The Journal of experimental biology* 217: 2825-2833, 2014.

50.     **Hood DA, Adhihetty PJ, Colavecchia M, Gordon JW, Irrcher I, Joseph AM, Lowe ST, and Rungi AA**. Mitochondrial biogenesis and the role of the protein import pathway. *Medicine and science in sports and exercise* 35: 86-94, 2003.

51.     **Ikeda M, Ide T, Fujino T, Arai S, Saku K, Kakino T, Tyynismaa H, Yamasaki T, Yamada K, Kang D, Suomalainen A, and Sunagawa K**. Overexpression of TFAM or twinkle increases mtDNA copy number and facilitates cardioprotection associated with limited mitochondrial oxidative stress. *PLoS One* 10: e0119687, 2015.

52.     **Ikeuchi M, Matsusaka H, Kang D, Matsushima S, Ide T, Kubota T, Fujiwara T, Hamasaki N, Takeshita A, Sunagawa K, and Tsutsui H**. Overexpression of mitochondrial transcription factor a ameliorates mitochondrial deficiencies and cardiac failure after myocardial infarction. *Circulation* 112: 683-690, 2005.

53.     **Irrcher I, Ljubicic V, and Hood DA**. Interactions between ROS and AMP kinase activity in the regulation of PGC-1alpha transcription in skeletal muscle cells. *American journal of physiology Cell physiology* 296: C116-123, 2009.

54.     **Iyer S, Thomas RR, Portell FR, Dunham LD, Quigley CK, and Bennett JP, Jr.** Recombinant mitochondrial transcription factor A with N-terminal mitochondrial transduction domain increases respiration and mitochondrial gene expression. *Mitochondrion* 9: 196-203, 2009.

55.     **Jackman RW, and Kandarian SC**. The molecular basis of skeletal muscle atrophy. *American journal of physiology Cell physiology* 287: C834-843, 2004.

56.     **Jang J, Yun HY, Park J, and Lim K**. Protective effect of branched chain amino acids on hindlimb suspension-induced muscle atrophy in growing rats. *Journal of exercise nutrition & biochemistry* 19: 183-189, 2015.

57.     **Jee H, Sakurai T, Lim JY, and Hatta H**. Changes in alphaB-crystallin, tubulin, and MHC isoforms by hindlimb unloading show different expression patterns in various hindlimb muscles. *Journal of exercise nutrition & biochemistry* 18: 161-168, 2014.

58.     **Johnson ML, Robinson MM, and Nair KS**. Skeletal muscle aging and the mitochondrion. *Trends Endocrinol Metab* 24: 247-256, 2013.

59.     **Jørgensen SB, Richter EA, and Wojtaszewski JFP**. Role of AMPK in skeletal muscle metabolic regulation and adaptation in relation to exercise. *The Journal of physiology* 574: 17-31, 2006.

60.     **Jornayvaz FR, and Shulman GI**. Regulation of mitochondrial biogenesis. *Essays in biochemistry* 47: 10.1042/bse0470069, 2010.

61.      **Joseph AM, Pilegaard H, Litvintsev A, Leick L, and Hood DA**. Control of gene expression and mitochondrial biogenesis in the muscular adaptation to endurance exercise. *Essays Biochem* 42: 13-29, 2006.

62.      **Joza N, Pospisilik JA, Hangen E, Hanada T, Modjtahedi N, Penninger JM, and Kroemer G**. AIF: not just an apoptosis-inducing factor. *Annals of the New York Academy of Sciences* 1171: 2-11, 2009.

63.      **Ju JS, Jeon SI, Park JY, Lee JY, Lee SC, Cho KJ, and Jeong JM**. Autophagy plays a role in skeletal muscle mitochondrial biogenesis in an endurance exercise-trained condition. *The journal of physiological sciences : JPS* 66: 417-430, 2016.

64.      **Kanazashi M, Tanaka M, Murakami S, Kondo H, Nagatomo F, Ishihara A, Roy RR, and Fujino H**. Amelioration of capillary regression and atrophy of the soleus muscle in hindlimb-unloaded rats by astaxanthin supplementation and intermittent loading. *Experimental physiology* 99: 1065-1077, 2014.

65.      **Kang C, Chung E, Diffee G, and Ji LL**. Exercise training attenuates aging-associated mitochondrial dysfunction in rat skeletal muscle: role of PGC-1alpha. *Experimental gerontology* 48: 1343-1350, 2013.

66.      **Kang C, Goodman CA, Hornberger TA, and Ji LL**. PGC-1alpha overexpression by in vivo transfection attenuates mitochondrial deterioration of skeletal muscle caused by immobilization. *Faseb j* 29: 4092-4106, 2015.

67.      **Kang C, and Li Ji L**. Role of PGC-1alpha signaling in skeletal muscle health and disease. *Annals of the New York Academy of Sciences* 1271: 110-117, 2012.

68.     **Kang C, O'Moore KM, Dickman JR, and Ji LL**. Exercise activation of muscle peroxisome proliferator-activated receptor-gamma coactivator-1alpha signaling is redox sensitive. *Free radical biology & medicine* 47: 1394-1400, 2009.

69.     **Kang C, Yeo D, and Ji LL**. Muscle Immobilization Activates Mitophagy and Disrupts Mitochondrial Dynamics in Mice. *Acta physiologica (Oxford, England)* 2016.

70.     **Kang D, Kim SH, and Hamasaki N**. Mitochondrial transcription factor A (TFAM): roles in maintenance of mtDNA and cellular functions. *Mitochondrion* 7: 39-44, 2007.

71.     **Kazior Z, Willis SJ, Moberg M, Apró W, Calbet JAL, Holmberg H-C, and Blomstrand E**. Endurance Exercise Enhances the Effect of Strength Training on Muscle Fiber Size and Protein Expression of Akt and mTOR. *PLOS ONE* 11: e0149082, 2016.

72.     **Kienhofer J, Haussler DJ, Ruckelshausen F, Muessig E, Weber K, Pimentel D, Ullrich V, Burkle A, and Bachschmid MM**. Association of mitochondrial antioxidant enzymes with mitochondrial DNA as integral nucleoid constituents. *Faseb j* 23: 2034-2044, 2009.

73.     **Kim JJ, Lee SB, Park JK, and Yoo YD**. TNF-alpha-induced ROS production triggering apoptosis is directly linked to Romo1 and Bcl-X(L). *Cell death and differentiation* 17: 1420-1434, 2010.

74.     **King-Himmelreich TS, Schramm S, Wolters MC, Schmetzer J, Moser CV, Knothe C, Resch E, Peil J, Geisslinger G, and Niederberger E**. The impact of endurance exercise on global and AMPK gene-specific DNA methylation. *Biochemical and biophysical research communications* 474: 284-290, 2016.

75.     **Koltai E, Hart N, Taylor AW, Goto S, Ngo JK, Davies KJ, and Radak Z**. Age-associated declines in mitochondrial biogenesis and protein quality control factors are minimized by

exercise training. *American journal of physiology Regulatory, integrative and comparative physiology* 303: R127-134, 2012.

76.     **Krustrup P, Soderlund K, Mohr M, Gonzalez-Alonso J, and Bangsbo J**. Recruitment of fibre types and quadriceps muscle portions during repeated, intense knee-extensor exercise in humans. *Pflugers Archiv : European journal of physiology* 449: 56-65, 2004.

77.     **Kühl I, Miranda M, Posse V, Milenkovic D, Mourier A, Siira SJ, Bonekamp NA, Neumann U, Filipovska A, Polosa PL, Gustafsson CM, and Larsson N-G**. POLRMT regulates the switch between replication primer formation and gene expression of mammalian mtDNA. *Science Advances* 2: e1600963, 2016.

78.     **Kukat C, Davies KM, Wurm CA, Spåhr H, Bonekamp NA, Kühl I, Joos F, Polosa PL, Park CB, Posse V, Falkenberg M, Jakobs S, Kühlbrandt W, and Larsson N-G**. Cross-strand binding of TFAM to a single mtDNA molecule forms the mitochondrial nucleoid. *Proceedings of the National Academy of Sciences* 112: 11288-11293, 2015.

79.     **Kunkel GH, Chaturvedi P, and Tyagi SC**. Mitochondrial pathways to cardiac recovery: TFAM. *Heart failure reviews* 21: 499-517, 2016.

80.     **Laplante M, and Sabatini DM**. mTOR signaling at a glance. *Journal of Cell Science* 122: 3589-3594, 2009.

81.     **Larsen S, Nielsen J, Hansen CN, Nielsen LB, Wibrand F, Stride N, Schroder HD, Boushel R, Helge JW, Dela F, and Hey-Mogensen M**. Biomarkers of mitochondrial content in skeletal muscle of healthy young human subjects. *The Journal of physiology* 590: 3349-3360, 2012.

82.	**Larsson NG, Wang J, Wilhelmsson H, Oldfors A, Rustin P, Lewandoski M, Barsh GS, and Clayton DA**. Mitochondrial transcription factor A is necessary for mtDNA maintenance and embryogenesis in mice. *Nature genetics* 18: 231-236, 1998.

83.	**Leeuwenburgh C, Gurley CM, Strotman BA, and Dupont-Versteegden EE**. Age-related differences in apoptosis with disuse atrophy in soleus muscle. *American journal of physiology Regulatory, integrative and comparative physiology* 288: R1288-1296, 2005.

84.	**Liang C, Curry BJ, Brown PL, and Zemel MB**. Leucine Modulates Mitochondrial Biogenesis and SIRT1-AMPK Signaling in C2C12 Myotubes. *Journal of nutrition and metabolism* 2014: 239750, 2014.

85.	**Liang H, and Ward WF**. PGC-1α: a key regulator of energy metabolism. *Advances in Physiology Education* 30: 145-151, 2006.

86.	**Liu J, Peng Y, Wang X, Fan Y, Qin C, Shi L, Tang Y, Cao K, Li H, Long J, and Liu J**. Mitochondrial Dysfunction Launches Dexamethasone-Induced Skeletal Muscle Atrophy via AMPK/FOXO3 Signaling. *Molecular Pharmaceutics* 13: 73-84, 2016.

87.	**Lundby C, and Jacobs RA**. Adaptations of skeletal muscle mitochondria to exercise training. *Experimental physiology* 101: 17-22, 2016.

88.	**Lynch CJ, Xu Y, Hajnal A, Salzberg AC, and Kawasawa YI**. RNA sequencing reveals a slow to fast muscle fiber type transition after olanzapine infusion in rats. *PLoS One* 10: e0123966, 2015.

89.	**Matsushima Y, Goto Y, and Kaguni LS**. Mitochondrial Lon protease regulates mitochondrial DNA copy number and transcription by selective degradation of mitochondrial

transcription factor A (TFAM). *Proceedings of the National Academy of Sciences of the United States of America* 107: 18410-18415, 2010.

90.     **McBride A, and Hardie DG**. AMP-activated protein kinase--a sensor of glycogen as well as AMP and ATP? *Acta physiologica (Oxford, England)* 196: 99-113, 2009.

91.     **McKinsey TA, Zhang CL, and Olson EN**. MEF2: a calcium-dependent regulator of cell division, differentiation and death. *Trends in Biochemical Sciences* 27: 40-47.

92.     **McLeod M, Breen L, Hamilton DL, and Philp A**. Live strong and prosper: the importance of skeletal muscle strength for healthy ageing. *Biogerontology* 17: 497-510, 2016.

93.     **Morita M, Gravel S-P, Chénard V, Sikström K, Zheng L, Alain T, Gandin V, Avizonis D, Arguello M, Zakaria C, McLaughlan S, Nouet Y, Pause A, Pollak M, Gottlieb E, Larsson O, St-Pierre J, Topisirovic I, and Sonenberg N**. mTORC1 Controls Mitochondrial Activity and Biogenesis through 4E-BP-Dependent Translational Regulation. *Cell Metabolism* 18: 698-711.

94.     **Morita M, Gravel SP, Hulea L, Larsson O, Pollak M, St-Pierre J, and Topisirovic I**. mTOR coordinates protein synthesis, mitochondrial activity and proliferation. *Cell cycle (Georgetown, Tex)* 14: 473-480, 2015.

95.     **Moulin M, and Ferreiro A**. Muscle redox disturbances and oxidative stress as pathomechanisms and therapeutic targets in early-onset myopathies. *Seminars in cell & developmental biology* 2016.

96.     **Mukai R, Matsui N, Fujikura Y, Matsumoto N, Hou DX, Kanzaki N, Shibata H, Horikawa M, Iwasa K, Hirasaka K, Nikawa T, and Terao J**. Preventive effect of dietary quercetin on disuse muscle atrophy by targeting mitochondria in denervated mice. *The Journal of nutritional biochemistry* 31: 67-76, 2016.

97.     **Muller FL, Song W, Jang YC, Liu Y, Sabia M, Richardson A, and Van Remmen H**.
Denervation-induced skeletal muscle atrophy is associated with increased mitochondrial ROS
production. *American journal of physiology Regulatory, integrative and comparative physiology*
293: R1159-1168, 2007.

98.     **Nagano K, Suzaki E, Nagano Y, Kataoka K, and Ozawa K**. The activation of apoptosis
factor in hindlimb unloading-induced muscle atrophy under normal and low-temperature
environmental conditions. *Acta histochemica* 110: 505-518, 2008.

99.     **Nagatomo F, Fujino H, Kondo H, Suzuki H, Kouzaki M, Takeda I, and Ishihara A**. PGC-
1alpha and FOXO1 mRNA levels and fiber characteristics of the soleus and plantaris muscles in
rats after hindlimb unloading. *Histology and histopathology* 26: 1545-1553, 2011.

100.    **Ngo HB, Lovely GA, Phillips R, and Chan DC**. Distinct structural features of TFAM drive
mitochondrial DNA packaging versus transcriptional activation. *Nature communications* 5: 3077,
2014.

101.    **Nishiyama S, Shitara H, Nakada K, Ono T, Sato A, Suzuki H, Ogawa T, Masaki H,
Hayashi J, and Yonekawa H**. Over-expression of Tfam improves the mitochondrial disease
phenotypes in a mouse model system. *Biochemical and biophysical research communications*
401: 26-31, 2010.

102.    **Nuoc TN, Kim S, Ahn SH, Lee JS, Park BJ, and Lee TH**. The analysis of antioxidant
expression during muscle atrophy induced by hindlimb suspension in mice. *The journal of
physiological sciences : JPS* 2016.

103.     **Ogasawara R, Fujita S, Hornberger TA, Kitaoka Y, Makanae Y, Nakazato K, and Naokata I**. The role of mTOR signalling in the regulation of skeletal muscle mass in a rodent model of resistance exercise. *Sci Rep* 6: 31142, 2016.

104.     **Ohno Y, Fujiya H, Goto A, Nakamura A, Nishiura Y, Sugiura T, Ohira Y, Yoshioka T, and Goto K**. Microcurrent electrical nerve stimulation facilitates regrowth of mouse soleus muscle. *International journal of medical sciences* 10: 1286-1294, 2013.

105.     **Olesen J, Kiilerich K, and Pilegaard H**. PGC-1alpha-mediated adaptations in skeletal muscle. *Pflugers Archiv : European journal of physiology* 460: 153-162, 2010.

106.     **Owusu-Ansah E, Yavari A, and Banerjee U**. A protocol for _in vivo_ detection of reactive oxygen species. 2008.

107.     **Paschen SA, and Neupert W**. Protein import into mitochondria. *IUBMB life* 52: 101-112, 2001.

108.     **Pasternak C, Wong S, and Elson EL**. Mechanical function of dystrophin in muscle cells. *The Journal of cell biology* 128: 355-361, 1995.

109.     **Pedersen BK**. Muscle as a secretory organ. *Comprehensive Physiology* 3: 1337-1362, 2013.

110.     **Pelicano H, Zhang W, Liu J, Hammoudi N, Dai J, Xu R-H, Pusztai L, and Huang P**. Mitochondrial dysfunction in some triple-negative breast cancer cell lines: role of mTOR pathway and therapeutic potential. *Breast Cancer Research : BCR* 16: 434, 2014.

111.     **Peralta S, Wang X, and Moraes CT**. Mitochondrial transcription: lessons from mouse models. *Biochimica et biophysica acta* 1819: 961-969, 2012.

112.     **Petrini AC, Ramos DM, Gomes de Oliveira L, Alberto da Silva C, and Pertille A**. Prior swimming exercise favors muscle recovery in adult female rats after joint immobilization. *Journal of physical therapy science* 28: 2072-2077, 2016.

113.     **Powers SK, Lynch GS, Murphy KT, Reid MB, and Zijdewind I**. Disease-Induced Skeletal Muscle Atrophy and Fatigue. *Medicine and science in sports and exercise* 48: 2307-2319, 2016.

114.     **Powers SK, Wiggs MP, Duarte JA, Zergeroglu AM, and Demirel HA**. Mitochondrial signaling contributes to disuse muscle atrophy. *American journal of physiology Endocrinology and metabolism* 303: E31-39, 2012.

115.     **Rebbeck RT, Karunasekara Y, Board PG, Beard NA, Casarotto MG, and Dulhunty AF**. Skeletal muscle excitation-contraction coupling: who are the dancing partners? *The international journal of biochemistry & cell biology* 48: 28-38, 2014.

116.     **Remels AH, Pansters NA, Gosker HR, Schols AM, and Langen RC**. Activation of alternative NF-kappaB signaling during recovery of disuse-induced loss of muscle oxidative phenotype. *American journal of physiology Endocrinology and metabolism* 306: E615-626, 2014.

117.     **Rudrappa SS, Wilkinson DJ, Greenhaff PL, Smith K, Idris I, and Atherton PJ**. Human Skeletal Muscle Disuse Atrophy: Effects on Muscle Protein Synthesis, Breakdown, and Insulin Resistance-A Qualitative Review. *Frontiers in physiology* 7: 361, 2016.

118.     **Russell AP, Foletta VC, Snow RJ, and Wadley GD**. Skeletal muscle mitochondria: a major player in exercise, health and disease. *Biochimica et biophysica acta* 1840: 1276-1284, 2014.

119.     **Saleem A, and Hood DA**. Acute exercise induces tumour suppressor protein p53 translocation to the mitochondria and promotes a p53-Tfam-mitochondrial DNA complex in skeletal muscle. *The Journal of physiology* 591: 3625-3636, 2013.

120.	**Sandri M**. Protein breakdown in muscle wasting: Role of autophagy-lysosome and ubiquitin-proteasome()(). *The international journal of biochemistry & cell biology* 45: 2121-2129, 2013.

121.	**Santos JM, and Kowluru RA**. Impaired Transport of Mitochondrial Transcription Factor and the Metabolic Memory Phenomenon Associated with the Progression of Diabetic Retinopathy. *Diabetes/metabolism research and reviews* 29: 204-213, 2013.

122.	**Schmidt O, Pfanner N, and Meisinger C**. Mitochondrial protein import: from proteomics to functional mechanisms. *Nature reviews Molecular cell biology* 11: 655-667, 2010.

123.	**Schneider CA, Rasband WS, and Eliceiri KW**. NIH Image to ImageJ: 25 years of image analysis. *Nature methods* 9: 671-675, 2012.

124.	**Schwalm C, Jamart C, Benoit N, Naslain D, Premont C, Prevet J, Van Thienen R, Deldicque L, and Francaux M**. Activation of autophagy in human skeletal muscle is dependent on exercise intensity and AMPK activation. *Faseb j* 29: 3515-3526, 2015.

125.	**Seo S, Lee M-S, Chang E, Shin Y, Oh S, Kim I-H, and Kim Y**. Rutin Increases Muscle Mitochondrial Biogenesis with AMPK Activation in High-Fat Diet-Induced Obese Rats. *Nutrients* 7: 8152-8169, 2015.

126.	**Shenkman BS, Belova SP, Lomonosova YN, Kostrominova TY, and Nemirovskaya TL**. Calpain-dependent regulation of the skeletal muscle atrophy following unloading. *Arch Biochem Biophys* 584: 36-41, 2015.

127.	**Short KR, Bigelow ML, Kahl J, Singh R, Coenen-Schimke J, Raghavakaimal S, and Nair KS**. Decline in skeletal muscle mitochondrial function with aging in humans. *Proceedings of the National Academy of Sciences of the United States of America* 102: 5618-5623, 2005.

128. **Silva LA, Pinho CA, Scarabelot KS, Fraga DB, Volpato AM, Boeck CR, De Souza CT, Streck EL, and Pinho RA**. Physical exercise increases mitochondrial function and reduces oxidative damage in skeletal muscle. *European journal of applied physiology* 105: 861-867, 2009.

129. **Siu PM**. Muscle apoptotic response to denervation, disuse, and aging. *Medicine and science in sports and exercise* 41: 1876-1886, 2009.

130. **Siu PM, Wang Y, and Alway SE**. Apoptotic signaling induced by H(2)O(2)-mediated oxidative stress in differentiated C2C12 myotubes. *Life sciences* 84: 468-481, 2009.

131. **Srivastava S**. Emerging therapeutic roles for NAD+ metabolism in mitochondrial and age-related disorders. *Clinical and Translational Medicine* 5: 1-11, 2016.

132. **St John JC**. Mitochondrial DNA copy number and replication in reprogramming and differentiation. *Seminars in cell & developmental biology* 52: 93-101, 2016.

133. **Steinbacher P, and Eckl P**. Impact of oxidative stress on exercising skeletal muscle. *Biomolecules* 5: 356-377, 2015.

134. **Stiles AR, Simon MT, Stover A, Eftekharian S, Khanlou N, Wang HL, Magaki S, Lee H, Partynski K, Dorrani N, Chang R, Martinez-Agosto JA, and Abdenur JE**. Mutations in TFAM, encoding mitochondrial transcription factor A, cause neonatal liver failure associated with mtDNA depletion. *Molecular genetics and metabolism* 119: 91-99, 2016.

135. **Strobel NA, Peake JM, Matsumoto A, Marsh SA, Coombes JS, and Wadley GD**. Antioxidant supplementation reduces skeletal muscle mitochondrial biogenesis. *Medicine and science in sports and exercise* 43: 1017-1024, 2011.

136. **Sun LW, Blottner D, Luan HQ, Salanova M, Wang C, Niu HJ, Felsenberg D, and Fan YB**. Bone and muscle structure and quality preserved by active versus passive muscle exercise on a

new stepper device in 21 days tail-suspended rats. *Journal of musculoskeletal & neuronal interactions* 13: 166-177, 2013.

137.    **Suwa M, Nakano H, Radak Z, and Kumagai S**. Endurance exercise increases the SIRT1 and peroxisome proliferator-activated receptor gamma coactivator-1alpha protein expressions in rat skeletal muscle. *Metabolism: clinical and experimental* 57: 986-998, 2008.

138.    **Taanman JW**. The mitochondrial genome: structure, transcription, translation and replication. *Biochimica et biophysica acta* 1410: 103-123, 1999.

139.    **Tawa NE, Jr., Odessey R, and Goldberg AL**. Inhibitors of the proteasome reduce the accelerated proteolysis in atrophying rat skeletal muscles. *The Journal of clinical investigation* 100: 197-203, 1997.

140.    **Theilen NT, Kunkel GH, and Tyagi SC**. The Role of Exercise and TFAM in Preventing Skeletal Muscle Atrophy. *J Cell Physiol* 232: 2348-2358, 2017.

141.    **Tisdale MJ**. The ubiquitin-proteasome pathway as a therapeutic target for muscle wasting. *The journal of supportive oncology* 3: 209-217, 2005.

142.    **Todd JS, Shurley JP, and Todd TC**. Thomas L. DeLorme and the science of progressive resistance exercise. *Journal of strength and conditioning research* 26: 2913-2923, 2012.

143.    **Tokusumi Y, Zhou S, and Takada S**. Nuclear respiratory factor 1 plays an essential role in transcriptional initiation from the hepatitis B virus x gene promoter. *Journal of virology* 78: 10856-10864, 2004.

144.    **Turrens JF**. Mitochondrial formation of reactive oxygen species. *The Journal of physiology* 552: 335-344, 2003.

145.    **Tyml K, and Mathieu-Costello O**. Structural and functional changes in the microvasculature of disused skeletal muscle. *Frontiers in bioscience : a journal and virtual library* 6: D45-52, 2001.

146.    **Umanskaya A, Santulli G, Xie W, Andersson DC, Reiken SR, and Marks AR**. Genetically enhancing mitochondrial antioxidant activity improves muscle function in aging. *Proceedings of the National Academy of Sciences of the United States of America* 111: 15250-15255, 2014.

147.    **Valero T**. Mitochondrial biogenesis: pharmacological approaches. *Current pharmaceutical design* 20: 5507-5509, 2014.

148.    **van Gisbergen MW, Voets AM, Starmans MHW, de Coo IFM, Yadak R, Hoffmann RF, Boutros PC, Smeets HJM, Dubois L, and Lambin P**. How do changes in the mtDNA and mitochondrial dysfunction influence cancer and cancer therapy? Challenges, opportunities and models. *Mutation Research/Reviews in Mutation Research* 764: 16-30, 2015.

149.    **van Osch FHM, Voets AM, Schouten LJ, Gottschalk RWH, Simons CCJM, van Engeland M, Lentjes MHFM, van den Brandt PA, Smeets HJM, and Weijenberg MP**. Mitochondrial DNA copy number in colorectal cancer: between tissue comparisons, clinicopathological characteristics and survival. *Carcinogenesis* 36: 1502-1510, 2015.

150.    **Vandenburgh H, Chromiak J, Shansky J, Del Tatto M, and Lemaire J**. Space travel directly induces skeletal muscle atrophy. *Faseb j* 13: 1031-1038, 1999.

151.    **Vigelso A, Andersen NB, and Dela F**. The relationship between skeletal muscle mitochondrial citrate synthase activity and whole body oxygen uptake adaptations in response to exercise training. *International journal of physiology, pathophysiology and pharmacology* 6: 84-101, 2014.

152.     **Wang C, and Youle RJ**. The Role of Mitochondria in Apoptosis(). *Annual review of genetics* 43: 95-118, 2009.

153.     **Wang W, Yang X, López de Silanes I, Carling D, and Gorospe M**. Increased AMP:ATP Ratio and AMP-activated Protein Kinase Activity during Cellular Senescence Linked to Reduced HuR Function. *Journal of Biological Chemistry* 278: 27016-27023, 2003.

154.     **Wang Y, and Pessin JE**. Mechanisms for fiber-type specificity of skeletal muscle atrophy. *Current opinion in clinical nutrition and metabolic care* 16: 243-250, 2013.

155.     **Warburton DER, Nicol CW, and Bredin SSD**. Health benefits of physical activity: the evidence. *CMAJ : Canadian Medical Association Journal* 174: 801-809, 2006.

156.     **Wei YH**. Oxidative stress and mitochondrial DNA mutations in human aging. *Proceedings of the Society for Experimental Biology and Medicine Society for Experimental Biology and Medicine (New York, NY)* 217: 53-63, 1998.

157.     **Wredenberg A, Wibom R, Wilhelmsson H, Graff C, Wiener HH, Burden SJ, Oldfors A, Westerblad H, and Larsson NG**. Increased mitochondrial mass in mitochondrial myopathy mice. *Proceedings of the National Academy of Sciences of the United States of America* 99: 15066-15071, 2002.

158.     **Yajid F, Mercier JG, Mercier BM, Dubouchaud H, and Prefaut C**. Effects of 4 wk of hindlimb suspension on skeletal muscle mitochondrial respiration in rats. *Journal of applied physiology (Bethesda, Md : 1985)* 84: 479-485, 1998.

159.     **Yan Z, Lira VA, and Greene NP**. Exercise training-induced Regulation of Mitochondrial Quality. *Exercise and Sport Sciences Reviews* 40: 159-164, 2012.

160.     **Yang J, Liu X, Bhalla K, Kim CN, Ibrado AM, Cai J, Peng TI, Jones DP, and Wang X**.

Prevention of apoptosis by Bcl-2: release of cytochrome c from mitochondria blocked. *Science*

275: 1129-1132, 1997.

161.     **You JS, Anderson GB, Dooley MS, and Hornberger TA**. The role of mTOR signaling in the

regulation of protein synthesis and muscle mass during immobilization in mice. *Disease models*

*& mechanisms* 8: 1059-1069, 2015.

162.     **Zhang P, Chen X, and Fan M**. Signaling mechanisms involved in disuse muscle atrophy.

*Medical hypotheses* 69: 310-321, 2007.

163.     **Zhou Q, Li H, Li H, Nakagawa A, Lin JLJ, Lee E-S, Harry BL, Skeen-Gaar RR, Suehiro Y,**

**William D, Mitani S, Yuan HS, Kang B-H, and Xue D**. Mitochondrial endonuclease G mediates

breakdown of paternal mitochondria upon fertilization. *Science* 353: 394-399, 2016.

# APPENDIX

Chapter 1 is a published review article while Chapter 2 and Chapter 3 are under review for publication as original research manuscripts. Proper copyright materials have been obtained for all published material contained within this dissertation and are referenced within this document.

CURRICULUM VITAE

Nicholas T. Theilen
419 Reba Jackson Dr.
Jeffersonville, IN, 47130
Phone: (Cell) 502.314.9661
Email: nick.theilen@gmail.com

---

## EDUCATION

| | |
|---|---|
| 05/2009 | B.S. in Business Management, University of Louisville, Louisville, KY |
| 05/2013 | M.S. in Exercise Science, University of South Florida, Tampa, FL |
| 03/2017 | M.S. in Physiology, University of Louisville, Louisville, KY |
| *05/2018* | *PhD in Physiology, University of Louisville, Louisville, KY* |

## ACADEMIC APPOINTMENTS

08/2011-05/2013    Graduate Teaching Assistant
Department of Exercise Science
University of South Florida
Tampa, FL

08/2014-12/2014    Adjunct Professor
Department of Exercise Science
University of Bellarmine
Louisville, KY

08/2015-05/2018    PhD Candidate
Department of Physiology
University of Louisville
Louisville, KY

## HONORS AND AWARDS

08/2004    President's Scholarship, University of Louisville

08/2011    Graduate Teaching Assistantship, Department of Exercise Science, University of South Florida

08/2015        Integrated Program in Biomedical Sciences Fellowship, Department of Physiology, University of Louisville

03/2017        Graduate Research Assistantship, Department of Physiology, University of Louisville

04/2017        Department of Physiology Travel Award, University of Louisville

10/2017        Alicia L. Jee Young Investigator Award, Orthopaedic Research Society-Musculoskeletal Workshop, Sun Valley, ID

04/2018        Graduate Dean's Citation, University of Louisville School of Interdisciplinary and Graduate Studies Awards Committee


## OTHER WORK EXPERIENCE

11/2013-06/2015        Fitness Coordinator - Corporate Fitness Works, Humana Clocktower Building, Louisville, KY

- Managerial experience as coordinator of equipment budgets, maintenance, training and wellness programs, marketing materials, and customer relations.
- Creator of a monthly health and wellness newsletter on the national company website chosen to be used by the CEO in traveling presentations.
- Developer of relationships in one-on-one settings to coach and advise employees as well as in a large group setting routinely delivering presentations to Humana groups and departments while garnering a near 100% satisfaction in survey ratings.

01/2011-10/2011        Patient Liaison – Moffitt Cancer Research Center, Tampa, FL

- Widespread exposure to multiple oncology research areas.
- Responsible for checking patients into appointments, ordering diagnostics, bloodwork, and discussing physician's orders with patients.
- Constant communication with MD, PA, and RNs to ensure patient experience and correct orders.

05/2005-11/2010        Nursing Administration / Patient Transporter - University of Louisville Hospital, Louisville, KY

- Problem solving experience shown by improving departmental timing efficiency of up to 12% after applying an operations productivity method to our operating procedures.
- In-depth experience working with patients, MDs, nurses, and hospital staff to provide effective care and production in a healthcare setting.
- Healthcare law knowledge gained through years of navigating HIPAA regulations and standards of care.

## PROFESSIONAL MEMBERSHIP

04/2015-Present     American College of Sports Medicine (ACSM) – Health and Fitness Specialist, Louisville, KY

02/2017-Present     American Physiological Society (APS) – Student member

08/2017-Present     Orthopaedic Research Society (ORS) – Student member

## WRITINGS AND PUBLICATIONS

1) Theilen, N.T., Jeremic, N., Weber, G.J., Tyagi, S.C. (2018). Exercise Preconditioning Diminishes Skeletal Muscle Atrophy. *Journal of Applied Physiology*. (article under review)
2) Theilen, N.T., Jeremic, N., Weber, G.J., Tyagi, S.C. (2018). TFAM Overexpression Diminishes Skeletal Muscle Atrophy. *Journal of Applied Physiology.* (article under review).
3) Jeremic, N., Weber, G.J., Theilen, N.T., Tyagi, S.C. (2018). Alteration of microRNAs in Heart as Underlying Mechanism for Beneficial Effects of High Intensity Interval Training. *AJP-Heart and Circulation.* (article under review).
4) Theilen, N. T., Kunkel, G. H. and Tyagi, S. C. (2017), The Role of Exercise and TFAM in Preventing Skeletal Muscle Atrophy. J. Cell. Physiol., 232: 2348–2358. doi:10.1002/jcp.25737
5) Kunkel GH, Chaturvedi P, Theilen N, Nair R, and Tyagi SC. Mechanisms of TFAM-mediated cardiomyocyte protection. *Canadian journal of physiology and pharmacology* 96: 173-181, 2018.
6) Theilen, N.T., Tyagi, S.C. (2017), Exercise and TFAM: Protectors of Skeletal Muscle. J Cell Signaling. (Open Access Online)
7) O'Halloran, J., Campbell, B., Martinez, N., O'Connor, S., Fuentes, J., Theilen, N., Kilpatrick, M. (2014). The effects of practical vascular blood flow restriction training on skeletal muscle hypertrophy. *Journal of the International Society of Sports Nutrition*, *11*(Suppl 1), P18. http://doi.org/10.1186/1550-2783-11-S1-P18

8) Theilen, N., Campbell, B., Zourdos, M., O'Halloran, J. (2013). "Comparisons of acute neuromuscular fatigue and recovery after maximal effort strength training using powerlifts" (2013). Graduate Theses and Dissertations. http://scholarcommons.usf.edu/etd/4593-

9) Martuscello J, Theilen N. 2014. Do the Benefits of Strength Training Out-Weigh the Dangers for Endurance Athletes? Strength & Conditioning Journal 36(4):49-51.

## JOURNAL REVIEWER

1) APS – Journal of Applied Physiology, 2017 (1 review)

## RESEARCH PROJECTS

1) **'Exercise Preconditioning and TFAM Overexpression Diminish Skeletal Muscle Atrophy'**
University of Louisville, Mentor: Dr. Suresh C. Tyagi, 2015-Present

- Lead Investigator, *Alicia L. Jee Young Investigator Award Winner 2017*.
- Responsible for all aspects of project idea generation, study design, treatments, experiments, presentations, and writings.
- Molecular laboratory techniques used as well as genetically modified mouse lines.
- Poster presentation at Experimental Biology Conference, Chicago, IL, 2017.
- Poster presentation at Orthopedic Research Society, Sun Valley, ID, 2017.

2) **'Alteration of microRNAs in Heart as Underlying Mechanism for Beneficial Effects of High Intensity Interval Training'**
University of Louisville, 2017-Present

- Co-author; podium award nominee for lead author Dr. Nevena Jeremic, *International Academy of Cardiovascular Sciences 2017.*
- Experience in idea generation, echocardiogram, polymerase chain reaction, western blotting, laser Doppler blood flow imaging, and morphological assessments.

3) '**Mechanism of TFAM Mediated Cardiomyocyte Protection'**
University of Louisville, 2016-2017

- Co-authorship of an *in vitro* study on cardiomyocytes.
- Experience using CRISPR-Cas9 technology.

- Conducted Bradford Assay protein estimations, western blots, and treatments on cell lines.

4) **'Comparisons of Acute Neuromuscular Fatigue and Recovery in Maximal Effort Strength Training Using Powerlifts'**
University of South Florida, Mentor: Dr. Bill Campbell, 2011-2013

- Lead Investigator: self-designed and coordinated 4week study using 12 human participants in training and measurement sessions.
- Complete experience with IRB (internal review board) submission, editing, and clearance.
- Equipment experience: TENDO Speed and Power Analyzer, blood analysis equipment
- Advised by Dr. Mike Zourdos (FAU) and Dr. Jonathan Oliver (TCU) in all phases of study creation and completion.
- Accepted for podium presentation and poster presentation at the NSCA conference, July 2013, Las Vegas, NV.

5) **'The Hypertrophic Effects of Practical Venous Blood Flow Restriction Training'** University of South Florida, Mentor: Dr. Bill Campbell, 2012-2013

- Co-authorship under lead investigator.
- Contributed to study design, piloting, and data collection.